

DISS. ETH NO. 29120

**STUDY OF THE ROLE OF CIRCULATING EXTRACELLULAR
VESICLES IN EPIGENETIC INHERITANCE**

A thesis submitted to attain the degree of
DOCTOR OF SCIENCES
(Dr. sc. ETH Zurich)

presented by

ANAR ALSHANBAYEVA

MSc - Arts et Métiers ParisTech,
Paris Descartes University

born on 20.02.1992

accepted on the recommendation of

Prof. Isabelle Mansuy, examiner

Prof. Magdalini Polymenidou, co-examiner

Prof. Gerhard Schratt, co-examiner

2023

Summary

Exposure to environmental stressors can affect functioning of an organism in various ways. In some cases, in addition to the generation directly exposed to a stressor, its unexposed offspring and grand offspring may also be affected. Studies have suggested that epigenetic alterations in germ cells could be a mechanism for this mode of inheritance. These alterations include changes in DNA methylation patterns, histone modifications and a differing composition of RNA. Although different environmental insults, such as stress, low and high-protein diets, high-fat diet, toxicants, and others can impact peripheral tissues and the information delivered by sperm upon fertilization, it is not well-understood how changes in the periphery can reach germ cells in the gonads. In recent years, blood, as a biological fluid that captures components secreted from various organs and serves as a signalling medium across distant tissues in the body, has emerged as a potential vector for soma-to-germline communication in males. Previously, such a possibility was strongly argued against, due to the existence of blood-organ barriers, which prevent direct access of bloodstream to germ cells in males, such as the blood-testis barrier and the blood-epididymis barrier. However, additional factors should be considered when examining the possibility of soma-to-germline communication via the bloodstream: (i) the pool of stem cells from which germ cells develop is located outside the blood-testis barrier and is therefore directly exposed to the components in circulation; (ii) both barriers consist of somatic cells that are connected to blood vessels and send signals to differentiating and maturing germ cells; (iii) both barriers are not fully formed during early development, allowing easier access for components from blood or neighbouring tissue to germ cells; (iv) both barriers are permeable to small molecules from the bloodstream. Taking these points into account, we investigate the possibility that signals from the periphery, carrying information about changes in the environment, reach the germ cells via the bloodstream.

To study this, we used a mouse model of early life stress (ELS), due to its consistency and reproducibility in transmitting metabolic and behavioral phenotypes for several generations through the patriline. Furthermore, ELS is prevalent in our society, and its long-term effects on mental health and well-being of those affected are well known. Mice exposed to ELS show increased risk-taking behavior, memory deficits, altered social recognition, depressive-like symptoms, and insulin/glucose

dysregulation. To understand the role of different circulating factors in ELS, we first divided ELS and control blood into fractions enriched in either extracellular vesicles (EVs) or proteins and injected them into naïve mice. We found that both EV-enriched and protein-enriched fractions from mice exposed to ELS caused significant changes in circulating metabolites and lipids when injected into naïve mice, but only EVs-enriched fractions gave rise to metabolic alterations that could also be observed in the next generation. When we examined which cargoes in circulating EVs might cause such an effect, we identified small RNAs and lipids as possible candidates. Interestingly, both small and long RNAs in sperm were significantly altered in males injected with ELS EVs. To link sperm RNA changes to phenotypic changes in the offspring, we performed *in vitro* fertilizations with sperm from males injected with either ELS EVs or control EVs and found several differentially expressed transcripts in early embryos. Further, we have demonstrated that germ cell-like cells can take up EVs from blood *in vitro*. Finally, we wanted to understand the response of germ cells at different stages of their development to EV-injections. To evaluate this, we analyzed sperm RNA at different time-points after the injections. In addition to studying EVs in the bloodstream, we also examined the impact of early life stress on the EVs produced in the epididymis. Here, we observed that ELS led to changes in their small RNA cargo. In summary, this thesis supports the existence of communication between the bloodstream/periphery with the germline in males and demonstrates that changes in circulating factors can affect the germ cells in ways that may ultimately affect the next generation.

We conclude this work by addressing how our findings contribute to the present knowledge on the potential of circulating factors communicating with germ cells in males, commenting on the limitations of the study, and exploring further experimental opportunities to build on the current results.

Zusammenfassung

Die Exposition gegenüber Umweltstressoren kann die Funktionsweise eines Organismus auf verschiedene Weise beeinträchtigen. In einigen Fällen können neben der Generation, die einem Stressor direkt ausgesetzt ist, auch die nicht exponierten Nachkommen und Enkel betroffen sein. Studien haben ergeben, dass epigenetische Veränderungen in Keimzellen ein Mechanismus für diese Art der Vererbung sein könnten. Zu diesen Veränderungen gehören Änderungen der DNA-Methylierungsmuster, Histonmodifikationen und eine unterschiedliche Zusammensetzung der RNA. Obwohl verschiedene Umwelteinflüsse wie Stress, eiweißarme und eiweißreiche Ernährung, fettreiche Ernährung, Giftstoffe usw. Auswirkungen auf periphere Gewebe und die von den Spermien bei der Befruchtung übermittelten Informationen haben können, ist noch nicht geklärt, wie Veränderungen in der Peripherie die Keimzellen in den Gonaden erreichen können. In den letzten Jahren hat sich das Blut als biologische Flüssigkeit, die Komponenten aufnimmt, die von verschiedenen Organen abgesondert werden, und als Signalmedium zwischen entfernten Geweben im Körper dient, als potenzieller Vektor für die Kommunikation zwischen Soma und Keimbahn bei Männern erwiesen. Bisher wurde diese Möglichkeit aufgrund der Blut-Organ-Schranken, die den direkten Zugang des Blutstroms zu den männlichen Keimzellen verhindern, wie die Blut-Hoden-Schranke und die Blut-Nebenhoden-Schranke, stark abgelehnt. Bei der Untersuchung der Möglichkeit einer Kommunikation zwischen Soma und Keimbahn über den Blutkreislauf sollten jedoch weitere Faktoren berücksichtigt werden: (i) der Pool von Stammzellen, aus denen sich Keimzellen entwickeln, befindet sich außerhalb der Blut-Hoden-Schranke und ist daher den Bestandteilen im Blutkreislauf direkt ausgesetzt; (ii) beide Schranken bestehen aus somatischen Zellen, die mit Blutgefäßen verbunden sind und Signale an sich differenzierende und reifende Keimzellen senden; (iii) beide Schranken sind während der frühen Entwicklung nicht vollständig ausgebildet, was den Zugang von Bestandteilen aus dem Blut oder benachbartem Gewebe zu Keimzellen erleichtert; (iv) beide Schranken sind für kleine Moleküle aus dem Blutkreislauf durchlässig. Unter Berücksichtigung dieser Punkte untersuchen wir die Möglichkeit, dass Signale aus der Peripherie, die Informationen über Veränderungen in der Umgebung transportieren, die Keimzellen über den Blutkreislauf erreichen.

Um dies zu untersuchen, haben wir ein Mausmodell für frühen Lebensstress (ELS) verwendet, da es Stoffwechsel- und Verhaltensphänotypen über mehrere Generationen hinweg konsistent und reproduzierbar über die Patriline weitergibt. Außerdem ist ELS in unserer Gesellschaft weit verbreitet, und seine langfristigen Auswirkungen auf die psychische Gesundheit und das Wohlbefinden der Betroffenen sind bekannt. Mäuse, die ELS ausgesetzt sind, zeigen ein erhöhtes Risikoverhalten, Gedächtnisdefizite, eine veränderte soziale Anerkennung, depressionsähnliche Symptome und eine Dysregulation von Insulin und Glukose. Um die Rolle verschiedener zirkulierender Faktoren bei ELS zu verstehen, teilten wir zunächst ELS- und Kontrollblut in Fraktionen auf, die entweder mit extrazellulären Vesikeln (EVs) oder Proteinen angereichert waren, und injizierten sie naiven Mäusen. Wir fanden heraus, dass sowohl mit EVs als auch mit Proteinen angereicherte Fraktionen von Mäusen, die ELS ausgesetzt waren, signifikante Veränderungen der zirkulierenden Metaboliten und Lipide verursachten, wenn sie naiven Mäusen injiziert wurden, aber nur mit EVs angereicherte Fraktionen führten zu metabolischen Veränderungen, die auch in der nächsten Generation beobachtet werden konnten. Als wir untersuchten, welche Ladungen in zirkulierenden EVs einen solchen Effekt verursachen könnten, identifizierten wir kleine RNAs und Lipide als mögliche Kandidaten. Interessanterweise waren sowohl kleine als auch lange RNAs in Spermien von Männern, denen ELS EVs injiziert wurden, signifikant verändert. Um die Veränderungen der Spermien-RNA mit den phänotypischen Veränderungen der Nachkommen in Verbindung zu bringen, führten wir In-vitro-Fertilisationen mit Spermien von Männern durch, denen entweder ELS-EVs oder Kontroll-EVs injiziert worden waren, und fanden mehrere unterschiedlich exprimierte Transkripte in frühen Embryonen. Außerdem haben wir gezeigt, dass keimzellenähnliche Zellen in vitro EVs aus dem Blut aufnehmen können. Schließlich wollten wir die Reaktion von Keimzellen in verschiedenen Stadien ihrer Entwicklung auf EV-Injektionen verstehen. Zu diesem Zweck analysierten wir die Spermien-RNA zu verschiedenen Zeitpunkten nach den Injektionen. Neben der Untersuchung der EVs im Blutkreislauf untersuchten wir auch die Auswirkungen von frühem Lebensstress auf die in den Nebenhoden produzierten EVs. Dabei konnten wir feststellen, dass ELS zu Veränderungen in der Ladung der kleinen RNAs führte.

Wir schließen diese Arbeit ab, indem wir darauf eingehen, wie unsere Ergebnisse zum derzeitigen Wissensstand über das Potenzial zirkulierender

Faktoren, die mit männlichen Keimzellen kommunizieren, beitragen, die Grenzen der Studie kommentieren und weitere experimentelle Möglichkeiten erkunden, um auf den aktuellen Ergebnissen aufzubauen. Zusammenfassend lässt sich sagen, dass diese Arbeit die Existenz einer Kommunikation zwischen dem Blutkreislauf/der Peripherie und der Keimbahn bei Männern belegt und zeigt, dass Veränderungen der zirkulierenden Faktoren die Keimzellen in einer Weise beeinflussen können, die sich letztlich auf die nächste Generation auswirken kann.

Glossary

ELS	Early life stress
EVs	Extracellular vesicles
DNAme	DNA methylation
PTMs	Post-translational modifications
ncRNA	Noncoding RNA
scnRNA	Small noncoding RNA
miRNA	microRNA
tRF	tRNA-derived fragment
MERVL	Murine endogenous retrovirus-L
piRNAs	Piwi-interacting RNAs
circRNA	circular RNA
IAP	Intracisternal A-particle
LINE1	Long interspersed nuclear elements
DMR	Differentially methylated region
PGC	Primordial germ cell
E7.25	Embryonic day 7.25
E10.5	Embryonic day 10.5
SCC	Spermatogonia stem cell
BBB	Blood-brain-barrier
BTB	Blood-testis-barrier
BEB	Blood-epididymis-barrier
TJ	Tight junction
HPA	Hypothalamic-pituitary-adrenal
HPG	Hypothalamic–pituitary–gonadal
BPA	Bisphenol A
EGFP	Enhanced green fluorescent protein
ATF7	Activating transcription factor-7
PPAR	Peroxisome proliferator-activated receptor
CNS	Central nervous system
Cre	Cyclization recombinase
VLDL	Very-low-density lipoprotein
LDL	Low-density lipoprotein

IDL	Intermediate-density lipoprotein
HDL	High-density lipoprotein
MVB	Multivesicular body
rRNA	Ribosomal RNA
tRNA	Transfer RNA
snoRNA	Small nucleolar RNA
mtRNA	Mitochondrial RNA
vtRNA	Vault RNA
CHOL	Cholesterol
PC	Phosphatidylcholine
PE	Phosphatidylethanolamine
PS	Phosphatidylserine
EM	Electron microscopy
WB	Western blotting
NTA	Nanoparticle-tracking analysis
FFC	Fluorescence flow cytometry
UC	Ultracentrifugation
SEC	Size-exclusion chromatography
DGUC	Density-gradient ultracentrifugation
UF	Ultrafiltration
ELISA	Enzyme-linked immunosorbent assay
eWAT	Epididymal white adipose tissue
AhR	Aryl hydrocarbon receptor
IRS-1	Insulin receptor substrate-1
IRS-2	Insulin receptor substrate-2
HFD	High-fat diet
LXR	Liver X-receptor
PXR	Pregnane X-receptor
PPARalpha	Peroxisome proliferator-activated receptor alpha
AAV	Adeno-associated virus

*“Does anything genuinely beautiful need supplementing? No more than justice does
– or truth, or kindness, or humility.” – Marcus Aurelius*

Table of Contents

Summary	1
Zusammenfassung	3
Glossary	3
1. Introduction	12
1.1 Epigenetic inheritance.....	12
1.2 Vectors of epigenetic inheritance.....	13
1.3 Germ cell development and supporting structures in males.....	16
1.4 Blood-organ barriers to the germ cells in males.....	18
1.5 Developmental processes affected by early life exposures	21
1.6 Evidence of soma-to-germline communication of environmental exposures	23
1.7 Broad classification of circulating factors.....	25
1.8 Changes in circulating factors due to environmental exposures	26
1.9 Extracellular vesicles.....	27
1.10 Extracellular vesicles in cell-to-cell communication across the body	30
1.11 Extracellular vesicles in male reproductive tract and their potential role in epigenetic inheritance	31
1.12 Characterization and identification of circulating extracellular vesicles	33
1.13 Aim of the Doctoral study.....	39
2. Circulating extracellular vesicles can vehicle signals from the periphery to the male germline	40
2.1 Abstract.....	41
2.2 Introduction	44
2.3 Results	46
2.3.1 Circulating EVs have distinct RNAs, lipids and metabolites content.	46
2.3.2 ELS persistently modifies the composition of circulating EVs.	49
2.3.3. Chronic injections of circulating EVs can alter metabolic state of naïve mice.	52
2.3.4 Circulating EVs can signal to germ cells in males.	55
2.3.5 Exposure to EVs can alter metabolism intergenerationally.	58
2.3.6 EV injections give rise to developmental changes in early embryos.	61
2.4 Discussion	64
2.5 Materials and Methods.....	67
2.5.1 Mice	67
2.5.2 ELS.....	67
2.5.3 Blood collection	68
2.5.4 Nanoparticle tracking analysis.....	68
2.5.5 Characterization of EVs by TEM	68
2.5.6 Isolations of plasma EVs	69
2.5.7 Western blotting.....	69
2.5.8 Intravenous injections of EVs	69
2.5.9 Preparation of sperm samples.....	70
2.5.10 In vitro fertilization and collection of embryos.....	70
2.5.11 Metabolic testing.....	71

2.5.12 Metabolomics	71
2.5.13 Lipidomics.....	72
2.5.14 RNA extraction	74
2.5.15 Preparation of sequencing libraries	74
2.5.16 Bioinformatic data analyses.....	75
2.6 Acknowledgments.....	76
2.7 Authors contribution.....	76
2.8 Conflict of interest.....	77
2.9 Supplementary Figures	77
3. Early life stress affects the miRNA cargo of epididymal extracellular vesicles in mouse	87
3.1 Graphical Abstract.....	89
3.2 Abstract.....	89
3.3 Introduction	90
3.4 Results	91
3.4.1 Isolation of cauda epididymosomes confirmed by several methods	91
3.4.2 The number and size of epididymosomes in adult males are not altered by postnatal stress	92
3.4.3 miRNAs are persistently altered by postnatal stress in cauda epididymosomes	94
3.4.4 mRNA targets of miRNAs from cauda epididymosomes are altered by postnatal stress in sperm and in zygotes	97
3.5 Discussions	99
3.6 Materials and Methods.....	101
3.6.1 Animals.....	101
3.6.2 MSUS	101
3.6.3 Tissue collection	102
3.6.4 Electron microscopy images.....	102
3.6.5 Epididymosomes isolation by ultracentrifugation.....	102
3.6.6 Immunoblotting	102
3.6.7 Nanoparticle tracking analysis.....	103
3.6.8 RNA isolation and epididymosomes profiling	103
3.6.9 Preparation and sequencing of sRNA-seq libraries from epididymosomes	103
3.6.10 RT-qPCR.....	104
3.6.11 Cholesterol measurements.....	104
3.6.12 Bioinformatics data analysis	104
3.7 Data availability	105
3.8 Acknowledgements.....	105
3.9 Authors contributions.....	106
3.10 Conflict of interest.....	106
3.11 Supplementary Figures	106
4. Conclusions and Outlook	113
4.1 Summary of research questions and major findings	113
4.2 Novelty of the research.....	115
4.3 Challenges and limitations.....	116
4.4 Recommendations for implementation of future research	119
4.5 Concluding summary.....	122

References.....	123
5. Annex - Omnisperm: Versatile analyses of sperm and offspring production from a single mouse male	139
5.1 Introduction	140
5.2 Results	142
5.2.1 OmniSperm to collect increased numbers of sperm cells for multi-layered analyses	142
5.2.2 Isolation of mature sperm cells confirmed by several methods.....	143
5.2.3 Association of sperm DNAm with RNA expression in sperm and embryos.....	143
5.3 Discussion	144
5.3 Methods.....	153
5.4 Conflict of interest.....	160
5.5 Author contributions.....	160
5.6 Acknowledgements.....	160
5.7 References	160
Acknowledgements	164
Curriculum Vitae	167

1. Introduction

1.1 Epigenetic inheritance

Epigenetics refers to modifications in gene expression patterns, without direct alterations to the DNA sequence. In Greek, “epi” means “on” or “above”, and therefore, epigenetic mechanisms concern the factors that surround the genetic code. Epigenetic mechanisms include DNA methylation (DNAm), histone post-translational modifications (PTMs), noncoding RNAs (ncRNAs) and histone variants. Those factors are important in healthy cell, tissue and organismal development, since they guide different cellular functions, such as cell differentiation and response to outside stimuli. Epigenetic regulation of gene expression during development is governed through spatial and temporal factors, and determines cellular fate. Therefore, through epigenetic mechanisms, cells destined to be part of the central nervous system will turn off gene expression patterns corresponding to for example muscle cells and vice-versa. Not only can the various epigenetic mechanisms define cellular fate, but they can also be altered due to a diverse range of environmental exposures, such as stress, toxicants, and changes in diet. A classic example of epigenetic gene regulation is cold-induced suppression of genes that control flowering in plants, which governs gene expression at a temperature-sensitive locus. Patterns of epigenetic response to environmental stimuli vary among different organisms, tissues within the same organism, and among the cells within a tissue, and some information can even be carried over to the unexposed offspring intergenerationally or transgenerationally.

Scientists have entertained the idea of passage of acquired traits due to changes in the environmental conditions for centuries. However, only in the 1900s, reports of such phenomenon emerged. A major criticism against potential inheritance of epigenetic marks in the early days was the reprogramming of epigenetic states during embryogenesis, when most acquired epigenetic marks are erased. However, understanding germ cell and early embryonic development shed light on many possibilities of skipping this challenge. In addition, the progress in assisted reproductive techniques helped dissecting the contribution of germ cells and other factors present at fertilization in understanding the offspring phenotype. Today, indisputable evidence persists in support of epigenetic inheritance and the notion has been demonstrated from plants, *C.elegans* to rodents and humans. It is important to

keep in mind the distinction of intergenerational and transgenerational epigenetic inheritance, where the germ cells that give rise to the offspring in question are directly exposed in the former and unexposed in the latter.

Although not classified at the moment of their discovery as an epigenetic mechanism, the first reports of epigenetic inheritance were in plants in 1956, observed by Brink et al. Almost 40 years later, following the discovery of RNA interference in *C.elegans*, Mello and Fire demonstrated that, injections of dsRNA into germ cells of *C.elegans* led to silencing of genes with homologous sequences to the dsRNA in injected animals and their progeny, up to 5 generations. Interestingly, the authors also showed that dsRNA injections into somatic cells of *C.elegans* can transfer the silenced phenotype of the target gene to the offspring.

In mammals, the first studies involving epigenetic inheritance were in the late 1990s through the study of the agouti fur color in mice, which was dependent on metastable epialleles that maintained their methylation status throughout developmental epigenetic reprogramming (Morgan et al., 1999, Rakyan et al. 2003). Later on, Anway et al. demonstrated that exposure to endocrine disruptor vinclozolin in rats caused phenotypic alterations up to several generations of unexposed offspring. At the same time, emerging studies in humans reported smoking and nutritional changes to lead to metabolic alterations in the next generation (Kaati et al. 2002, Pembrey et al. 2006).

Due to the presence of comprehensive research in mice as an animal model and the studies included in this thesis on male mice, the following chapters will concentrate the attention on the mouse as an animal model, with focus on the male males. When relevant, information on humans and other model organisms will be briefly covered.

1.2 Vectors of epigenetic inheritance

In order to affect the next generation, some marks need to be established in male germ cells and delivered to the oocyte upon fertilization. These marks also need to escape embryonic reprogramming and be relevant in terms of their amount, in comparison to the information that comes from the oocyte. Regardless of the fact that sperm is known to be around 2000 times smaller than the oocyte, the ability of sperm-contributed epigenetic information to influentially pass to the next generation, altering

the phenotype of the unexposed offspring has been demonstrated by a number of studies.

Although initial focus on the vectors of epigenetic inheritance was on DNA methylation, subsequent studies explored the significant role of histone PTMs and noncoding RNA. In this section, we will cover major studies that cover these 3 vectors.

RNAs

Despite the initial belief that sperm cells are transcriptionally silent, a few studies displayed contradicting data to this notion (Gur et al. 2006, Ren et al. 2017). Regardless of the transcriptional status of sperm, some RNAs are endogenously expressed in sperm, while other RNAs, such as small noncoding RNAs (sncRNAs), can be taken up through uptake of vesicles. Throughout male germ cell differentiation and maturation, there are many sources that could deliver sncRNAs to sperm - among those are extracellular vesicles (EVs) in the testis, epididymis and seminal fluid. Some of these sncRNAs are susceptible to environmental insults, such as changes in the diet, exposure to stress and exposure to toxicants. In this section, we briefly cover the most prominent concepts in understanding the role of germ cell RNAs in epigenetic inheritance.

Several studies preceded the boom of RNA-related epigenetic inheritance research. First, Krawetz and a few others demonstrated that male germ cell RNAs could be delivered to the oocyte upon fertilization (Krawetz et al. 2005, Ostermeier 2004). A few years later, Rassoulzadegan et al. showed that injections of sperm RNA from transgenic animals into fertilized oocytes could alter offspring phenotype. Almost a decade following these experiments, several research groups revealed that sperm RNA repertoire is susceptible to environmental exposures, such as stress and diet (Fullston et al. 2013, Gapp et al. 2014, Rodgers et al. 2015, Grandjean et al. 2015). In addition, they demonstrated that sperm RNA injections from exposed animals into naïve zygotes or *in vitro* fertilizations with sperm of the exposed males could transmit some of the behavioral and metabolic phenotype to the offspring. Most of these initial studies concentrated on a type of sncRNAs – the microRNAs (miRNAs). Involvement of miRNAs has been later explored in relation to stress and several other models of environmental insults.

tRNA-derived fragments (tRFs), the most abundant sncRNA type in sperm, have gained importance as another sncRNA type in sperm with potential role epigenetic inheritance. Involvement of tRFs in father to offspring transmission was first

shown by Kiani et al in 2013. In this study, tRF methylation by RNA methyltransferase Dnmt2 was demonstrated as a mechanism of Kit paramutation model. To discard the contribution of scnRNAs other than tRFs in paternal high-fat diet transmission, Chen et al. size-selected sperm total RNA to enrich for tRFs and demonstrated, that indeed the tRFs and not the miRNAs of sperm were responsible for the phenotype observed in the offspring (Chen et al. 2016). Sharma et al. further extended understanding the role of sperm tRFs by looking at the embryonic development in low-protein diet animal model (Sharma et al. 2016). They demonstrated that the transmission of the low-protein induced phenotype to the offspring could partially be due to a specific sperm tRF, which regulates a group of genes that are targets of endogenous retroviral element murine endogenous retrovirus-L (MERVL). In addition to tRFs and microRNAs, other sperm RNAs such as piwi-interacting RNAs (piRNAs) and circular RNAs (circRNAs) have been linked to paternal transmission of environmental changes to offspring (Rodgers et al. 2015, Gapp et al. 2020).

DNAme

DNAme is a process by which gene expression is altered, due to the attachment of a methyl group to the 5th position of a cytosine residue (5mC). Although DNA methylation is an important mechanism to keep the cellular identity during division, it is also subjected to massive erasure and re-establishment after fertilization. However, certain imprinted regions, such as intracisternal A-particle (IAP) and long interspersed nuclear elements (LINE1) retrotransposons escape this process.

Differentially methylated regions (DMRs) were reported in the sperm of rodents exposed to endocrine disruptors, plastics or alcohol during early embryonic days and were found in progeny (Bohacek et al. 2015). Vincozolin treatment during embryonic days 8 through 14 induced several DMRs in primordial germ cells, spermatogonia, and sperm. These DMRs were still detected in sperm several generations later (Bohacek et al. 2015). Postnatal exposure to environmental insults, such as early life stress, also induces differential methylation in sperm of the exposed males and their offspring. In mice fed high-fat-diet from weeks 9 to 12, DNA methylation pattern is drastically altered in their sperm and in the following 3 generations. Due to its heritability during cell division and environmentally-induced adaptability, DNAme is one of the most characterized mechanisms of epigenetic inheritance in mammals.

Histone modifications

To facilitate paternal genome re-organization and packaging of chromatin to the sperm nuclei, the mammalian sperm undergoes histone-to-protamine transition during spermiogenesis. This process leads to a significant loss of histones in male germ cells, hence most mature sperm carries only around 1-5% histones. The most common histone PTMs include phosphorylation, acetylation, methylation, and ubiquitylation, although mature germ cells lack some PTMs such as acetylation (Bohacek et al. 2015). Histone modifications are yet another mechanism by which environmental exposures were shown to alter gene expression patterns and phenotype in the offspring.

Various environmental exposures, such as cocaine-treatment, unpredictable traumatic experience, and low-protein diet have shown to alter histone PTMs in sperm. More recently, Yoshida et al. showed the direct involvement of a reduction in H3K9me2 in testicular germ cells in males subjected to low-protein diet to the RNA expression in spermatozoa and metabolic reprogramming of the unexposed offspring (Yoshida et al. 2020). The direct effect of differential sperm histone PTMs has also been demonstrated by Siklenka et al. In addition to their direct involvement, the ability of histone PTMs to modulate DNA methylation is a secondary mechanism by which histone PTMs might relay information of environmental exposures to the next generation.

1.3 Germ cell development and supporting structures in males

The earliest precursors of functional gametes in mice are the primordial germ cells (PGCs) (Richardson et al. 2010, Saitou et al. 2012). After their initial discovery and characterization by Ginsburg in the 1990s (Ginsburg et al. 1990), the current knowledge has expanded and identified the subsequent evolution of trajectories occurring during mouse germline development (Richardson et al. 2010, Saitou et al. 2012). At embryonic day 7.25 (E7.25), the primary PGCs are formed within the endoderm of the yolk sac, they then migrate and populate the gonadal ridges by embryonic day 10.5 (E10.5). PGCs that populated the gonadal ridges are referred to as gonocytes. Gonocytes stay in mitotic arrest during the whole time of embryonic development, while other developmental processes occur. Only at postnatal day 1-2, the gonocytes exit the mitotic arrest. They then migrate to the basement membrane of the seminiferous cord and continue spermatogenesis as spermatogonial cells.

Male germ cell development in the testis

Testicular development brings the spermatogonial cells to the basement membrane of the seminiferous tubules of the testis (Oatley et al. 2006). They then develop into elongated spermatids and are released into the lumen of the seminiferous tubules. In rodents, this process lasts around 35 to 37 days. In order to have a lifetime pool of spermatogenic stem cells, the spermatogonial cells first divide continuously and form the pool of spermatogonia stem cells (SCCs) in the testis. For the subsequent differentiation, a part of the cells in this pool lose their stem cell potential and become an A-type and then a B-type spermatogonia. By the end of postnatal day 10, we have the first preleptotene spermatocytes, which are still diploid. After meiosis I, the preleptotene diploid spermatocytes undergo several divisions and give rise to haploid spermatocytes by the end of postnatal day 14. During meiosis II, spermatocytes further differentiate into round spermatids. During the last stage of testicular development, many important processes occur in round spermatids, which transform round spermatids into elongated spermatids. One of these processes is histone to protamine transitions, following which only 5% of initial histones remain. The elongated spermatids are then released into the lumen of seminiferous tubules to conclude their maturation in the epididymal tract. The release of the mature spermatids into the lumen of seminiferous tubules is directed by Sertoli cells. This process, also known as spermiation, lasts several days and includes processes such as remodeling of the spermatid cytoplasm and head, and removal of attachment structures to finalize the de-attachment process from Sertoli cells (O'Donnell et al. 2011).

In addition to the above-mentioned cells in the apical compartment of the seminiferous tubules, the outside or the basal compartment of the tubules is occupied by other cells, such as Sertoli cells, Leydig cells, testicular resident macrophages and vasculature-associated cells. All these cells play an important role in germ cell protection, differentiation and maturation. Sertoli cells, the only cells that have physical contact to the differentiating germ cells, hold the blood-testis barrier and serve as the nursing cells to the developing germ cells. They do so by several mechanisms, such as providing nutrients, removing cellular waste and forming the protective barrier. Leydig cells produce testosterone, which is the governing hormone for testicular germ cell differentiation and maturation, whereas resident macrophages play a role in spermatogonia cell differentiation and in immunological protection.

Epididymal transit of germ cells and vas deferens

Following the release into the lumen of seminiferous tubules in the testis, the elongated spermatids are transported through the testicular fluid movement to the rete testis and several ductuli, which form the head of the epididymis. In mice, the epididymal transit lasts around 5-7 days, which follows the storage period of ejaculation-ready spermatozoa. The epididymis itself consists of 3 main segments - caput, corpus, and cauda, and is then further extended and connected to form the vas deferens. During the transit through the epididymis, spermatozoa undergoes alterations in membrane fluidity, protein and small RNA composition, lipid content as well as some changes to its net surface charge. Additionally, the concentration of spermatozoa drastically increases during the epididymal transit. Although self-modifications of spermatozoa also occur, many of these modifications are known to be driven by secretion or absorption of molecules by epididymal epithelial cells. Importantly, abnormal or old spermatozoa are partially reabsorbed by epididymal epithelial cells in cauda, and overall cycling period and quality of germ cells is maintained through spontaneous ejaculations from the vas deferens, where the sperm is also stored for future ejaculation (Durairajanayagam et al. 2015).

1.4 Blood-organ barriers to the germ cells in males

The ways by which somatic cells in the body could communicate to germ cells regarding environmental insults could be broadly divided into the group of direct and indirect mechanisms. Indirect mechanisms involve the relay of information to male germ cells through secondary paths, such as modifying gene expression patterns in the somatic cells surrounding the germ cells; whereas direct mechanisms involve information transfer from the somatic cells in the periphery to the germ cells, in the forms of circulating, lymphatic and other factors. There are several challenges when studying the possibility of direct soma-to-germline communication, due to the existing blood-organ barriers and protection of the developing germ cells from the outside environment. In the following section, we will describe some of these challenges in detail and cover the recent developments that address them.

Almost 100 years after Weismann's theory on the existence of a barrier between somatic cells and germ cells, intravenous dye injection experiments showed the absence of dye in the testis and brain, indicating resistance of the blood-organ barriers in the testis and brain to the dye in the bloodstream (Cheng et al. 2012). At

the same time, experiments conducted by Kormano and others demonstrated the ability of dyes to penetrate into the lumen of seminiferous tubules in pre-pubertal but not adult rats (Cheng et al. 2012). This phenomenon was later linked to the initiation of blood-testis-barrier (BTB) formation by postnatal day 15 and completion by postnatal day 21 in rats. Today, blood-organ barriers are known to not only exist in the testis, but also in the brain (blood-brain-barrier or BBB), the epididymis (blood-epididymal-barrier or BEB) and the thymus (blood-thymus-barrier), among others.

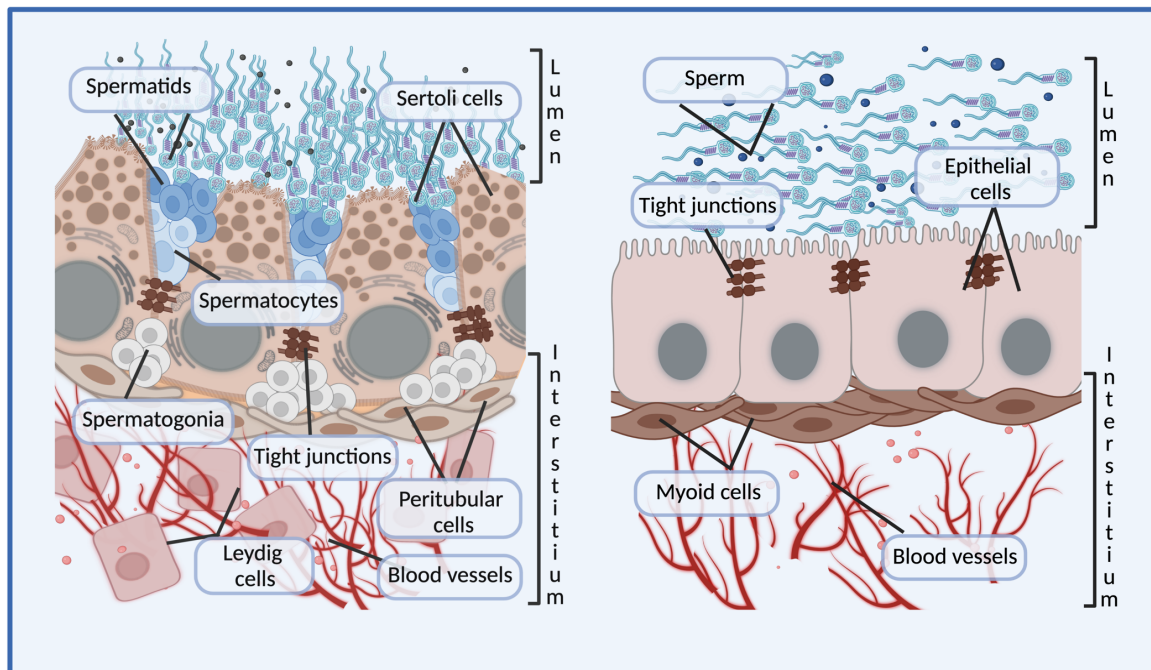


Figure 1-1. Components of blood-testis and blood-epididymis barriers. The blood-testis-barrier is created by Sertoli cells held together with tight junctions and peritubular cells (left). Interstitial compartment of blood-testis-barrier contains spermatogonia stem cells, Leydig cells and blood vessels, whereas the luminal compartment contains spermatocytes and spermatids. The blood-epididymis-barrier consists of epithelial cells connected by tight junctions and myoid cells (right). The sperm cells swim in the luminal compartment, and are separated from the blood vessels in interstitium by the blood-epididymal-barrier. Created with BioRender.com.

The BTB separates the lumen of seminiferous tubules from the interstitium by tight junctions (TJs) (Cheng et al. 2012, Mital et al. 2011). It allows filtering of cells, large molecules, proteins, and lipids, while being permeable to small molecules such as some hormones and metabolites. The interstitium contains the myoid cells, immune cells (T cells and macrophages), Leydig cells, the blood vessels, germ stem cells, and germ cells at their early stages of differentiation (**Figure 1-1**). These germ cells include spermatogonia stem cells, together with A and B type spermatogonia. The myoid cells

along the basal membrane serve as the first line of defense in the BTB, preventing around 85% of weakly charged molecules from passing. The main barrier is built by the Sertoli cell TJs, although additional components such as ectoplasmic specializations, desmosomes, hemidesmosomes, and gap junctions play a role as well.

The structure of the BEB is similar to that of the BTB, with epididymal epithelial cell TJs creating the barrier and also dividing the space into luminal compartment with developing germ cells, interstitium with blood vessels and myoid cells (**Figure 1-1**). The main difference between the BTB and BEB are the location of the TJs, which are located basally in BTB and apically in BEB. Apical location is also common in other epithelial cell TJs (Mital et al. 2011).

In addition to creating anatomical and physiological barriers, BTB and BEB comprise an immunological barrier (Cheng et al. 2012, Mital et al. 2011). Xenogenic tissues transplanted into the interstitium of the testis could persist longer compared to other organs, such as liver and kidney (Mital et al. 2011). This is attributed to the presence of immunoglobulins, T cells, and macrophages in the testicular interstitium and involvement of locally-produced immunosuppressive factors (Mital et al. 2011). BEB has shown to have a lower potential as an immunological barrier. While immune cells and immunoglobulin were found within the epididymal epithelial cells, xenogeneic tissue transplants did not show significantly higher survival rate within the epididymal interstitium compared to other tissues (Cheng et al. 2012, Mital et al. 2011).

When it comes to the strength of different blood-organ barriers measured by electrical resistance, BBB performs as the tightest barrier, followed by barriers formed within endothelial cells in the periphery, and then BTB and BEB (Cheng et al. 2012). BBB is unique in that it solely consists of TJs between capillary endothelial cells. Irrespective of the strength of these barriers, the field has accumulating evidence that, even the strongest blood-organs barrier as BBB is permeable to some circulating factors and is affected by disease conditions. For example, an emerging number of studies in the recent years have shown that circulating EVs can cross BBB and deliver RNA and protein, informing neuronal cells of disease states (Dardet et al. 2022, Ramos-Zaldívar et al. 2022). If factors from the circulation are capable of crossing the tightest of blood-organs barriers such as BBB, it is no surprise that circulating factors could potentially cross more permeable blood-organ barriers, such as BTB and BEB. Indeed, fluorescently-labeled testicular EVs injected into the interstitial space

were found both in the interstitium and in the lumen of seminiferous tubules (Choy et al. 2022).

1.5 Developmental processes affected by early life exposures

The impact of environmental exposures on the germline and the next generation depends on a variety of factors, such as the developmental timing of exposures (early life, youth, adulthood), dosage and length of exposures, waiting time post-exposures, type of exposures (stress, toxicants, diet), and other factors. Studies where all parameters except the waiting time post-exposure is shifted show differential impact on germ cells. The effect of the developmental timing and waiting timing are significant, since an organism undergoes a diverse set of changes throughout its lifespan.

Environmental insults in early postnatal life are detrimental, since many tissues and their cells are undergoing developmental initiation processes and establish the tissue-specific niche during this period. These include the establishment of a pool of spermatogonia stem cells in the testis (by early postnatal day 15), the process of creating fully divided and differentiated Sertoli cells in the testis (by early postnatal day 15), the accelerated adipogenesis process (early postnatally until weaning), the differentiation and expansion of epididymal epithelial cells (early postnatally until puberty), developmental processes in central nervous system, including many other processes.

Developmental processes that happen early postnatally in germ cells are covered elsewhere (Chapter 1.3). Therefore, we will next describe some of the other processes that can also be affected by early life exposures.

Sertoli cells, the somatic cells of the testis responsible for nurturing and supporting male germ cells through spermatogenesis, are known to fully differentiate and establish a pool of cells that are present through the lifespan of a mouse by early postnatal day 21. After this time point, the cells in this pool growth and performs their supportive functions, without altering their number. Therefore, if the establishment and the differentiation of this early Sertoli pool is affected by an environmental exposure, it could potentially be carried into adulthood.

Adipogenesis starts during the last week of gestation and accelerates significantly postnatally until weaning. Thus, adipocyte stem cells are especially sensitive to experiences of early postnatal life. The developmental and metabolic

processes that program adipocyte number are set in early development, increasing the adipocyte cell number until puberty and leaving the total amount and size of adipocytes stable after puberty, with a turnover rate of 10-20%. Many studies observe metabolic alterations in the exposed and in some cases unexposed offspring regardless of exposure type. Thus, the niche establishment of metabolic organs such as the adipose tissue could be affected by environmental exposures. This is important, since adipose tissue is suggested to be the major source of circulating miRNAs, with the ability to regulate gene expression in other tissues (Bond et al. 2022).

The epididymal epithelial cells are also undergoing differentiation and expansion between early postnatal days and puberty (Robaire et al. 2006). Completing this expansion, the number of epididymal epithelial cells is constant in adulthood, possibly carrying comparable information to sperm throughout adulthood. The postnatal development and differentiation of the epididymal epithelial cells, heavily but not solely, depends on testicular signals. Since environmental exposures such as stress affect the coupling of the hypothalamic-pituitary-adrenal (HPA) and the hypothalamic-pituitary-gonadal (HPG) axes, stress-related decrease in steroidogenesis can have profound implications on the differentiation and expansion of the epididymal cells early postnatally, thus affecting the secretion profile of adult epididymal epithelial cells. This is significant, since male germ cells finalize their maturation through the transit in the epididymis, where information exchange between germ cells and epididymal cells take place in terms of EVs, lipids, and proteins.

Another important developmental process relevant to male reproduction is the formation of the BTB by postnatal day 21 in rodents. Some toxicants, such as cadmium or bisphenol A (BPA), can disrupt the formation of BTB. Cadmium disrupts the TJs and other junctions of the BTB. It was shown in rodents that once the BTB barrier is disrupted by cadmium, there is no more spermatogenesis, even if the spermatogonia stem cell pool is revived after several weeks and is present throughout the lifetime. This was partially explained by the oxidative stress of Sertoli cells caused by the cadmium exposure. Cadmium-injected animals have the required pool of spermatogonia cells, but do not have the essential differentiation and support signals as well as the protection barrier that is provided by the BTB. Interestingly, in humans, 80% of clinically infertile men reported long-term exposure to some type of toxicant. This accentuates the necessity of functional BTB development early in development.

1.6 Evidence of soma-to-germline communication of environmental exposures

In recent years, many studies supported the evidence of altered information in male germ cells due to various environmental insults such as stress, changes in diet and toxicant exposure (Bohacek et al. 2015, Conine et al. 2022). Still, there has been only a few studies that addressed soma-to-germline transmission of information. Therefore, the possibility of soma-to-germ cell information transfer, either directly to germ cells or indirectly through somatic cells in male reproductive organs, either in the form of vesicles, RNA, protein, lipids, metabolites or other factors from the circulation, has evolved into an exciting research area with a few progressive studies in the recent years. A number of different experimental models, such as a Cre-dependent systems, human melanoma cell xenografts, and adeno-associated viral (AAV) gene delivery systems, were used to address the possibility of soma-to-germline information transfer and to understand its underlying mechanisms.

One of the pioneering mechanistic studies to address the possibility of soma-to-germline DNA- or RNA-mediated information transfer was performed in mice (Cossetti et al. 2014). The researchers xenografted human melanoma cells expressing enhanced green fluorescent protein (EGFP) plasmids and detected the presence of EGFP-specific RNA 45 days in circulation and in sperm, but not in epididymis. Interestingly, they observed that circulating EGFP-specific RNA was co-purified in the EV-enriched blood fraction. The authors therefore speculated on the ability of xenografted melanoma cells to secrete EVs that carry the EGFP-RNA to the germ cells. However, they did not demonstrate EVs crossing the BEB or being uptaken by the germ cells *in vitro*.

O'Brien et al. brought another likely communication medium of somatic cells with germ cells - the lymph nodes (O'Brien et al. 2020). Lymph nodes are known to be present in the testicular interstitium together with blood vessels, Leydig, and immune cells. By stereotactically injecting AAV virus expressing human pre-miR-491 into one striatal hemisphere in mice, they were able to detect expression of the human pre-miR in the epididymis, lymph nodes, and striatum, but not in blood or liver, 2 weeks after injections. Not only the directly exposed males, but also 30% and 50% of the embryos, obtained by natural breeding from these males 8 weeks and 16 weeks following injections, carried detectable levels of the human pre-miR-491. Contrary to the previous studies in melanoma cells, the researchers did not detect presence of pre-

miR-491 in the vesicular preparations from blood. Since the lymph nodes in the testes are located outside the BTB, it is still to be addressed, how the foreign RNA entered the apical interstitium.

The aforementioned studies concentrated on tackling the possibility of soma-to-germline transfer of information through exposure to exogenous couriers. On the contrary, Yoshida and colleagues analyzed the effect of a natural stressor, such as low-protein diet and examined the effect of this alteration on testicular germ cells in mice (Yoshida et al. 2020). Briefly, low-protein diet proved to phosphorylate the activating transcription factor-7 (ATF7), which in its inactive state is bound to promoters of around 2300 genes. Activation of ATF7 led to its release from the promoter regions of its target genes and to a decrease of H3K9 dimethylation on these genes. This resulted in an increase of several tRNAs in testicular germ cells. The authors did not directly validate the mechanistics of how the increased tRNAs in testicular germ cells altered information passed by mature germ cells to the offspring. However, there are several prior studies from other groups that have demonstrated the relevance of some of these tRNAs, such as tRNA-Gly-GCC, tRNA-Glu-CTC and tRNA-His-GTG, in inheritance of paternal low-protein phenotype (Conine et al. 2022).

More recently, circulating factors, such as lipid-derived metabolites emerged as a novel potential mechanism of soma-to-germline information transfer. van Steenwyk et al. used a mouse model of early life stress to study the role of circulating metabolites in epigenetic inheritance of environmental exposures (van Steenwyk et al. 2020). The study found that early life stress alters the repertoire of circulating metabolites in the exposed adult mice and their unexposed offspring. The transmission of the metabolic alterations is further linked to the peroxisome proliferator-activated receptor (PPAR) pathway. Both serum injections from stressed to naïve animals as well as pharmacological activation of PPAR *in vivo* reveal comparable metabolic phenotypes. Strikingly, the researchers observe similar changes in circulating metabolites in a human cohort of children exposed to early life adversity.

Most recently, Cre expression in the central nervous system detected Cre-dependent reporter gene expression in the epididymis, bringing more support to the direct soma-to-germline contact (Rinaldi et al. 2022). The authors were able to also demonstrate a similar event by expressing Cre in adipose tissue. Although the researchers did not fully dissect which mode of transmission from periphery to germ cells was involved, they have demonstrated the potential involvement of serum factors,

by performing Parabiosis to join the circulatory systems of 2 animals. Additionally, this study highlighted the absence of any “sink” tissues that take up the majority of circulating factors, but rather detects Cre-dependent gene expression in many tissues.

In summary, these studies support the possibility of direct information exchange between the soma and germline and propose several possible mechanisms, that need to be explored further, emphasizing on such potential of factors in blood, such as EVs.

1.7 Broad classification of circulating factors

Blood is filled with various circulating factors, which can be divided into three larger groups - cellular components, circulating particles, and biomolecules. Each of these factors carry a myriad of components within themselves.

Cellular components of blood.

Cellular components of blood involve the 4 major immune cell types, many of which have cellular subtypes of their own (Dean et al. 2005). These are erythrocytes, leukocytes, monocytes, and platelets. Erythrocytes and leukocytes are both derived from the hematopoietic stem cells in the bone marrow, but perform entirely different functions. Erythrocytes carry out oxygen transport across the body, whereas leukocytes defend the organism from pathogens as a part of adaptive immunity. Monocytes are another immune cell type that is involved in the fight against foreign pathogens. By producing reactive oxygen species that penetrate bacterial walls, they destroy foreign materials. As the main saviors of damaged blood vessels, platelets attach to the damaged vascular walls and create a clot through their interaction with fibrin to prevent further damage.

Other components of blood.

In addition to the cellular components, blood is packed with complex factors that allow its multi-functional capacity. These components include various types of lipoproteins (chylomicrons, very-low-density lipoproteins (VLDLs), intermediate-density lipoproteins (IDLs), low-density lipoproteins (LDLs), high-density lipoproteins (HDLs)), EVs and viruses. Whereas biomolecules such as metabolites, proteins and protein aggregates, lipids, cytokines, hormones, growth factors, RNAs, ions, and other components constitute another important component of the circulation.

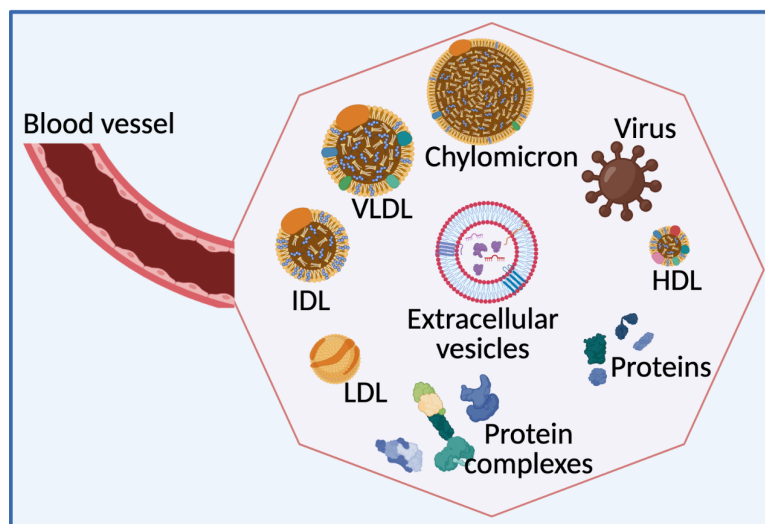


Figure 1- 2. Overview of non-cellular components in blood.

In addition to cellular components, blood consists of other circulating components that vary in size. These include lipoproteins such as HDL, LDL, IDL, VLDL, chylomicrons, circulating extracellular vesicles, protein complexes, and viruses. Created with *BioRender.com*.

1.8 Changes in circulating factors due to environmental exposures

Various environmental exposures lead to alterations in not only the cellular, but also non-cellular components of the circulation in both rodents and humans. In the following paragraph, we will highlight some of the data in different animal models as well as clinical studies in humans that support that environmental exposures alter non-cellular blood factors.

In humans, exposure to 23 different persistent organic pollutants increased circulating total cholesterol and LDL-cholesterol levels long term (Penell et al. 2014). Exposure to sleep deprivation in humans significantly decreased levels of choline plasmogens and increased triglycerides and phosphatidylcholines in blood (Chua et al. 2015). Such lipid changes indicate that continuous sleep deprivation alters the metabolic status of the organism, causing changes in metabolic balance. Circulating lipids are also affected by temperature, since both cold and heat exposure in mice and humans have shown to significantly impact brown adipose function. This in turn leads to changes in blood lipids (Coolbaugh et al. 2019, Yamamoto et al. 2003). Dietary insults, such as high-fat- and low-protein diets, some of which are used to model cardiovascular diseases, extensively alter the lipidomic profile of an organism. Major mechanisms of significant lipid changes in models of environmental exposures are traced to liver, brown adipose tissue, and kidneys (Jain et al. 2022). Together with lipids, emerging evidence suggests that changes in circulating metabolites cause

metabolic perturbations in mice exposed to early life stress and their offspring (van Steenwyk et al. 2020).

In addition to lipid constituents of blood, environmental exposures such as obesity or differing caloric intakes, are also associated with differential protein expression. Analyses of several publicly available datasets in humans and experimental models in mice showed that toxicants, such as BPA, air pollutants, gamma and X-ray irradiation as well as heat exposure create changes in circulating proteins (Trigg et al. 2021, Rokad et al. 2019, Samanta et al. 2018, Jelonek et al. 2016).

Last, but not least, numerous changes in circulating sncRNAs have been reported. Dietary differences in humans result in a specific circulating microRNA profile (Ferrero et al. 2020). For example, obese versus healthy overweight humans display distinct changes in several microRNAs, such as miR-139, let-7c, and miR-432 (Giardina et al. 2019). Blood microRNAs are also involved in stress response (Guelfi et al. 2022, Leung et al. 2015). Changes in circulating EV number, EV RNAs and EV proteins due to obesity and stress is not uncommon (Driedonks et al. 2018, Castaño et al. 2018, Abey et al. 2017). For example, obese mice carried several altered EV microRNAs that were modulating glucose and lipid metabolism (Castaño et al. 2018). Other circulating EV-associated sncRNAs, such as Y-RNAs and tRNAs have also been associated with environmental exposures like stress-related immune response and dietary modifications (Driedonks et al. 2018, Weng et al. 2022).

1.9 Extracellular vesicles

EVs are small particles delineated by a lipid bilayer, released into extracellular space by many cell types, are evolutionary conserved from bacteria and plants to humans. EVs carry active molecules such as proteins, nucleic acids, metabolites, and lipids. Depending on the mode of secretion, EVs could be classified into 3 major categories: small EVs of 30-200nm, microvesicles (MVs) of 100-1000nm, and apoptotic bodies of 100nm-5 μ m. Small EVs are secreted through fusion of multivesicular bodies (MVBs) with parental cell membrane and MVs are produced by parental cell membrane blebbing, whereas apoptotic bodies are generated by dying cells.

EVs were first mentioned in 1946 by Chargaff and West, who described EVs as “breakdown products of the blood corpuscles”, when they studied thromboplastin and

platelets (Bazzan et al. 2021). This observation was further enriched in the 1970s by Wolf and Aaronson, who contributed to further descriptions of EVs using EM. They showed that EVs originate from larger cellular organelles, which are not known as MVBs and that they carry lipidic structures from the cells of origin. Additional studies in the late 1970s and 1980s further characterized EVs from different cell types and identified the heterogeneity of EVs in size as well as in mode of secretion. Regardless of their discovery and characterization, interest in EVs did not arise again until the mid 1990s, due to the commonly accepted idea that EVs were either a cell's way of disposing unneeded material or were artifacts of the plasma membrane fragments. The newly emerging interest in EVs arose following a series of experiments in the field of immunology, in which the role of EVs in many cell types such as platelets, lymphocytes, and dendritic cells was shown. This was followed by various other studies that demonstrated the presence of EVs in different cell types across the body, such as epithelial cells, neurons, and adipocytes (Bazzan et al. 2021). With advancements in isolation methods, even today previously unknown sources of EVs, such as testicular cells, are being described and added to the long list of EV secreting cell or tissue types.

Cargo of extracellular vesicles

Regardless of cell or tissue origin, most EVs have shown to carry a number of components such as RNAs, proteins, lipids, and metabolites. Due to alterations in external stimuli such as changes in hormones, psychological or metabolic state of an organism, the secreted EV number and content may vary.

Extracellular vesicle RNA

RNAs, particularly sncRNAs, are EV components that drew the highest interest in deciphering functions of EVs since their discovery. The most prominent EV sncRNAs are microRNAs (miRNAs), yet other RNAs such as long non-coding (lncRNAs), transfer RNAs (tRNAs), ribosomal RNAs (rRNAs), small nucleolar (snoRNAs), mitochondrial RNAs (mtRNAs), PIWI-interacting RNAs (piRNAs), Y RNAs and vault RNAs (vtRNAs), are also found (O'Brien et al. 2020). A number of studies support the «fluid state» of the EV cargo. This means that the RNA constituents of EVs only partially reflect the physiological state of the secreting cell or tissue. Involvement of EV RNAs in various biological and pathological processes has been demonstrated in many cell types such as adipocytes, cardiomyocytes, neuroprecursor cells, and various types of immune and cancer cells (O'Brien et al. 2020).

One of the major challenges in associating specific small RNAs with EV functionality among the studies is the difference in EV isolation methods, which greatly impacts the RNA biotype profiled in a given batch of EVs. Additionally, due to the variability in isolation methods, the proportion of other contaminating components of a biofluid would vary. Lastly, the proportion of the cargo to EV number should be considered, when interpreting mechanistic roles of EV small RNAs. A targeted EV isolation from serum with depletion of lipoproteins showed that around $5.69\% \pm 3.74\%$ (SD) of serum EVs, which equals to every 1 in 24 EVs, contain on average 1 miRNA molecule, signifying the majority of EVs carrying no or very few miRNA molecules (Otahal et al. 2021).

Extracellular vesicle protein

In addition to small RNAs, EV proteins are widely characterized. Together with the more common EV proteins (tetraspanin family of proteins such as CD63, CD81 and CD9), other proteins in EVs of different sizes and densities were distinguished by quantitative proteomic analysis following iodixanol gradient isolations (Kowal et al. 2016). Diagnostic and treatment potential of EV proteins has been demonstrated by several studies. For example, by analyzing 8 EV protein markers in plasma EVs, a study showed that EV proteins can be used to predict the therapeutic response to metastatic breast cancer (Tian et al. 2021). Another research group demonstrated that EVs from mesenchymal stem cells with enrichment in several cargo proteins were effective in reducing inflammation and liver damage in non-alcoholic steatohepatitis (Kim et al. 2021). Currently, due to their high immune-modulatory and remodeling abilities, stem cell derived EVs have emerged in new tissue reparative models (Roefs et al. 2020).

Other components of extracellular vesicles

Lipids, metabolites, and DNA are currently the least examined EV components. Lipids in EVs could be classified according to their location in the EV membrane, as lipids can either form the outside of the lipid-bilayer (SM, PC and CHOL), the inside of the lipid bilayer (PS, PE and CHOL) or connect the two bilayers (CHOL) (Skotland et al. 2020). In addition to its membrane lipids, EVs transport enzymes that are involved in lipid synthesis processes (Skotland et al. 2020). Interestingly, a small fraction of EVs have been shown to carry lipidic structures inside, in addition to their main lipid bilayer (Skotland et al. 2020). Metabolites in EVs were mostly covered in regard to changes in cell culture characteristics, whereas EV DNA cargo is gaining attention in

recent years, mainly due to its potential for monitoring the changes in natural ecosystems, involving prokaryotes and lower eukaryotes (Ghanam et al. 2022, Harmati et al. 2021, Williams et al. 2019, Palviainen et al. 2019).

1.10 Extracellular vesicles in cell-to-cell communication across the body

Regardless of the load carried, once EVs reach their destination, the uptake process varies. Some EVs could be internalized through receptor-facilitated internalization, direct fusion with plasma membrane, uptake through phagocytosis or a caveolae-dependent-mechanism, and others can be taken up by a clathrin-dependent-mechanism or by a formation of a lipid raft. EVs uptaken by the direct fusion with the plasma membrane deliver their functional cargo to the recipient cell, whereas EVs processed in lysosomes for degradation mainly provide metabolites and nutrients as their main contribution to the recipient cell (van Niel et al. 2018).

Even though originally considered as cellular waste products, EVs were shown to be transferred from one cell to another as early as the 1990s, with studies emerging on functional transfer of the EV nucleic acids in the mid 2000s. Today, EVs are the new addition to the diverse cellular communication mechanisms, such as cytokines, hormones, tight and gap junctions, and others. Due to their versatility and biodegradability, EVs are developed to be used for targeting specific cell types.

Heterogeneous EV populations are secreted by all cells, but major enrichment is observed in biofluids, particularly blood, milk, urine, bile, seminal fluid, and cerebrospinal fluid (Urabe et al. 2021, Van Der Pol et al., 2012; Van Niel et al., 2018; Yáñez-Mó et al., 2015). Tissue-related internal and external conditions modulate intensity and composition of EVs secreted into biofluids. These conditions could be related to pathological and disease conditions, or simply cellular adaptation or differentiation. For example, EV-associated miRNAs derived from adipose tissue have been shown to regulate gene expression in the liver. Injections of obesity-associated circulating EVs altered metabolic states of the otherwise naïve recipients. Studies have also demonstrated that EVs from peripheral blood of aged mice can cross the BBB and activate glial cells in the brain. In cancers, circulating EVs play a role in facilitating establishment of a microenvironment for tumor growth and fasten tumor progression. Circulating B-cell and dendritic-cell derived EVs can activate the immune response by delivering antigens to T-cells.

The potential ability of EVs in transferring information from circulation to germ

cells in males has yet to be explored. This stems partly due to the concept of "Weismann barrier" established by Weismann in 1982, stating that the hereditary information moves only from germ cells to somatic cells in the periphery and not vice-versa. Moreover, deciphering soma-to germ cell communication is complex, since male germ cells undergo a complex differentiation process in the testis and epididymis. This makes it necessary to track all alterations to specific developmental phases. Currently, tracking changes to several stages of spermatogenesis in the same animal is not feasible due to technical/methodological limitations. Moreover, studying this phenomenon in females carries additional difficulties, such as mate preference and related behavioral changes, maternal grooming and care, differential delivery, and abundance of milk components.

1.11 Extracellular vesicles in male reproductive tract and their potential role in epigenetic inheritance

In addition to the various tissue and biofluid EVs described above, male reproductive tract-associated EVs have a potential role in epigenetic inheritance. Apart from the well-studied EVs from epididymis (epididymosomes) and less-known EVs from prostate (prostasomes), a recent report demonstrated the presence of testicular-derived EVs (Choy et al. 2022).

Testicular EVs

The testicular microenvironment is rich in different cell types, such as the feeder or supporter Sertoli cells, hormone-secreting Leydig cells, germ cells at different stages of spermatogenesis, various types of immune cells, and endothelial cells. In addition, factors such as cytokines, metabolites, and hormones conduct cellular signaling and govern spermatogenesis. Pioneering work on isolated testicular EVs demonstrated that: (i) testicular EVs are a heterogeneous mixture of exosomes and microvesicles of different sizes, similar to EVs from other tissues; (ii) testicular EVs can be taken up by somatic cells and germ cells in the testis, specifically Sertoli cells, spermatogonia, and spermatozoa; (iii) testicular EVs are potentially involved in germ cell development; and (iv) testicular EVs can make their way across the blood-testis-barrier; (v) testicular EVs are originated from Leydig or immune cells in the testis, according to their proteomic profiling (Choy et al. 2022). The authors, however, were unable to determine if testicular EVs can directly cross BTB and access germ cells, or are first taken up by Sertoli cells to elicit responses in Sertoli cells, which are then

passed to the germ cells. Nevertheless, by blocking EV release in testis, the researchers showed that EVs are important for normal germ cell development. Whether testicular EVs are affected by environmental insults or could carry the memory of exposure to the germ cells and the next generation, remains an open question.

Epididymal EVs

The most extensively studied EVs in the mammalian male reproductive tract are epididymal EVs, or epididymosomes. They were first described in Chinese hamsters by Yanagimachi et al. in 1985. Epididymosomes are secreted by epithelial cells of the epididymis, which includes principal, basal, clear and narrow cells (Rinaldi et al. 2020). Connected through TJs, the epididymal epithelial cells form the BEB and maintain a protective luminal environment that facilitates sperm maturation (Robaire et al. 2006). The protein, lipid, and RNA content of epididymosomes differs between the three luminal compartments of the epididymis, namely caput, corpus, and cauda. The content closely resembles the biochemical composition of the respective compartment but carries its unique signature as well. Functionally, epididymosomes perform a range of roles, such as neutralizing dead sperm, delivering or removing enzymes to alter sperm's energy production, modifying sperm fluidity, and supplying proteins for proper sperm capacitation and adhesion to oocytes (Munoz et al. 2022).

Both small and long RNAs are found in epididymosomes. Environmental insults such as low protein, stress or toxicant exposure were shown to alter the small RNA content of epididymosomes (Alshanbayeva et al. 2021, Trigg et al. 2021, Chan et al. 2020, Sharma et al. 2016). Epididymosomes carry a vast assortment of sncRNAs, such as snoRNAs, tRFs, miRNAs, piRNAs and several others. However, the focus is yet to be diverted from tRFs and miRNAs. Needless to say, epididymosomal proteins and lipids receive even less attention. Such a gap might partially be explained due to the concept that proteins and lipids are mainly known to affect physical properties of the sperm, such as fluidity, capacitation, and fertilization, rather than crucially altering information inside the sperm, which is transferred to the oocyte. Nevertheless, there are some indications for a role of epididymal proteins in signaling to the offspring. Trigg et al. demonstrated that the epididymal epithelial cell proteome is altered by acrylamide, which in turn potentially alters epididymosomal proteins delivered to mature sperm.

Prostate EVs

Prostasomes are EVs secreted by the epithelial cells of the prostate (Munoz et al. 2022). They were the first EVs associated with male germ cells discovered in seminal plasma in the 1970s. Similar to other EVs, prostasomes range from 30 to 500 nm in size. The main functions of prostasomes involve prevention of premature capacitation of sperm, by delivering high amounts of sphingomyelin, and the delivery of agents for sperm protection. For example, human prostasomes protect sperm from bacterial infection, by delivering a protein that aggressively permeabilizes the bacterial walls. The fusion of prostasomes to sperm as well as the mechanisms of their delivery are not well-understood. The seminal plasma does not only advance sperm motility, but it also evokes immunological responses from the maternal pre-implantation uterine environment (Watkins et al. 2018). These responses facilitate postfertilization development of embryos. Watkins and colleagues showed that seminal fluid alone carries enough information about an environmental insult to affect the offspring metabolism. They particularly highlighted that, when seminal fluid and sperm have similar metabolic backgrounds, the embryonic development progresses normally. Whereas, seminal fluid with unmatched background to that of sperm, does not program appropriate uterine response, somewhat hindering offspring metabolic health development (Watkins et al. 2018).

1.12 Characterization and identification of circulating extracellular vesicles

This chapter provides information on the different methods for identification and characterization of circulating EVs, in addition to describing the most commonly used methods to isolate EVs from blood.

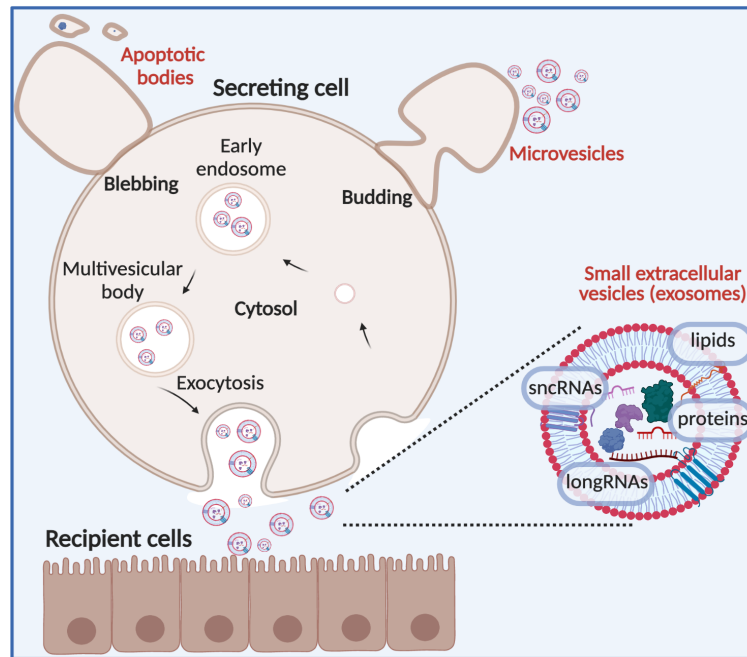


Figure 1-3. Broad overview of extracellular vesicles formation and release pathways.

Exosomes or small extracellular vesicles (exosomes) are formed as intraluminal vesicles in early endosomes, with a subsequent release into the intercellular space from the fusion of multivesicular bodies with plasma membrane. Microvesicles are formed by outward budding of the plasma membrane, whereas apoptotic bodies are formed by blebbing of the plasma membrane due to programmed cells death. The main components of extracellular vesicles include lipids, scnRNAs, proteins and longRNAs. Created with *BioRender.com*.

Analysis of circulating extracellular vesicles

Blood is a rich medium, composed of a range of heterogeneous molecules secreted from different tissues throughout the body. It is therefore important to differentiate EVs from other circulating components, such as lipoproteins, proteins, lipids, hormones and other circulating particles. Isolation and characterization of EVs from blood carries many challenges, due to several reasons: (i) size and density of EVs and other circulating components, such as lipoproteins are similar, depending on the sub-type; (ii) within EVs, subpopulations exist that differ in secretion mechanism and cellular function, but overlap in size (exosomes, microvesicles, apoptotic bodies); (iii) low abundance and fragility of EVs create additional difficulties in the processing and long-term storage.

Currently, several validation methods for EVs are established, following the minimal guidelines published by the *Society of Extracellular Vesicles* (Théry et al. 2018). These methods include electron microscopy (EM), western blotting (WB), nanoparticle-tracking analysis (NTA) and fluorescence flow cytometry (FFC).

To validate the shape and morphology of EVs, negative stain EM remains to be the standard imaging technique. More detailed structural information on EVs can be obtained by EM, since the resolution of EM is much smaller than the EV size, allowing even imaging of protein aggregates. EVs typically have a cup-shaped round morphology in EM, which results from the fixation in the preparation process for EM (Chuo et al. 2018).

NTA, on the other hand, extrapolates the particle size by analyzing Brownian motion of particles in a fluid. Through this, NTA allows estimation of several EV quantitative and qualitative parameters, such as particle size, number, and presence of surface markers. The videos of particles moving in real time are used for calculations of final concentrations. However, NTA is not as reliable with smallest EVs (<30-50 nm) and is only used as an additional validation method, secondary to WB, EM and FFC.

In addition to EM and NTA, WB is providing crucial complementary information on the EV isolation and purity. The majority of markers used to determine the presence of EVs are the tetraspanin markers CD9, CD63, and CD81. Other commonly used EV markers include TSG101, Alix, and HSP70. Depending on the cell of interest, the most common EV proteins can be found on the *Vesiclepedia* database. The field of circulating EV proteome has progressed rapidly, due to many studies that concentrate on purer isolation of EVs, involving depletion from lipoproteins (Trigg et al. 2021, Karimi et al. 2018, Kowal et al. 2016).

EVs can also be imaged by labeling with fluorescent dyes, such as lipophilic Paul Karl Horan (PKH) dyes or luminal carboxyfluorescein succinimidyl ester (CFSE) dyes. These dyes allow one to obtain direct quantification of EVs, track their uptake by cells, and image tissue localization of injected EVs by flow cytometry or microscopy (Dehghani et al. 2020). Labeling of EVs can nevertheless lead to several issues that can alter their functionality. When labeling, it is important to preserve the size and shape of EVs, due to the necessity of interaction with cells. It is also crucial to deplete the labeled EV preparation from the dye-only aggregates, which are not distinguished from labeled EVs in downstream analyses. Lastly, dyes could interact with EV cargo and alter the functional properties of EVs.

Current methods and challenges in EV isolations

Since their discovery in 1970, EV isolation methods have evolved from 1-2 day long protocols to a few hours or even minutes of isolation time, depending on the

protocol used. However, regardless of the isolation method, the major issues of purity and sufficiency of the isolated material for downstream experiments still remain, when it comes to the biofluid of major interest - the blood. In the early days of their discovery, EVs were identified through EM and chemical lysis (through nitrogen cavitation). Only in the mid- and late- 1980s, following determination of the size range of EVs, researchers started to use ultracentrifugation (UC) as the main method of isolation, which was previously widely used for viral particles. Today, EV isolation methods differ in their yield, purity, processing time, and specific downstream applications. In the next paragraphs, we will cover the commonly used EV isolation methods such as UC, kit-based isolations, size-exclusion chromatography (SEC), density-gradient ultracentrifugation (DGUC), ultrafiltration (UF) and microfluidic approaches. In addition to these main methods, there are a number of other EV isolation methods, such as rate-zonal and isopycnic centrifugation, sequential filtration, flow field-flow fractionation, ELISA, lectin induced agglutination, and others, that are extensively covered elsewhere (Doyle et al. 2019).

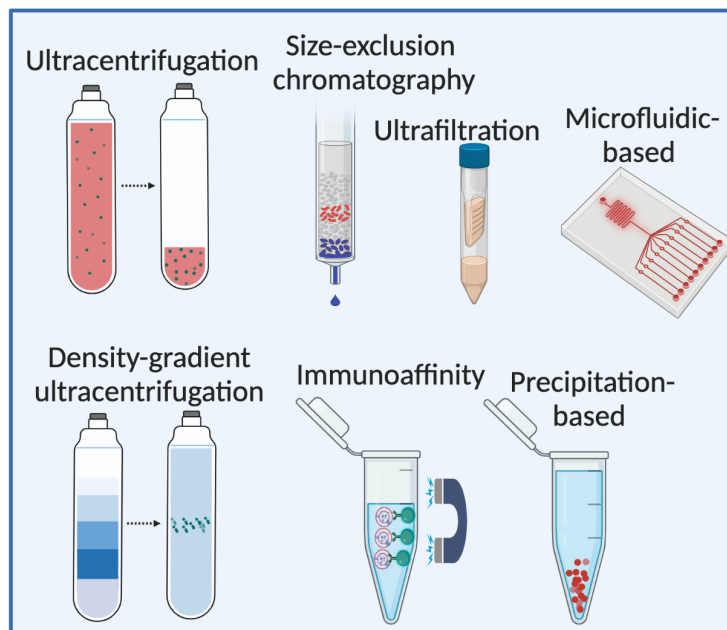


Figure 1-4. Overview of commonly used methods for isolation of extracellular vesicles from blood.

Extracellular vesicle isolation methods vary in many parameters, such as processing time, purity, yield and reproducibility. Ultracentrifugation, ultrafiltration and chemical precipitation-based methods produce higher yield, yet have larger amounts of other circulating factors contaminating the preparations. Density-gradient ultracentrifugation, immunoaffinity, size-exclusion chromatography and microfluidic-based methods offer cleaner preparation, although with forfeit in yield. Created with *BioRender.com*.

One of the most common methods is a simple high-speed UC. UC has relatively high yield, but low purity, since it pellets not only EVs, but rather a mix of particles from the experimental biofluid used. One advantage of UC is that it could be widely applied to isolate EVs from practically any fluid source. Therefore, it is known as the «quick and dirty» method to isolate EVs from biofluids. The purity of UC could be improved by performing sequential UCs, at the cost of yield.

An improved method for isolation of EVs is the DGUC, which also uses high speed UC, but applies it to separate particles based on their densities. DGUC results in much lower yield compared to the standard UC, due to dilution of the sample with iodixanol to create a gradient and long centrifugation times (up to 18-20h).

Similar to UC, commercial-based kits also elute EVs in a mix with other biofluid components, but methods specific to EVs with certain markers have been recently developed. They are generally less time-consuming than other methods and are based on different techniques, such as magnetic bead-based pulling of EVs, polymer-based precipitation, and immunoaffinity. Regardless of the kit used, the costs are relatively high when performing high throughput research.

Another «quick and dirty» way of EV isolation from biofluids is ultrafiltration. It is based on the size of particles in a biofluid and shear force that pushes the fluid through a membrane that has a molecular cut-off filter. Even though it is relatively fast compared to other popular methods like UC or DGUC, there are several disadvantages such as clogging of the membrane filter, wasting the filters due to clogging, damage to particles due to shear stress, or trapping of EVs on the membrane.

SEC is a method for EV isolation from biofluids with comparably purer and higher yield. However, since the particles in a fluid injected onto the column are separated by their size, larger circulating lipoproteins and smaller apoptotic bodies partially elute in the EV fractions. The new generation of commercially available SEC columns allow better separation from lipoproteins and require lower input volumes. Since SEC does not involve a long processing time, it allows rapid sample isolation, without freezing prior to processing. When it comes to *in vivo* studies requiring EV injections, SEC is the most appropriate isolation method, since it allows immediate processing of a biofluid and injection of EVs. This ensures minimal disruptions to natural functioning of the injected EVs.

Still at their early stage of development and usage, microfluidic-based isolation techniques hold several advantages, such as separation of particles in a biofluid simultaneously based on size and biochemical composition, fast operation, reproducibility, and low amount of starting material. There are currently 2 major microfluidic approaches for EV isolations - the sound-based and the immuno-affinity-based methods (Doyle et al. 2019). In the prior, the ultrasound waves are used to vibrate the particles in a flow of fluid, causing higher vibration and therefore faster speed for larger particles. However, this method allows particles to be isolated based on the size property only. The immuno-affinity-based isolation of EVs instead uses antibodies that are immobilized on a chip to bind various membrane proteins on the EV surface. It allows higher specificity and isolation of more homogeneous population of EVs.

Challenges in the isolation of EVs

There are several important empirical aspects to consider when performing isolations of EVs from biofluids. Depending on these practical aspects, the results of experiments carried out on the same sample may differ.

Firstly, storage and handling conditions greatly contribute to the overall EV yield. Regardless of the isolation method used, increasing the number of freeze-thaw cycles negatively impacts EV yield, by damaging the EV membrane. This subsequently affects all the downstream applications performed on EVs, such as RNA-seq, proteomics, and others. When making cross-study interferences and integrating datasets from different experiments, such information is important for appropriate interpretation of results.

Secondly, treatment procedures performed before and after EV isolation should be considered. Major changes are observed when purified EVs are treated with RNAses or proteases before RNA isolations. Additionally, the treatment with protease can impact EV natural functions by disrupting proteins on the surface of EVs that are involved in the uptake or secretion processes. Similarly, RNase treatment would affect the RNA that could be bound to the EV membrane, instead of being encapsulated inside the lipid bilayer. Such details are important, since both EV RNAs and proteins play a role in intercellular communication and can affect the target cells.

Another important aspect to consider is the proportion of other circulating components in the isolated EV material from biofluids. Since most of the EV isolation

methods produce a mixture of particles with enrichment of EVs, the proportion of other components, such as lipoproteins, should be recorded.

Overall, depending on the application, one or a combination of the EV isolations methods described above could be appropriate. When EV-specific RNA or protein is of interest, or EV injections are performed, techniques requiring less pre-processing and manipulation such as SEC or immunoaffinity should be the methods of choice. On the other hand, when overall characterization or exploratory analysis is performed, UC or UF could be used instead.

1.13 Aim of the Doctoral study

Using molecular, cellular, and bioinformatic approaches, this thesis aims to understand the role of circulating factors as conveyors of changes caused by environmental exposures to male germ cells (**Chapter 1, Chapter 2**). In addition, it explores the role of circulating extracellular vesicles as carriers of information to germ cells in males that can give rise to phenotypic alterations in the offspring (**Chapter 2**). It also investigates the modifications in male reproductive tract extracellular vesicles due to an environmental insult during early life (**Chapter 3**). To address these outstanding questions, this thesis uses a mouse model of early life stress as a model of an environmental exposure during early life. The thesis concludes with a discussion of the relevant challenges in the research field, other significant questions that are yet to be answered and recommendations on future experiments and research directions (**Chapter 4**).

2. Circulating extracellular vesicles can vehicle signals from the periphery to the germ cells in males

Anar Alshanbayeva^{1,2,3}, Leonard Steg^{1,2,3}, Alaa Othman⁴, Francesca Manuella^{1,2,3}, Rodrigo G. Arzate-Mejía^{1,2,3}, Nicola Zamboni⁴ and Isabelle M. Mansuy^{1,2,3*}

Affiliations:

¹Laboratory of Neuroepigenetics, Brain Research Institute at the Medical Faculty of the University of Zurich

²Institute for Neuroscience of the Department of Health Sciences and Technology, ETH Zurich, Zurich, Switzerland

³Zurich Neuroscience Center, ETH and University of Zurich, Zurich, Switzerland

⁴Institute of Molecular Systems Biology, ETH Zurich, Zurich, Switzerland

Corresponding author: Isabelle M. Mansuy; E-mail: mansuy@hifo.uzh.ch and imansuy@ethz.ch.

Research Article in Preparation

Description of the contributions to the manuscript.

Contributions of Anar Alshanbayeva:

- i. Performed half of the ELS paradigm and breeding workload, collected plasma samples, and isolated EVs for all experiments with EVs.
- ii. Pre-processed plasma and prepared plasma EVs for metabolomic and lipidomic analyses. Performed explorative and characterization analyses on lipidomic and metabolomic datasets, and differential expression analyses on lipidomic datasets.
- iii. Performed all characterization experiments of EVs, which include immunoblotting, nanoparticle-tracking characterization and electron microscopy images.
- iv. Performed all the breedings with the EV-injected males to obtain the 12- and 46-days post-injection offspring and tracked body-weight of the injected males and their offspring.
- v. Performed intravenous injections of EVs, metabolic tests on EV-injected males and the offspring of EV-injected males, sacrificed the EV-injected males and collected tissues and sperm samples, isolated sperm RNA from EV-injected males.
- vi. Performed *in vitro* fertilization with the sperm of EV-injected males, followed by embryo culture and collection.
- vii. Prepared small RNA-sequencing libraries of plasma EVs isolated by size-exclusion chromatography and density-gradient ultracentrifugation.
- viii. Analyzed embryo RNA-sequencing data, sperm small and total RNA-sequencing datasets, and small RNA-sequencing dataset from plasma EVs isolated by size-exclusion chromatography and density-gradient ultracentrifugation.
- ix. Performed *in vitro* EV-uptake experiments with GC-1 cells.
- x. Generated plots from all the datasets, with the input from Rodrigo G. Arzate-Mejía and Isabelle M. Mansuy.
- xi. Wrote the Manuscript together with Isabelle M. Mansuy, with the input from Rodrigo G. Arzate-Mejía.

Contributions of the other authors:

- i. Leonard Steg prepared sperm total RNA-sequencing libraries from EV-injected males 12- and 46-days post-injections.
- ii. Alaa Othman and Nicola Zamboni performed metabolomic and lipidomic experiments, data pre-processing and differential expression of metabolomic datasets.
- iii. Francesca Manuella assisted with animal experiments planning and execution.
- iv. Rodrigo G. Arzate-Mejía assisted with generation of the figures, data interpretation and writing of the Manuscript.
- v. Isabelle M. Mansuy designed, coordinated and funded the study, performed data interpretation and wrote the Manuscript together with Anar Alshanbayeva.

2.1 Abstract

Paternal exposure to environmental stressors drives changes to the information carried by the sperm. The knowledge whether these stressors modify information in the germline by directly acting on the germ cells or indirectly via somatic cells in the gonads is limited. In recent years, the possibility that soma-to-germline communication contributes to the transfer of paternal experiences to the offspring has been suggested by studies in rodent models. However, how signals in the periphery can reach germ cells in gonads is still not well understood. As a biological fluid that captures physiological changes in the body and brings signaling components across different tissues, blood has emerged as a potential vector of such communication. Here, using early life stress as an environmental insult, we identified circulating extracellular vesicles as vectors of communication with germ cells that can reproduce several symptoms of exposure in the offspring when injected to fathers *in vivo*. These results highlight the importance of circulating factors in the mechanisms of epigenetic inheritance.

Keywords: Epigenetics, extracellular vesicles, miRNAs, early life stress, sperm, intergenerational inheritance, metabolism, lipids, father, offspring.

2.2 Introduction

Intercellular communication is a fundamental process necessary for the development and functioning of multicellular organisms. Cells can communicate by exocytosis or direct exchange of small cytoplasmic components via gap junctions, which are efficient modes of information transfer for cells in close proximity (Armingol et al. 2021; Di Fiore et al. 2001). However, cells far apart are also known to exchange information, such as by secreting components into the blood, a process known as endocrine signaling. Long distance communication between cells is however more challenging and involves different mechanisms such as secretion of messengers or formation of thin tubular membranous channels to transfer signaling molecules, proteins, lipids and RNAs. Recent research identified extracellular vesicles (EVs) as another efficient mode of long distance communication between cells (Raposo et al. 2019). EVs are small particles delineated by a lipid bilayer and released into extracellular space by many cell types. EVs carry active molecules such as proteins, nucleic acids, metabolites, and lipids and were shown to carry a variety of roles in intercellular communication in different systems, such as immune, cardiovascular, reproductive systems and more (Buzas et al. 2022; Yates et al. 2022).

Circulating EVs produced by some tissues can transfer their cargo to other cells in the body via endocrine signaling, and in some cases lead to changes in the recipient cells (Morales-Prieto et al. 2022; Thomou et al. 2017). For example, miRNAs from EVs derived from adipose tissue can regulate gene expression in liver (Thomou et al. 2017). EVs from peripheral blood can activate glial cells in the brain, suggesting they can cross the blood-brain-barrier (Morales-Prieto et al. 2022). In some pathological states such as inflammation, cancer and cardiovascular diseases, composition as well as functionality of EVs can be altered. For example, in models of cerebral ischemia, EVs from brain endothelial cells can transfer a pro-neuronal transcription factor to astrocytes, transforming them into neuronal progenitor cells (Li et al. 2022). Whereas, EVs released from cancer cells can affect growth, differentiation, proliferation and migration of their recipient cells (Zhang et al. 2021).

However, communication of circulating EVs with gonads or gonadal germ cells in mammals has not been well studied. In males, this stems partly due to the presence of the blood-testis-barrier and the concept of hereditary information moving only from germ cells to somatic cells in the periphery and not vice-versa, also known as

Weismann's theory. In addition, addressing this question is technically challenging, since male germ cells undergo several differentiation stages in testis and epididymis, creating a barrier with the number of cell types and differentiation stages to look at.

Here we examined the potential communication between circulating EVs and germ cells in males by using a mouse model of early life stress (ELS), as a model of changes to environmental conditions. We show that circulating ELS EVs and their cargo are sufficient to affect the physiology of directly exposed animals and of their unexposed progeny. Injections of ELS EVs into the circulation of naïve animals result in the long-term reprogramming of the sperm transcriptome, which also correlates with altered transcriptional programs in the embryo and metabolic changes in the adult offspring. Our data provide evidence that environmental exposures can persistently rewire circulating factors such as EVs, which in turn can modify physiology across generations. These findings highlight the important role of circulating factors in communication processes in the body and identify their contribution to information transfer to germ cells.

2.3 Results

2.3.1 Circulating EVs have distinct RNAs, lipids and metabolites content.

To characterize the components of circulating EVs from the plasma of adult mice, we first isolated plasma EVs by size-exclusion chromatography, a method that can separate particles in a fluid based on their size (**Fig. 2-1a**). Nanoparticle tracking analysis showed enrichment of particles of 50-120 nm diameter in fractions 4-5 of our preparations, consistent with the expected size of exosomes, which are the smallest EVs in mammals (**Fig. 2-1b**). Electron microscopy confirmed the typical cup shape morphology of EVs in these fractions (**Fig. 2-1c**). Western blot analyses indicated the presence of common EV markers known to be abundant in EV preparations from various sources (Odaka et al. 2022; Komarova et al. 2021; Kowal et al. 2016), including the heat-shock protein HSP70 in fractions 4-5 and 6-7, and the tetraspanin family protein CD63 in fractions 4-13. We also checked the high-density lipoprotein (HDL) marker ApoA1, to confirm the absence of HDL in EV-enriched fractions. ApoA1 was absent from fractions 1-6 but detectable in fractions 6-9 (**Fig. 2-1d**). Therefore, to avoid HDL contamination, we used only fractions 4-5, instead of all fractions that displayed the presence of EV markers HSP70 and CD63, as the source of EVs for all further analyses and experiments.

We next characterized the RNA, lipids and metabolites content of plasma EVs. Profiling of small RNA populations by RNA sequencing (RNA-seq) revealed that the majority of RNA reads map to tRNAs, microRNAs (miRNAs) and protein coding regions, consistent with previous reports (**Fig. 2-1e**) (Thomou et al. 2017; Otahal et al. 2021; Vickers et al. 2011; Skotland et al. 2011). We found that specific miRNAs, known to be enriched in EVs (Otahal et al. 2021), were abundant in our preparations while miRNAs enriched in HDL were in low amount, confirming the specificity of our EV preparations (**Supplementary Fig. 2-1a**). Analyses of lipids by liquid chromatography coupled with mass spectrometry revealed the presence of major lipid classes such as lysophosphatidylcholines (LPC), phosphatidylcholines (PC), sphingomyelins (SM), phosphatidylethanolamine (PE) and triacylglycerols (TAG), with PCs and SMs being the most predominant classes (**Fig. 2-1f**). Analyses of functional categories related to the cellular localization of lipid moieties indicated that the majority of lipids in EVs belong to lysosomes and membrane (**Supplementary Fig. 2-1b**), which are both

involved in EVs secretion (Skotland et al. 2020). Finally, the profiling of EVs metabolites by time-of-flight mass spectrometry showed that carbohydrates, fatty acyls, benzoids and steroids among others metabolite sets are enriched in plasma EVs (**Fig. 2-1g**). Together, these results identify complex RNA, lipids and metabolites signatures of plasma EVs from adult mouse.

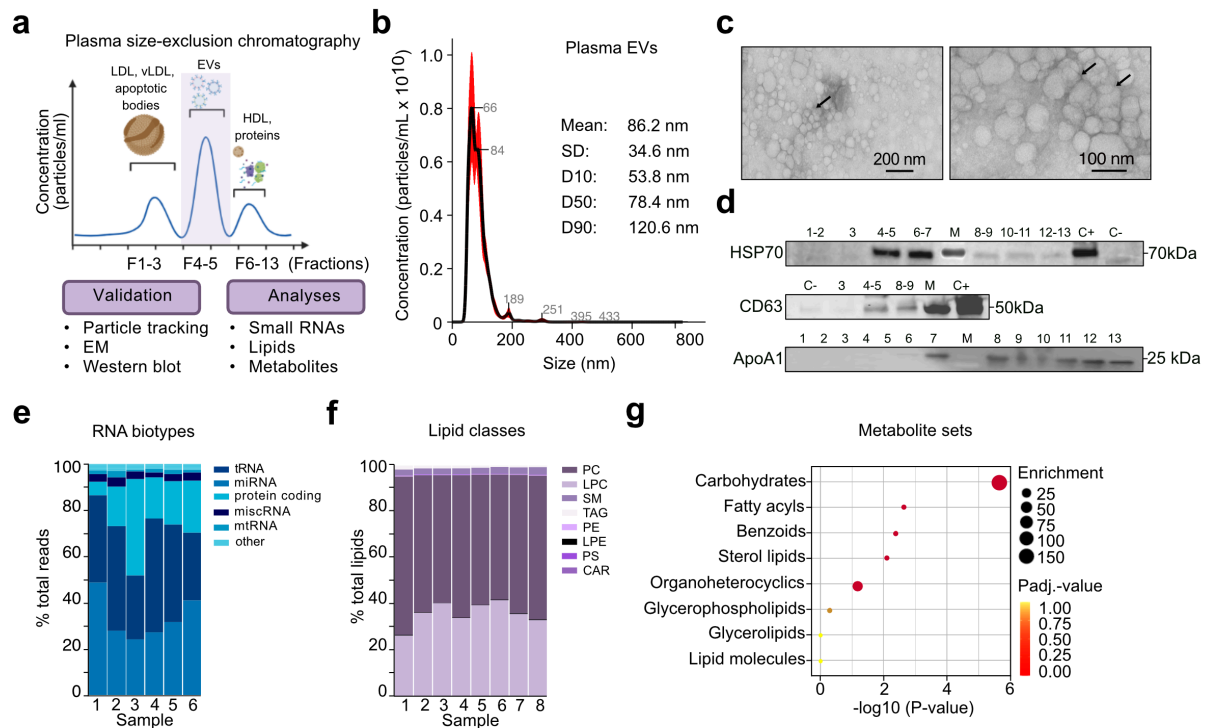


Figure 2-1. Isolation of plasma EVs and characterization of RNA, lipid and metabolite components.

a. Purification of plasma EVs by size-exclusion chromatography. EVs are enriched in fractions 4-5 (F4-5) and are separated from larger circulating components, including LDL (low-density lipoprotein), vLDL (very low-density lipoprotein) and apoptotic bodies in fractions 1-3 (F1-3) and smaller components including HDL (high-density lipoprotein) and proteins in fractions (F6-13). Created with *Biorender.com*.

b. Concentration of plasma EVs (particles/ml) by size (nm) obtained by nanoparticle tracking. SD (Standard Deviation), D10-50-90 (points at which 10%, 50% and 90% of the sample is contained).

c. Electron microscopy images of EV enriched fractions 4-5. Arrows point to individual EVs.

d. Protein levels of EV markers, a transmembrane protein associated to plasma membrane (CD63) and cytosolic protein (HSP 70), and a high-density lipoprotein marker (ApoA1). C+ (positive control, human exosome lysate), C- (negative control, buffer), M (Molecular weight marker).

e. Distribution of RNA biotypes as % of total reads in plasma EVs from size-exclusion chromatography F4-5. $n=6$ biologically independent samples.

f. Distribution of lipid classes in plasma EVs from size-exclusion chromatography F4-5. $n=8$ biologically independent samples. PC (Phosphatidylcholine), LPC (Lysophosphatidylcholine), SM (Sphingomyelin), TAG (Triglyceride), PE (Phosphatidylethanolamine), LPE (Lysophosphatidylethanolamine), PS

(Phosphatidylserine), CAR (Acylcarnitine). $n=6$ biologically independent samples.

g. Enriched sets of metabolites in plasma EVs from size-exclusion chromatography F4-5. $n=8$ biologically independent samples.

2.3.2 ELS persistently modifies the composition of circulating EVs.

We next wanted to understand if early life experiences can alter circulating EV components in adulthood. To achieve this, we used a mouse model of ELS, where pups are separated from mothers during postnatal days 1-14 and mothers are subjected to a forced-swim or restrain stress daily at unpredictable times (**Fig. 2-2a**) (Franklin et al. 2010). We previously demonstrated that serum of adult animals exposed to ELS, when chronically injected into naïve animals, can lead to metabolic perturbations in the offspring of the injected animals (van Steenwyk et al. 2020). We compared plasma EVs of ELS and control males in EV number, RNA, lipid and metabolite composition (**Fig. 2-2a**). While no differences were detected in the mean particle size between control and ELS EVs, the total number of EVs was significantly higher in ELS plasma (**Fig. 2-2b, 2c**).

Remarkably, ELS significantly altered RNA cargo of EVs (**Fig. 2-2d**). In particular, we detected 7 down- and 63 up-regulated RNAs ($P\text{-adj.} < 0.05$) respectively (**Fig. 2-2d**). The majority of differentially-altered sncRNAs are microRNAs and tRNAs (**Supplementary Table 2-1**). Many of these sncRNAs, such as the microRNA families miR-let-7, miR-30, and tRNA-Lys, were found by others to be altered in response to different environmental exposures (Gapp et al. 2014; Trigg et al. 2021; Sharma et al. 2016; Chan et al. 2020; Rodgers et al. 2015).

To confirm the specificity of our RNA findings to EVs, we isolated plasma EVs by yet another method known as density-gradient ultracentrifugation (DGUC) and performed small RNA-seq (**Supplementary Fig. 2-2a**). DGUC differs from SEC in that it separates particles based on their density rather than size (**Fig. 1a, Supplementary Fig. 2-2a**). Overall, DGUC EVs were of similar size range of EVs and shape as those from SEC (**Fig. 2-1e, 1c; Supplementary Fig. 2-2b-e**), while the difference in number between control and ELS plasma EVs was also present in the DGUC EVs (**Fig. 2-1, Supplementary Fig. 2-2f**). However, the overall number of EVs from DGUC isolations was significantly lower compared to the number from SEC isolations, which stems from the technical differences between the two methods (**Fig. 2-2c, Supplementary Fig. 2-2f**). We observed significant differences in the abundance of microRNAs in ELS

EVs isolated by DGUC. Namely, both SEC and DGUC showed a significant increase of miR-30 and miR-let-7 miRNA families in ELS plasma EVs, while differences in the abundance of other sncRNAs were unique to either of the isolation methods (**Fig. 2-2d, Supplementary Fig. 2-2g**).

In addition to RNAs, differential analysis of EV lipids isolated by SEC showed significant increase in 5 lipids in ELS plasma EVs compared to controls, with no difference in overall distribution of lipid classes and functional categories (**Fig. 2-2e, Supplementary Fig. 2-3a, 3b**). These increased lipids include 3 PCs and 1 PE, that form the EV lipid bilayer and 1 TAG (**Fig. 2-2g, 2h**).

The type or number of different EV metabolites in ELS plasma were not altered compared to controls (**Fig. 2-2f**). When looking at the top metabolites in ELS plasma EVs ($P < 0.1$), we observed overrepresentation in several metabolite sets, such as monosaccharides, fatty acids and conjugates, such as steroid conjugates and bile acids (**Supplementary Fig. 2-4a, 4b**). Enrichment in these metabolite sets is consistent with what we previously observed from plasma of adult ELS males.

Overall, our findings suggest that ELS alters the number, sncRNAs cargo and lipid composition of circulating EVs in adult male mice.

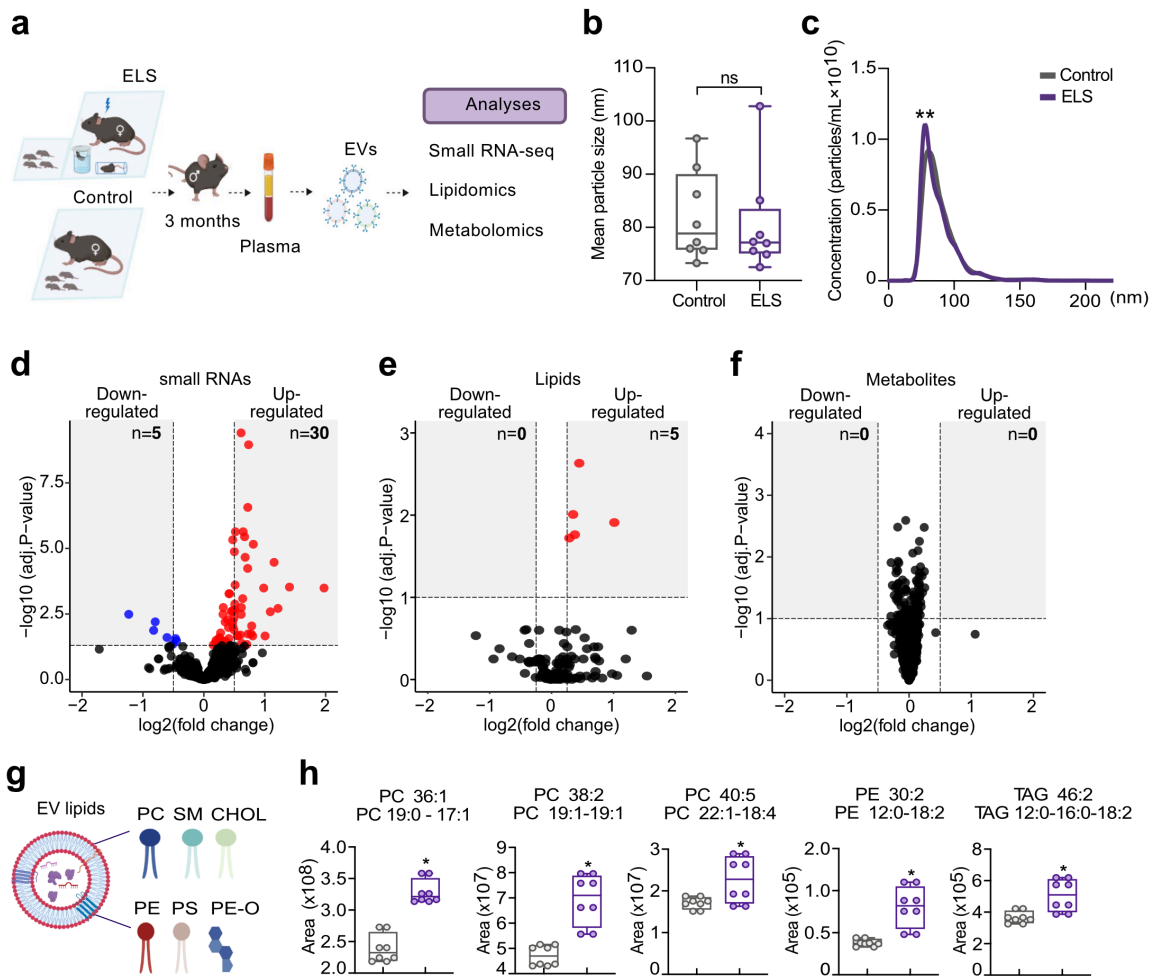


Figure 2-2. The effect of ELS on plasma EVs RNA, lipid and metabolite components.

a. Experimental design. Plasma EVs are isolated from ELS and Controls, and analyzed by small RNA-sequencing, lipidomics and metabolomics. Created using *Biorender.com*.

b. Mean particle size of plasma EVs from ELS and Controls (two-tailed unpaired Student's t-test, ns=non-significant, $n=8$ biologically independent samples/group). Error bars are SEM.

c. Concentration of plasma EVs in ELS and Controls ($n=8$ biologically independent samples/group, $*P < 0.05$).

d-f. Volcano plots of differentially-expressed small RNAs (**d**), lipids (**e**) and metabolites (**f**) in ELS plasma EVs compared to Controls. ($n=6$ biologically independent samples/group for small RNAs, $n=7$ /group for metabolites, $n=8$ /group for lipids). Corrected for multiple testing with Benjamini-Hochberg test. Significance: $P_{adj.} < 0.05$.

g. Lipid composition of plasma EVs. PC (Phosphatidylcholine), SM (Sphingomyelin), CHOL (Cholesterol), PE (Phosphatidylethanolamine), PS (Phosphatidylserine), PE-O (Phosphatidylethanolamine-O). Created using *Biorender.com*.

h. Differentially altered lipids in ELS plasma EVs. Mann–Whitney, Significance: $P^* > 0.05$. Nomenclature: number of carbons in the fatty acid chain : number of double-bonds in the fatty acid chain.

2.3.3. Chronic injections of circulating EVs can alter metabolic state of naïve mice.

Since circulating EVs can influence physiological states across organs, and ELS resulted in robust alterations in circulating EV composition, we wanted to test if alterations in EV components brought by ELS in naïve animals. To do this, we isolated plasma EVs from 3 months old control and ELS males by SEC and chronically injected them into naïve age-matched males for 4 weeks, twice per week (**Fig. 2-3a**). SEC was the method of choice due to the higher amount of EVs isolated compared to DGUC (**Fig. 2-1a, Supplementary Fig. 2-2**).

We looked at glucose metabolism, circulating metabolites and lipids in the injected males long-term post-injections (**Fig. 2-3a**), since ELS alters glucose metabolism and circulating components, whereas circulating EVs were shown to play a role in glucose metabolism (Castaño et al. 2018). We observed no differences in body weight immediately after or long-term post-injections (**Fig. 2-3b**), while ELS EV-injected mice showed significantly lower insulin sensitivity and no difference in glucose clearance (**Fig. 2-3c, 3d**). Unbiased plasma metabolomic and lipidomic analyses of ELS EV-injected males 46 days after injections revealed many significantly up- and down-regulated metabolites and their subsequent pathways (**Fig. 2-3e, 3f; Supplementary Fig. 2-5a, 5b; Supplementary Table 2-2**). Overall, 18% of all metabolites detected in the plasma of Day-46 ELS EV-injected males were significantly altered between the 2 groups, with 132 up-regulated and 111 down-regulated metabolites (**Fig. 2-3e**). Compound analysis of these metabolites showed 100-300-fold enrichment of several compounds, including fatty acids, prenol lipids, steroid conjugates, and glycerophosphoethanolamines (**Fig. 2-3g**). Similar metabolic pathways and compounds were enriched in plasma of ELS adult males (van Stynweek et al. 2020). When looking at only significantly up- or down-regulated metabolites, we found that major compound differences originate from metabolites that are down-regulated (**Supplementary Fig. 2-5a, 5b**). Differential pathway enrichment of metabolites in plasma of Day-46 ELS EV-injected males showed up-regulation of alpha linolenic acid and linoleic acid metabolism, similar to that of ELS adults, up-regulation of bile acid

biosynthesis and steroidogenesis, opposite of ELS adults (**Fig. 2-3f**). When looking at the common metabolites that are altered in ELS and ELS EV-injected males, we observed that half of the common metabolites have opposite enrichment in the 2 groups (**Fig. 2-3h**).

In addition to the major changes in circulating metabolites, we found that around 50% of lipids assigned with high confidence to be significantly upregulated and <5% down-regulated in the circulation of males injected with ELS EVs 46 days compared to controls (**Fig. 2-3i**). Similar to ELS EV lipids, most of the significantly altered and upregulated lipids were PCs and PEs (**Fig. 2-3j**).

These findings indicate that chronic injections of circulating EVs from animals exposed to ELS can induce long-lasting changes in the metabolism of naïve adult males, and that some of the changes resemble those of adult ELS.

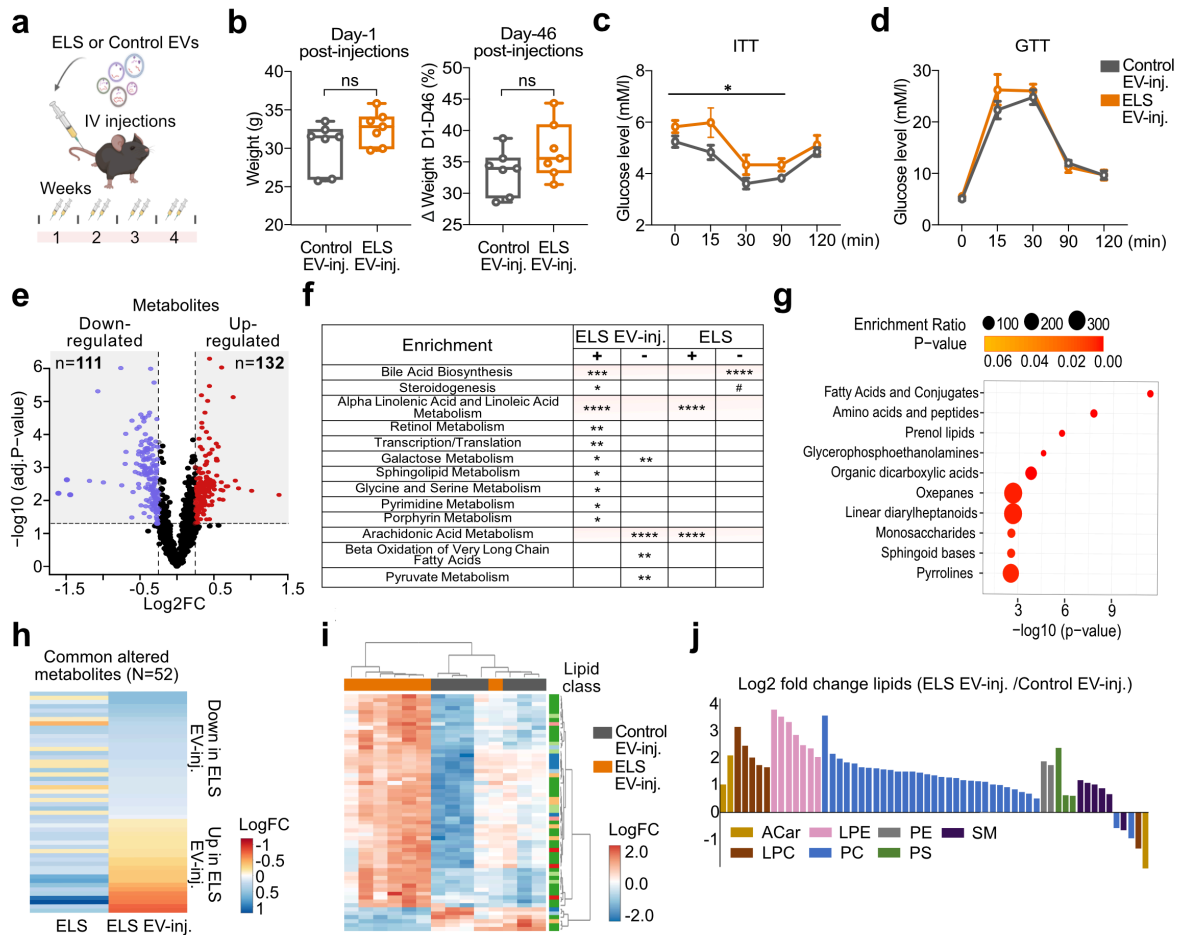


Figure 2-3. Impact of chronic injections of ELS EVs on metabolism.

a. Experimental design. Plasma EVs from ELS or Controls were intravenously injected into naïve mice for 4 weeks, 2 times per week ($n=7$ biologically independent samples/group). Created using *Biorender.com*.

b. Body weight of the ELS or Control EV-injected males at 1 day post-injections (Day-1) and % change in body weight at 46 days post-injections (Day-46). Two-tailed unpaired Student's t-test, ns=non-significant.

c-d. Glucose tolerance test (GTT) and insulin tolerance test (ITT) of ELS EV-injected males. Repeated-measures ANOVA, treatment effect $P < 0.05$.

e-g. Changes in circulating metabolites (**e**), metabolic pathways (**f**) and metabolic compounds (**g**) in plasma of ELS EV-injected males ($n=7$ biologically independent samples/group). Corrected for multiple testing with Benjamini-Hochberg test. Significance: $P_{adj.} < 0.05$. Metabolites with $P_{adj.} < 0.05$ were selected as input for Metaboanalyst tool to look at compound enrichment.

h. Heatmap of commonly altered ($P < 0.05$) plasma metabolites in adult ELS males and ELS EV-injected males compared to Controls.

- i. Heatmap of significantly changed ($P_{\text{adj.}} < 0.05$) plasma lipids in ELS EV injected males at 46 days post-injections compared to controls ($n=7$ biologically independent samples/group).
- j. Lipid classes of significantly changed ELS plasma EVs lipids. Corrected for multiple testing with Benjamini-Hochberg test. Significance: $P_{\text{adj.}} < 0.05$.

2.3.4 Circulating EVs can signal to germ cells in males.

We have shown that ELS circulating EVs can cause long-term systemic metabolic alterations in the periphery in naïve males, when injected chronically. However, whether circulating EVs can reach or affect germ cells is not known. Therefore, we incubated GFP-labeled plasma EVs with a testicular germ cell-like GC-1 cells *in vitro*. We detected the presence of GFP-signal in the cytoplasm of the GC-1 cells (**Fig. 2-4a**), suggesting the potential ability of circulating EVs to enter germ-like cells.

We next wanted to test if the circulating EVs can have an effect on male germ cells and looked at the examined the sperm of ELS EV-injected and control males in longRNA and sncRNA content at 12 and 46 days after the injections (**Fig 2-4b**). In mice, the epididymal transit of spermatozoa lasts ~7 days, then the mature sperm resides in cauda for ~5 days and is then removed by spontaneous ejaculation (**Fig 2-4b**) (Dadoune et al. 1984; Meistrich et al. 1975; Huber et al. 1980). Therefore, a delay of 12 days allows us to eliminate the sperm that was present in the epididymis during the injections (**Fig. 2-4b**).

At 12 days post-injections, we found 3 scnRNAs significantly increased and 2 long RNAs significantly decreased ($P_{\text{adj.}} < 0.05$, $\text{LogFC} > 1$) in the sperm of the ELS plasma EV-injected males compared to controls (**Fig. 2-4c, 4d**). Among the top increased scnRNAs are 2 piRNAs and miR-let-7c, whereas tRNA-Glycine and tRNA-Histidine showed an increased trend ($P_{\text{adj.}} < 0.1$) (**Supplementary Table 2-3**). Many of these small RNAs have been previously shown to be involved in paternal transmission of environmental changes to the offspring, including miR-let-7 family that we previously showed to be up-regulated in ELS sperm (Sharma et al. 2016; Gapp et al. 2020). Genes that have an increased trend ($P < 0.05$) in the sperm of ELS EV-injected Day-12 males showed enrichment of 340 transcription factor (TF) binding sites ($P_{\text{adj.}} < 0.01$) (**Supplementary Table 2-3**). One of the top enriched binding sites is a PPAR α -RXR α binding motif (**Supplementary Table 2-3**). PPAR-involving pathways were also found to be increased in adult ELS sperm (van Stynweek et al. 2020). Overall, regardless of significant changes in body weight of ELS EV-injected males 12 days post EV

injections (**Fig. 2-4c, 4d**), the effect of the injections to the germ cells was mild, at least when looking at the RNA signature of the sperm.

12 days following injections, the caudal sperm of the EV-injected males was exposed to the injected material during the latest stages of testicular development (**Fig. 2-4b**) (Meistrich et al. 1975; Cossetti et al. 2014). This time-point does not allow one to distinguish if the male germ cells could be perceptive to circulating factors at the earlier stages, such as spermatogonium or preleptotene spermatocyte, which take place outside the blood-testis barrier (BTB) (**Fig. 2-4b**). Therefore, we have further looked at the EV-injected males' caudal sperm small and long RNAs 46 days after injections (Day-46), a period which allows for a complete spermatogenesis cycle and clearance of mature sperm from cauda by spontaneous ejaculation (**Fig. 2-4b**). This replenishes all the germ cells that could be directly vulnerable to the injected material during maturation in the seminiferous tubules or during the epididymal passage (**Fig. 2-4b**).

Interestingly, at 46 days post-injections, the increase in body weight of ELS EV-injected males that we observed at 12 days post-injections was lost, with no differences in body weight between ELS and control EV-injected males (**Fig. 2-3b, Supplementary Fig. 2-6**). Both sperm small and long RNAs were significantly altered in males injected with ELS plasma EVs compared to controls, 46 days post-injections (**Fig. 2-4e, 4f**).

To compare transcript expression changes in Day-12 and Day-46 EV-injected males to ELS and ELS serum-injected males' sperm transcript expression changes, we used a rank-rank hypergeometric overlap (RRHO) analysis, which allows a threshold-free identification and expression comparison of common transcripts between 2 groups (**Fig. 2-4g, Supplementary Table 2-3, 4**). Sperm of Day-12 males displayed similar transcript expression patterns as ELS males and males injected with ELS serum (**Fig. 2-4g**). Whereas, the majority of common transcripts between Day-46 males and ELS or ELS serum-injected males had an opposite expression profile (**Fig. 2-4g**). Interestingly, RRHO analysis also showed that, among the common RNAs found in Day-12 and Day-46 sperm, there is a set with similar and a set with opposite expression pattern in the two groups (**Fig. 2-4g**).

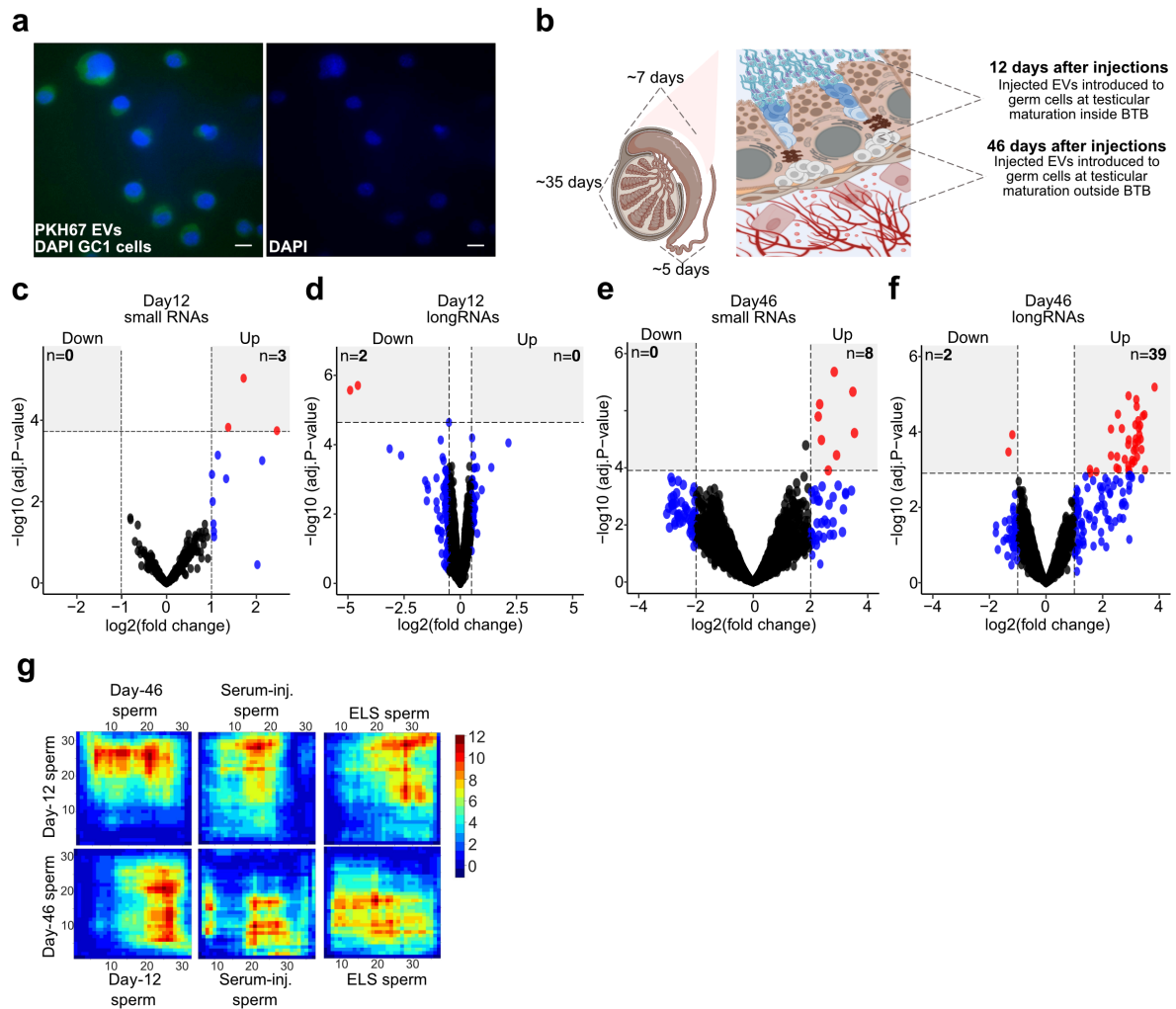


Figure 2-4. The effect of chronic injections of ELS EVs on sperm RNA.

a. Fluorescence microscopy images of germ cell-like GC-1 cells incubated with plasma EVs labeled with a green fluorescent PKH67 dye. Scale bar: 10 μ m.

b. Representation of male germ cell maturation and transit through testis and epididymis in mice. On average, male germ cells spend ~35 days in testicular maturation, whereas epididymal transit lasts ~7 days with waiting time of ~5 days in cauda epididymis. Created using *Biorender.com*.

c-f. Volcano plots of differentially expressed sperm small and long RNAs in ELS EV-injected males 12 days (**c-d**) and 46 days (**e-f**) post-injections. Corrected for multiple testing with Benjamini-Hochberg test. Significance: $P_{adj.} < 0.05$. ($n=7$ biologically independent samples/group for 46 days, $n=5$ biologically independent samples /group for 12 days).

g. Rank-rank hypergeometric overlap plot of sperm long RNA expression comparison between different groups. Comparisons made: sperm of ELS EV-injected males 12 and 46 days post-injections, ELS sperm and sperm of ELS serum-injected males 12 days post-injections. Expression level represents $-\log_{10}(P)$ of overlapping RNAs between any compared 2 groups.

2.3.5 Exposure to EVs can alter metabolism intergenerationally.

We showed that exogenous administration of EVs can rewire the RNA cargo of sperm from naïve mice (**Fig. 2-4c-f**). Since sperm RNA is sufficient to induce phenotypes in the offspring, we wanted to next understand if those otherwise naïve animals injected with ELS EVs have offspring that are metabolically different compared to control offspring. This question is especially relevant, since the effect of ELS is known to affect metabolism of the unexposed offspring (Franklin et al. 2010). To do this, we repeated the injections of ELS and control plasma EVs into naïve males as before (**Fig. 2-3a**) and looked at different parameters in the adult offspring that were obtained by pairing with naïve females at 12 (Day-12 offspring) and 46 (Day-46 offspring) days after injections (**Fig. 2-5a**). Interestingly, Day-12 offspring of ELS EV-injected males indeed had metabolic alterations, similar to that of ELS offspring and offspring of ELS serum-injected males (**Fig. 2-5b, 5c, 5f-g**) (van Stynweek et al. 2020). First, the body weight of Day-12 ELS EV-injected offspring was significantly decreased, similar to ELS offspring (**Fig. 2-5b**). This decrease came from overall changes in body composition, such as significantly lower body fat, water, and lean mass (**Fig. 2-5b**). Additionally, Day-12 offspring of ELS EV-injected males displayed insulin hypersensitivity and higher glucose in response to restraint, corresponding to ELS males and ELS offspring (**Fig. 2-5c**). Moreover, steroidogenesis and bile acid biosynthesis pathways were decreased, as in ELS males and ELS offspring (**Fig. 2-5f**). Day-12 offspring of ELS EV-injected males also had alterations in circulating lipids (**Fig. 2-5h**). Overall, Day-12 offspring of ELS EV-injected male displayed many metabolic alterations that are comparable to that of ELS offspring.

Similar to the different metabolic and sperm RNA signatures of ELS EV-injected males at 12- and 46-days post-injections, Day-46 offspring also showed a distinct phenotype in body weight and glucose tests from that of Day-12 offspring (**Fig. 2-5d, 5e**). Particularly, the Day-46 offspring of ELS EV-injected males had opposite changes to that of Day-12 offspring of ELS EV-injected males, in overall body weight, body composition and glucose metabolic tests, with only few changes overlapping in circulating lipids (**Fig. 2-5d, 5e, 5h**). Day-46 offspring of ELS-EV injected males had mild alterations in circulating lipids and metabolites (**Fig. 2-5f-h**). When comparing the common metabolites that have an increased or decreased trend ($P < 0.01$), Day-12 and Day-46 offspring have similar direction of change (**Fig. 2-5f**). However, there is

opposite enrichment ($P < 0.01$) between the two groups in 20% of all common lipids (**Fig. 2-5h**). Interestingly, the common plasma metabolites between Day-12 or Day-46 and ELS offspring all have an increased trend and all share a significant enrichment ($P_{\text{adj.}} < 0.05$) in metabolites involved in bile acid biosynthesis and steroidogenesis pathways (**Fig. 2-5f**).

To understand if metabolic alterations observed in the offspring were specific to the plasma EV-enriched fractions of ELS, we intravenously injected ELS or Control plasma protein-enriched fractions (PEF) (**Fig. 2-1a**, F 6-13) into naïve males twice per week for 4 weeks, similar to the EV-injections (**Supplementary Fig. 2-7a**), and obtained offspring 12 and 46 days post-injections. Interestingly, males injected with ELS plasma PEF showed no changes in glucose metabolism or insulin response, but exhibited many significantly altered circulating metabolites and lipids, compared to controls (**Supplementary Fig. 2-7b-e**). However, offspring, obtained at 12 or 46 days post-injections from the ELS PEF-injected males were not metabolically different from the control offspring (**Supplementary Fig. 2-7f, 7g**).

Overall, these findings suggest that alterations in sperm RNA signature of naïve mice brought by exogenous EV injections can affect the offspring and manifest similar metabolic changes to that of ELS offspring.

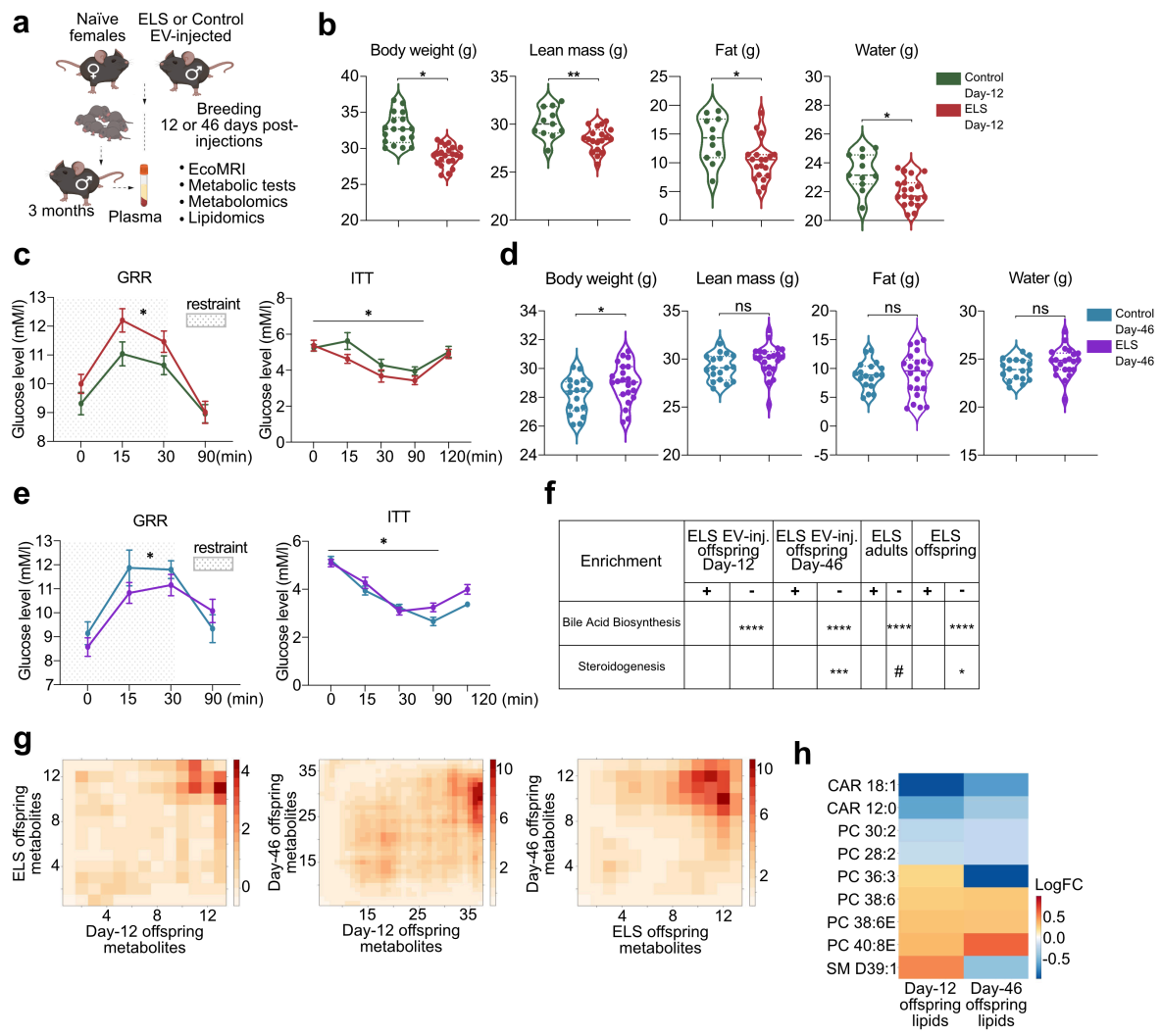


Figure 2-5. Metabolic changes in the offspring of ELS EV-injected males.

a. Experimental design. ELS or Control EV-injected males were paired with a naïve female at 12 days and 46 days post-injections. Offspring were subjected to EcoMRI, metabolic tests, plasma metabolomic and lipidomic analyses. Created using *Biorender.com*.

b. Body weight and body composition analysis of ELS and Control EV-injected males' offspring obtained 12 days post-injections. Two-tailed Student's t- test, treatment effect * $P < 0.05$, ** $P < 0.01$, *** $P < 0.001$, **** $P < 0.0001$. ns=non-significant.

c. Glucose in response to restraint (GTT) and insulin tolerance test (ITT) of the ELS EV-injected Day-12 offspring. Repeated-measures ANOVA, treatment effect $P < 0.05$.

d. Body weight and body composition analysis of ELS and Control EV-injected males' offspring obtained 46 days post-injections. Two-tailed Student's t- test, treatment effect * $P < 0.05$, ** $P < 0.01$, *** $P < 0.001$, **** $P < 0.0001$. ns=non-significant.

e. Glucose in response to restraint (GTT) and insulin tolerance test (ITT) of the ELS EV-injected Day-46 offspring. Repeated-measures ANOVA, treatment effect $P < 0.05$.

f. Common enriched metabolic pathways in the EV-injected males' 12 days and 46 days post-injections offspring, adult ELS males and ELS offspring. Asterisk and hashtag represent $P_{adj.}$ after multiple testing corrections using Benjamini–Hochberg (BH) test. Data significance: # $P_{adj.} < 0.1$, * $P_{adj.} < 0.05$, ** $P_{adj.} < 0.01$, *** $P_{adj.} < 0.001$, **** $P_{adj.} < 0.0001$. Columns indicate significance for positive (+) and negative (-) enrichment.

g. Rank-rank hypergeometric overlap plot of plasma metabolites between different groups. Comparisons made: ELS offspring, Day-12 EV-injected males offspring, Day-46 EV-injected males offspring. Expression level represents $-\log_{10}(P)$ of overlapping metabolites between any compared 2 groups.

h. Heatmap of commonly altered ($P < 0.05$) plasma lipids in ELS EV injected males' offspring 12 and 46 days post-injections compared to controls. CAR (Acylcarnitine), PC (Phosphatidylcholine), SM (Sphingomyelin).

2.3.6 EV injections give rise to developmental changes in early embryos.

In vitro fertilization allows us to discern the sole contribution of sperm in the development of offspring, in the absence of seminal fluid and other paternal factors. To understand the role of sperm in the early development of the offspring in the absence of other paternal factors, we carried out *in vitro* fertilizations with the sperm of ELS and Control EV-injected males 12 days post-injections and performed RNA-seq of 2-cell embryos via Smart-seq2 protocol (**Fig. 2-6a**). Mouse 2-cell embryos can be distinguished into early, mid and late stages by stage-specific gene expression. Therefore, to not miss information due to possible heterogeneity of the embryos, we first characterized the developmental stages of our 2-cell embryos. To do this, we used SCMAP, which is a tool for unsupervised projection of single cell RNA-seq data, to project our embryo-seq data onto a published dataset, in which gene expression profiles of early, mid, and late 2-cell embryos are identified (Deng et al. 2014). 90% of our 2-cell embryos were projected by their gene expression to be at mid or late 2-cell stage (**Fig. 2-6b, 6c**). Therefore, we did not split the 2-cell embryos by developmental stages for further differential-expression analyses. There was also no clear separation of the embryos by fathers when plotting the first two principal components, suggesting that differences in gene expression might be discrete between both groups. (**Supplementary Fig. 2-8a**). We found 100 differentially expressed RNAs ($P_{adj.} < 0.05$, $\log_{2}FC > 1$) in the 2-cell embryos obtained from the sperm of ELS EV-injected males, 90% of which were upregulated (**Fig. 2-6e**). We then performed TF binding-site enrichment analysis of differentially expressed genes in the embryos from ELS EV-injected males (**Fig. 2-6d, 6f; Supplementary Table 2-5**). The most enriched TF

motifs from downregulated genes were E2F family (17% of all motifs), Elk and Pax family (3.5%), GATA and Sox family (3%) (**Supplementary Table 2-5**). When looking at the gene ontology (GO) enrichment of the differentially expressed genes in the embryos from ELS EV-injected males, the top GO terms related to molecular function involved terms such as “translation imitation factor activity”, “translation factor activity and RNA binding”, “translation regulator activity” (**Supplementary Table 2-5**). In addition, GO terms related to biological processes and cellular function terms were “translation initiation”, “translation”, “spliceosome complex” and terms related to RNA splicing processes. These findings indicate overall transcriptional changes in the embryos originating from the sperm of males injected with ELS plasma EVs 12 days post-injections.

Since the 2-cell embryos come from the same sperm that was used for long and small RNA-seq 12 days post-injections, we wanted to see if any of the embryo transcripts targeted by differentially expressed miRNAs in sperm of Day-12 males are changed. As expected, all the RNA-targets of the miRNAs upregulated in sperm of Day-12 males had a decreasing trend in the embryos, as shown by the cumulative distribution plots of the corresponding target genes’ expression in embryos (**Supplementary Fig. 2-9**).

With these findings, we conclude that the information carried in the sperm of the ELS-EV injected males alone is sufficient to alter the initial stages of embryonic development in the offspring, with potential impact of these changes in the adult offspring.

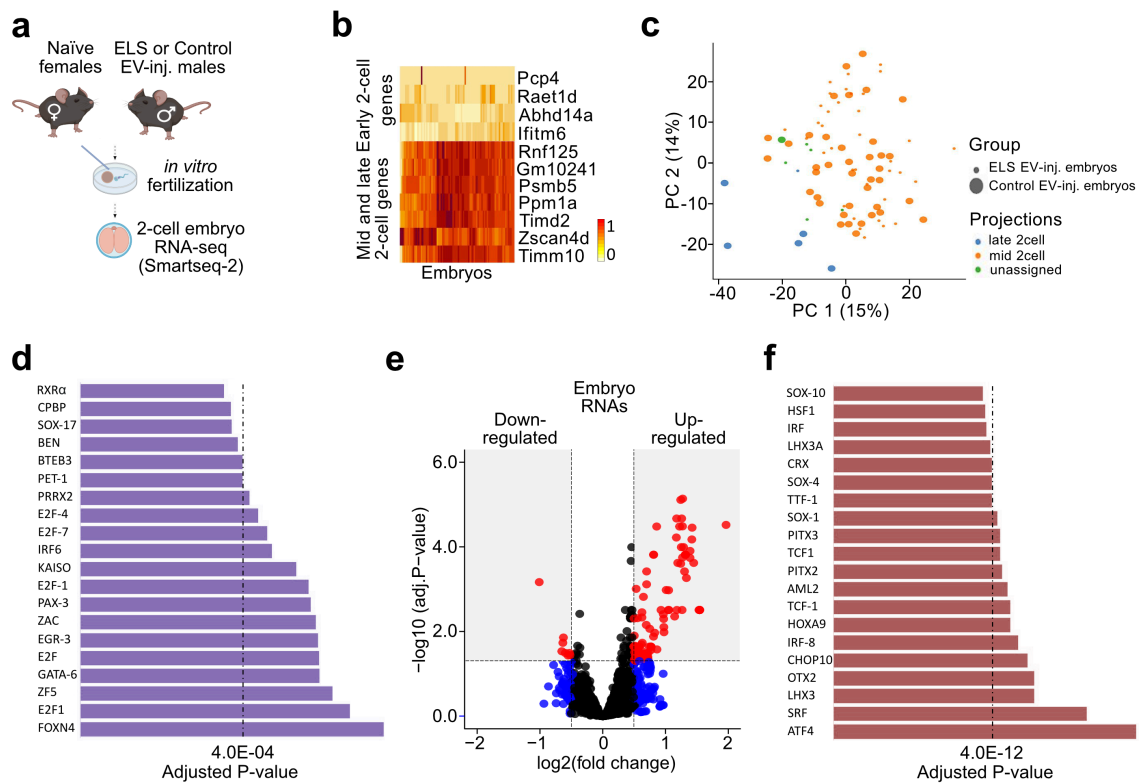


Figure 2-6. Chronic injections of ELS EVs give rise to developmental changes in 2-cell embryos.

a. Experimental schematic of *in vitro* fertilization and embryo RNA-sequencing experiments. Created using *Biorender.com*.

b. Gene expression heatmap of early 2-cell markers and mid to late 2-cell markers in embryos.

c. Plot of 2 main principal components in the embryo RNA-sequencing data. Colour coding: projection of single embryo RNA expression onto a known dataset (Deng et. al., 2014) shows classification of the single embryos into early, mid and late 2-cell stages.

d-f. Top transcription factors ($P_{adj.} < 0.0001$) with enrichment of binding motifs in genes significantly ($P_{adj.} < 0.05$) down-regulated (**d**) and up-regulated (**f**) in the embryos of ELS EV-injected males.

e. Volcano plot of differentially-expressed RNAs in ELS EV-injected males' embryos. Corrected for multiple testing with Benjamini-Hochberg test. Significance: $P_{adj.} < 0.05$.

2.4 Discussion

The inter-organ communicative abilities of circulating EVs have been explored with regard to a number of systems. It was shown that injections of circulating EVs from obese to lean mice caused glucose intolerance and insulin resistance via microRNA dependent pathways (Castaño et al. 2018). Even though overall metabolic changes were observed in the lean animals injected with obesity-associated EVs, the implications of the EV injections in the sperm or offspring of the injected males was not investigated. Here, we further extended the inter-organ communicative potential of circulating EVs to the germ cells in males. We do so by demonstrating that chronic injections of EVs with altered cargo can have long-term effects on the metabolism of the injected males as well as the information carried by their mature sperm. We also showed that the systemic impact established by circulating EVs influences the sperm RNA content delivered upon fertilization to the offspring. Additionally, we demonstrated that injections of circulating EVs from mice subjected to ELS into naïve mice can have an intergenerational impact on the offspring, causing varied metabolic alterations. To the best of our knowledge, this is the first study that demonstrates the role of circulating EVs as signaling factors of changes in the periphery to the germ cells in males, with a relevant effect in the offspring.

The possibility of soma to germline communication through the circulation has been previously explored with two different methods. In one of the studies, the authors xenotransplanted GFP-positive human melanoma cells in mice and observed the GFP mRNA in the sperm from cauda (Cossetti et al. 2014; O'Brien et al. 2020). The second study expressed human pre-miR941 with an AAV in the mouse brain and discovered the presence of miR941 in mature sperm (O'Brien et al. 2020). In both scenarios, the mice were subjected to unnatural invasion in terms of cancer cells or AAV, which are known in some cases to not behave innately (Cossetti et al. 2014; O'Brien et al. 2020). However, in our study, the EVs were not manipulated, derived from age-matched animals, and administered through simple intravenous injections.

Chronic environmental alterations such as chronic stress, have already been shown to alter circulating EV RNAs (Cuomo-Haymour et al. 2022). However, the relevance of EVs as small RNA carriers in the circulation has been questioned due to the fact that only a small proportion of small RNAs in the circulation originate from EVs (Arroyo et al. 2011). On average, there is one microRNA molecule per every 24 EVs

in the circulation (Otahal et al. 2021). Since the number of microRNAs in circulating EVs is low, our findings further accentuate the fact that plasma EVs of males subjected to ELS are enriched in certain microRNAs, such as miR-30 family, miR-let-7 family and several tRNAs. Strong evidence from other studies suggests that many of the small RNAs we observe altered in ELS plasma EVs are also involved in paternal transmission of information on experiences to the offspring. Nevertheless, we cannot exclude involvement of other EV components, such as proteins or DNA, in the effect we observe.

The term EVs instead of exosomes is used, since even if the enrichment is in particles of size 30-200 nm, there are larger particles in lower numbers in our preparations. The presence of microvesicles in our preparations cannot be excluded, since their size (0.1–1.0 μm) overlaps with that of larger exosomes. However, similar size range of particles is isolated by both SEC and DGUC methods. The variation in the number of isolated EVs between the two methods was reported by other studies (Onódi et al. 2018; Sidhom et al. 2020). It could be mainly attributed to the longer processing time and more processing steps involved in DGUC protocol, both of which decrease concentration of purified EVs. The differences in the small RNAs between the two methods could be explained by the loss of EVs in DGUC.

Changes to TF binding in mature sperm and embryos as a response to environmental stimuli from fathers was demonstrated before (Jung et al. 2020). We also observe enrichment of 340 TF binding sites ($P_{\text{adj.}} < 0.01$) in the genes expressed higher ($P < 0.05$) in the sperm of males injected with ELS EVs. Some recent reports indicated association of increased chromatin accessibility and TF-binding in mature sperm upon environmental stimuli (Jung et al. 2020). We showed that 90% of the TF-binding motif enrichments in embryos of ELS EV-injected males come from the 10% of genes that were all down-regulated. This suggests that most of the TFs that are differentially active among the embryos of two groups are repressors. Interestingly, the TF family with most binding sites (17% of all motifs) in downregulated genes from the embryos was E2F, a family of TFs conserved from *C.elegans* to mammals (Tsai et al. 2008). During early embryonic development, the E2F family of TFs are associated with differentiation and proliferation signals, and the defect in the E2F family during embryonic development causes metabolic changes, such as decreased body weight and adipose mass, in adult mice (Tsai et al. 2008; Palena et al. 2000).

Cell cycle progression and renewal is affected by E2F during embryonic growth, which impacts the adult animal body size significantly (Tsai et al. 2008).

There are several factors outside the scope of the current study. These include addressing several important questions, such as the potential role of seminal fluid and the lymph node in the transmission, the travel trajectory of injected EVs and downstream effect on the cells EVs are taken up by, the origins of alterations in sperm small and long RNAs, other possible changes in the sperm of the injected males and the rationale behind the different mechanisms that gave rise to the metabolic variability observed in the offspring obtained 12 and 46 days post-injections.

Seminal fluid was shown to partially transfer paternal exposure information to the offspring by others (Watkins et al. 2018). We do not exclude this possibility in our model. However, we showed with *in vitro* fertilization experiments that sperm alone is enough to affect the early embryonic development of the offspring of ELS EV-injected males. How the changes in gene expression in embryos unfolds remains to be explored further.

Another mode of transmission of environmental exposure information to the germ cells that was not explored in our study is the lymph node. Both testis and epididymis have access to lymphatic drainage (McDonald et al. 1988), and the capillaries responsible for nutrient and vesicle transport of the lymphatic and the circulatory systems are found near each other. Moreover, when a human AVV pre-miR941 is expressed in the mouse brain, the presence of the human pre-miR941 is persistently detected in the lymph nodes, in addition to other organs (O'Brien et al. 2020). Therefore, we cannot eliminate the possibility of circulating EVs acting on the germ cells in males through the lymphatic system.

In addition to the possible modes of transmission mentioned above, the origins of the changes in sperm RNA signature as well as metabolism in the males injected with ELS EVs 12 days and 46 days after injections is yet to be addressed. To do so, more time-points and animals are necessary. One would need to be able to continuously monitor changes in the blood as well as in the spermatozoa, ideally, at different stages of maturation in testis and epididymis. However, at present, there is no sensible method that enables sampling enough spermatozoa for molecular analysis, while keeping the animal alive. Potentially, tail sampling for plasma and electroejaculation for semen collection could be considered.

We have shown that exposure to stress in early postnatal life still has readable effects in the circulating EV components in adults. We have also shown that the changes in EV components are relevant to the overall metabolism of an organism as well as that of the offspring. We speculate that, the circulating components that drive metabolic alterations in the offspring are specific to ELS plasma fractions enriched with EVs, due to no apparent changes in the offspring of males injected with protein-enriched plasma fractions. These findings bring new potential applications to light. First, circulating EVs can be used as a diagnostic tool or an additional readout of an organism's metabolic state. Second, circulating EVs should be considered in the case of blood component transfusions in humans. When blood is separated into plasma, red and white blood cells for transfusions, no filtering of plasma components is performed to remove EVs from plasma. This becomes more relevant in the case of patients receiving regular transfusions, as we demonstrated the impact of chronic injections of plasma EVs with altered cargo. Lastly, with the advances in EV isolation and characterization methodologies, more targeted delivery of drugs or EVs with manipulated cargo could be considered, since the cell or tissue origin of a disease will be easier to be determined.

2.5 Materials and Methods

2.5.1 Mice

All C57Bl/6J mice that were used for the experiments were kept under a 12-h reverse light/dark cycle in an environment with temperature and humidity control. The animals had ad access to food and water ad libitum. All the experiments were performed on the animals during the period of their active cycle, in conformity with the guidelines of the Cantonal Veterinary Office, Zürich. The animals in this work belong to the license number: ZH083/2018. All experimental animals were between 3-4 months old of age, except females used for *in vitro* fertilization experiments (2 months old).

2.5.2 ELS

ELS was performed as previously described elsewhere (Franklin et al., 2010). Briefly, 3-month-old C57Bl/6J females were paired with age-matched males for 1 week. Following birth, the litters were separated to ELS or control groups, balancing the litter sizes and number of animals between the two groups. Control animals were left

undisturbed apart from a cage change once a week until weaning (postnatal day 21). Dams assigned to ELS group were subjected to a 3h separation (occurred at unpredictable times daily) from their pups from postnatal day 1 to postnatal day 14. During the separation, the dams were subjected to either an acute swim in cold water (18°C for 5 min) or a 20-min restraint stress in a tube. At postnatal day 21, pups from both groups were weaned and assigned into cages of 3-5 animals/cage, based on gender and treatment. To avoid cage effect, the pups coming from the same litter were assigned to different cages.

2.5.3 Blood collection

To avoid triggering the stress response in littermates, the adult males were single-house overnight with food and water before sacrifice and blood collection. Trunk blood was collected into EDTA-coated tubes (Microvette, Sarstedt) from the adult males after decapitation, inverting the tube gently several times. After 15 mins at room temperature, the blood was centrifuged at 2,000 × rcf for 10 min. Plasma was collected and centrifuged again at 2,000 × rcf for 5 min to remove any debris. Plasma was then stored at -80°C.

2.5.4 Nanoparticle tracking analysis

The number and size distribution of plasma EVs was measured on Nanosight NS300 (Malvern, UK) at 20 °C, according to manufacturer's guidelines. All samples were diluted to a 1:1000 concentration in filtered (0.22µm) PBS.

2.5.5 Characterization of EVs by TEM

EVs were visualized by TEM using a negative stain method with methylcellulose. Briefly, the carrier grid was glow-discharged in plasma for 10 min and then washed with a 100 ul drop of PBS, followed by incubation in 1% glutaraldehyde (GA) in water for 5 min and washing with water 5 times for 2 min per wash. The grid was then incubated in 1% UAc (uranyl acetate) for 5 min and kept on ice in Methylcellulose/UAc (900 ul Methylcellulose 2 % and 100 ul 3 % UAc) solution.

2.5.6 Isolations of plasma EVs

To isolate plasma EVs by size-exclusion chromatography, qEVoriginal columns were used (IZON, SP1). The column was prepared and run according to manufacturer's instructions. Briefly, immediately after loading 500 ul of plasma, 13 1 mL fractions were collected. Fractions 4-5 of SEC were used as EV-enriched fractions.

To isolate plasma EVs by density-gradient ultracentrifugation, the Iodoxanol (OptiPrep) density media (Sigma-Aldrich, St Louis, MO, USA) was used to prepare an OptiPrep gradient (40%, 20%, 10%, 5%) by diluting OptiPrep with 0.25M sucrose, 10mM Tris. 1 mL of plasma was layered onto the OptiPrep gradient and ultracentrifuged at 100,000 x g 4°C for 18 h. 10 fractions were collected from top to bottom, and each fraction was diluted with filtered cold PBS and subjected to 120,000 x g ultracentrifugation for 2 h at 4 °C. The supernatant was removed, and the final pellet was resuspended in cold phosphate buffer saline (10010-015, Gibco) and frozen in -80 °C. Fractions 5-7 were pulled as EV-enriched fractions.

2.5.7 Western blotting

The pellet containing EVs was mixed with 10X RIPA (Cell Signaling Technology) and incubated for 5 min at 4°C and mixed with 4X Laemmli Sample Buffer (Bio-Rad Laboratories, USA). The membranes were blocked in 5% SureBlock™ (LubioScience GmbH, Zürich, Switzerland) in Tris-buffered saline with 0.05% Tween-20 (Sigma-Aldrich, St Louis, MO, USA) for 1 h at 20°C and incubated with primary-antibodies overnight at 4°C (anti-HSP70 [1:1000; System Biosciences, EXOAB-Hsp70A-1], anti-CD63 [1:1000; System Biosciences, EXOAB-CD63A-1], anti-ApoA1 [1:10000; Genetex, GTX112692], anti-CD9 [1:1000; System Biosciences, EXOAB-CD9A-1], anti-TSG101 [1:2000; Abcam, ab125011]). Human exosome lysate (System Biosciences, EXOAB-POS-1) was used as a positive control. Next, the membranes were washed in TBS-T (3 times for 15 min), and incubated with an HRP-conjugated secondary- antibody (anti-rabbit [1:10000; Santa-Cruz Biotechnology, cs2357], anti-mouse [1:10000; Upstate Biotechnology, 12-349]) for 1h, followed by another round of washes in TBS-T.

2.5.8 Intravenous injections of EVs

EVs injections were performed immediately following isolations by size-exclusion chromatography. 100 ul of 10¹⁰ freshly isolated EVs from adult ELS or control mice

were injected intravenously twice per week for 4 weeks. For injections, mice were placed in a restraint tube and the tail was placed in a lukewarm water. The two lateral veins of the tail were alternated. The injections success was confirmed by absence of resistance and presence of blood. All injections were successful with maximum of 2 attempts. Each injected male was paired with a primiparous adult naïve female 12 days or 46 days after the last injection to obtain Day-12 and Day-46 post-injection offspring.

2.5.9 Preparation of sperm samples

Sperm was isolated as previously described (Roszkowski et al., 2021). Briefly, cauda epididymis was incised with several cuts, placed into M2 medium (M7167-100ml, Sigma-Aldrich) and incubated for 30 min at 37°C. The supernatant, containing the motile sperm was centrifuged at 2000 rcf for 10 min. The supernatant was then mixed with equal volume of somatic cell lysis buffer ((0.1 % sodium dodecyl sulfate and 0.05 % Triton X-100 in MilliQ water)), centrifuged again at 2000 rcf for 10 min and washed twice with phosphate buffer saline (10010-015, Gibco). The final sperm pellet was then snap-frozen and stored at -80 °C for molecular analysis.

2.5.10 In vitro fertilization and collection of embryos

2 months old female mice were superovulated with Card Hyperova (Cosmo Bio, KYD-010-EX-X5), followed by 5 Units of human chorionic gonadotropin (hCG) 48 hours after. 16 hours following the hCG administrations, the females were sacrificed by cervical dislocation and ampulla was cut with excised scissors. The cumulus-oocyte complexes (COC) were then released into HTF medium (Cosmo Bio LTD, CSR-R-B070) and incubated for 60 mins (5% CO₂, 37°C), before introducing the sperm. To prepare the freshly-harvested sperm samples for IVF, the adipose around cauda epididymis was removed carefully. The cauda was then placed into a petri dish with pre-incubated (30 mins, 5% CO₂, 37°C) Card FertiUP medium (Cosmo Bio LTD, KYD-005-EX) solution, overlaid with mineral oil (Sigma, M8410-1L). 1 incision per cauda was made and a small 'ball' of sperm was dragged through the oil into the drop of FertiUP. The sperm was then allowed to disperse throughout the medium (1h, 5% CO₂, 37°C). A few drops of the sperm from the FertiUP drop were then added into the oocyte-containing drop. After fertilization, the oocytes were washed

with 3 washes of HTF medium to remove the cell debris, degenerating oocytes and dead sperm. The zygotes were then moved into a fresh drop of HTP overlaid with the oil and cultured overnight. Next morning the 2-cell embryos were collected immediately into a tube containing the lysis buffer for Smartseq2.

2.5.11 Metabolic testing

Glucose in response to restraint

All animals were single-housed for 5h before the restraint. Mice were restrained in a cylindrical plastic tube (3.18 cm in diameter, Midsci) for 30 min. The blood was obtained by tail pinch using a 28-G needle at 0, 15, 30 and 90 min after restraint, and measured by AccuCheck aviva device. Data were analysed with repeated-measures ANOVA and corrected for multiple comparisons.

Glucose and insulin tolerance test

All animals were single-housed, fasted for 5 hours before to establish a baseline blood glucose level and the body weight was measured. All animals received a single injection of glucose or insulin, adjusted for the body weight (insulin: 1 mU/g, glucose: 2 mg/g). For blood glucose measurements, the blood was taken from tail vein by pinching with 28-G needle and measured by AccuCheck aviva device. Data were analysed with repeated-measures ANOVA and corrected for multiple comparisons.

Body Composition Analysis and weight measurement

The total body fat, lean and total water masses were measured by EchoMRI™ system, according to manufacturer's instructions. Briefly, the total body weight of the animals was measured, followed by placement and fixation in a plastic holder. The holder was then inserted into a tubular space at the side of the machine and scanned. The scanning took 2.5-3 minutes per animal.

2.5.12 Metabolomics

Extraction

Metabolite extraction was performed on the Hamilton STAR M liquid handling robot with the following protocol. In brief, 10 µl of the sample was aliquoted into 1.2 ml 96-deep well plates. Afterward, 300 µl of cold extraction solvent Methanol: H₂O, (4:1 v:v) was added. After brief vortexing on a plate shaker, the samples were kept at -20 °C for 2 hours. The samples were then centrifuged at 4000g for 20 min. After

centrifugation, the supernatant was transferred to another deep-well plate, and dried under N₂. Before mass spectrometric analysis, the dried extracts were then resuspended in 100 µl MilliQ H₂O and then transferred to PCR 96-well plates, and then sealed using heat sealing.

Mass Spectrometry

Flow injection mass spectrometry was performed as described previously (Fuhrer et al. 2011). In brief, the samples were injected directly into the mass spectrometer (Agilent QTOF 6546) using an autosampler (Gerstel, USA) and a quaternary pump Agilent 1100 (Agilent, Germany). The samples were injected at an isocratic flow rate of 150 µl/min of solvent isopropanol:H₂O (6:4, v:v) that contains ammonium fluoride (1 mM) and the reference compounds hexakis (2,2,3,3-tetrafluoropropoxy)phosphazene and Homotaurine (3-Amino-1-propane sulfonic acid). Electrospray ionization was used with the following source parameters: gas temperature 225 °C, drying gas 5 l/min, nebulizer 20 psi, sheath Gas Temperature 350 °C, sheath gas flow 10 l/min, Vcap 3500 V and Nozzle voltage 1000 V and Fragmentor was set 120 V, Skimmer to 65 V and the Oct1RF Vpp was set to 750 V. The mass spec was operated in full scan mode scanning the mass range (50-1000 m/z) at 1.4 spectra per second. Online mass correction using the reference masses 138.0230374 and 940.0003763

Data analysis

Raw mass spectrometric data was converted to an open source format (mz5) and then processed using an in-house data processing pipeline (FiaMiner) in Matlab. The m/z axis for the whole dataset was recalibrated using expected reference masses. Afterwards, annotation was performed based on m/z, with mass accuracy of 0.001 Da matching to HMDB. Differential analysis statistics were performed in Matlab for pairwise and group comparisons and correction of multiple comparisons was performed. Pathways enrichment analysis was performed using the HMDB pathway definition v 3.0.

2.5.13 Lipidomics

Extraction

Lipid extraction was performed as described previously (Pellegrino et al. 2014) with some modifications. To 20 µl of the sample, 1 ml of a mixture of methanol: MTBE:

chloroform (MMC) 1.33:1:1 (v/v/v) was added. After brief vortexing, the samples were continuously mixed in a Thermomixer (Eppendorf) at 25 °C (950 rpm, 30 min). Protein precipitation was obtained after centrifugation for 10 min at 16000 g and 25 °C. The single-phase supernatant was collected, dried under N₂, and stored at -20 °C until analysis. Before Analysis, the dried lipids were redissolved in 100µL MeOH:Isopropanol (1:1).

Liquid Chromatography

Liquid chromatography was done as described previously (Delabriere et al. 2021; Cajka et al. 2016) with some modifications. Vanquish LC pump (Thermo Scientific) was used with the following mobile phases; A) Acetonitrile:Water (6:4) with 10mM ammonium acetate and 0.1% formic acid and B) Isopropanol: Acetonitrile (9:1) with 10mM ammonium acetate and 0.1% formic acid. The lipids were separated using C18 reverse phase chromatography using Acquity BEH column (Waters) with the dimensions 100mm * 2.1mm * 1.7µm (length*internal diameter*particle diameter). The column temp was set to 60°C. The following gradient was used with a flow rate of 1.2 ml/minutes; 0.0-0.29 minutes (isocratic 15-30%B), 0.29-0.37 minutes (ramp 30-48% B), 0.37-1.64 minutes (ramp 48-82%B), 1.64-1.72 minutes (ramp 82-99%), 1.72-1.79 minutes (isocratic 99%B), 1.79-1.81 minutes (ramp 100-15% B) and 1.81-2.24minutes (isocratic 15%B). injection volume was 2µl. The needle wash solvent was Methanol:Isopropanol:Acetonitrile:H₂O (1:1:1:1, v:v:v:v)

Mass Spectrometry

The liquid chromatography was coupled to a hybrid quadrupole-orbitrap mass spectrometer (Q-Exactive HFX, Thermo Scientific, Germany). Heated electrospray ionization was used with the following source parameters: sheath gas flow rate 40, aux gas flow rate 8, spray voltage 3.5 kV, capillary temperature 300 °C, funnel RF level 50, and auxiliary gas heater temperature 300°C. The mass spec was operated in data-dependent acquisition mode DDA). First, A full scan was used scanning from 200-2000 m/z at a resolution of 60000 and AGC Target 1e6, max injection time 100 ms. Then the top 2 precursors were automatically selected for fragmentation using normalized collision energies (NCE) of 20, 30,50, a resolution of 7500, and an AGC target of 1e5.

Data Analysis

Raw mass spectrometric data were imported in Compound Discoverer 3.1 (Thermo Scientific) for data analysis. Peak picking, retention time alignment, and compound

grouping were performed, Afterwards, lipid annotation was performed by matching the MS2 spectra to the LipidBlast in-silico library. Lipid identification was manually confirmed based on lipidomics standards initiative criteria and annotations not matching the stringent criteria were filtered out. Peak areas were normalized using median normalization and differential analysis was performed between the different groups and the p values were corrected for multiple comparisons.

2.5.14 RNA extraction

RNA from EVs was extracted with Trizol reagent (Life Technologies, 15596026), according to manufacturer's instructions. Briefly, EV preparations from SEC or DGUC were lysed in Trizol, followed by phenol-chloroform extraction. The final RNA pellet was washed in 75% ethanol, air dried and dissolved in nuclease free water.

Mature sperm was collected according to the previously established sperm swim-up method (Roszkowski et al., 2021). Sperm RNA was extracted with Trizol (Life Technologies, 15596026) according to standard RNA extraction protocol. Briefly, the samples were homogenized in Trizol, using steel beads and a TissueLyser (TissueLyser II, Qiagen), followed by phenol-chloroform extraction. The final RNA pellet was washed in 75% ethanol, air dried and dissolved in nuclease free water. The RNA concentration and integrity was checked using 2100 Bioanalyzer (Agilent), according to the manufacturer's instructions.

2.5.15 Preparation of sequencing libraries

The small RNA libraries from plasma EVs were prepared according to the Smallseq protocol, designed for single-cell or low-input RNA sequencing experiments (Hagemann-Jensen et al., 2018). The libraries were sequenced with Illumina Novaseq6000, 100 bp read length, single-end sequencing with 18 M reads/sample depth. All samples were sequenced twice.

Small RNA-seq libraries of sperm samples were prepared using Reaseq Small RNA sequencing library preparation kit (Somagenics), according to the manufacturer's instructions. 3-5 ng of total starting RNA was used to prepare the libraries. The libraries were sequenced on Illumina Novaseq6000 platform, with 100bp single-stranded read-length with average sequencing depth of 30M reads/sample.

3-5 ng sperm RNA was use to prepare total RNA sequencing libraries using

SMARTer® Stranded Total RNA-Seq Kit v3 - Pico Input Mammalian (Takara Bio USA, #634486), according to the manufacturer's instructions, with a fragmentation time of 150 seconds and 12 PCR cycles at the final amplification. Bead purifications were performed using AMPure XP beads (Beckman Coulter Life Sciences, #A63881) The libraries were sequenced on Illumina Novaseq6000 platform, with 150bp read-length paired-end sequencing.

For embryo RNA-seq experiments, no prior RNA extraction was performed, and each single embryo was directly collected into 4 µl of the lysis buffer (Triton X-100, nuclease free water, RNasin Plus, Biotinylated Oligo-dT, dNTP mix), followed by reverse transcription, template switching, PCR preamplification, tagmentation and PCR purification steps, according to Smart-seq2 protocol (Simone Picelli et al., Nature protocols, 2014). The Smart-seq2 libraries were sequenced on Illumina Novaseq 6000 instrument in 1 lane SP Flowcell with single-read 100bp length parameters. On average, 5-10 M reads were obtained per embryo.

2.5.16 Bioinformatic data analyses

Plasma EVs small RNA-seq

FASTQ raw read files were processed as specified previously (Hagemann-Jensen et al., 2018). Briefly, the UMIs on the 5' of the reads were appended on the read name using UMI-tools (Smith et al., 2017) followed by the removal of adapters using Cutadapt (Martin et al., 2011) and CA-linker was removed from the beginning of each read. Next, the samples were mapped to the mouse genome with STAR aligner (Dobin et al., 2013). The final read count table was used to perform differential-expression analysis between the two groups using edgeR (Robinson et al., 2010). Batch correction was performed to avoid falsely increasing the power due to 2 sequencing runs performed on all samples.

Sperm small RNA-seq

Cutadapt (Martin et al., 2011) was used to trim the known sequence TGGAATTCTCGGGTGCCAAGG, according to the manufacturer's instructions. The reads were then processed, integrating the ExceRpt pipeline for small RNA analysis (Rozowsky et al., 2019).

Sperm long RNA-seq

UMItools (Smith et al., 2017) was used to trim the 8nt UMIs, followed by removal with

Cutadapt (Martin et al., 2011) of the 3nt UMI linker and 3nt Pico v3 SMART UMI Adapter from Read2 prior to mapping. Mapping to the mouse genome (mm10) was performed with hisat2 (Zhang et al., 2021), followed with sorting and indexing with samtools (Danecek et al., 2021). Final bam files were deduplicated with UMIttools and raw counts were calculated with featurecounts of Rsubread package (Liao et al., 2019).

Embryo Smart-seq2

After adapter removal with Cutadapt (Martin et al., 2011) reads were mapped to the mouse genome (mm10) with STAR aligner (cite, version), following raw count quantification with featureCounts (Liao et al., 2019). Differential expression was performed in edgeR (Robinson et al., 2010). Genes with FDR < 0.05 value were used for functional enrichment analysis using of g:Profiler web-tool (Reimand et al., 2017). To differentiate the 2-cell embryos into different stages of 2-cell development, we projected the gene-expression profiles of the 2-cell embryos onto an index that contained expression profiles from early, mid and late 2-cell embryos (Deng et al., 2014), using SCMAP tool (Kiselev et al., 2018).

2.6 Acknowledgments

We would like to thank Kristina Thumfart and Martin Roszkowski for their help and advice. Nancy Carullo for initial feedback on the Manuscript. Pawel Pelczar and his team for teaching and advising on IVF experiments. Dimitri Schmid, Lola Kourouma, Chiara Boschardin and Anastasiia Efimova for helping with IVF and animal experiments. Deepak Tanwar and Pierre-Luc Germain for their advice on data analysis. Ali Jawaid, Eloise Kremer and Mia Holmes for their help in the initial stages of the project. Katharina Gapp for advice on IVF and scientific concepts and methods. Alekhya Mazukhar for initial training with Nanoparticle tracking-analysis. Emilio Yangüez for his advice on RNA-seq experiments. Yvonne Zipfel for taking care of the animals. Johannes Riemann for his help with EM images. Simon Berger for his help with microscopy. Michael Hagemann-Jensen for his advice on Smallseq protocol. Emmanuel Maciel for her contributions to the project during her Master Thesis.

2.7 Authors contribution

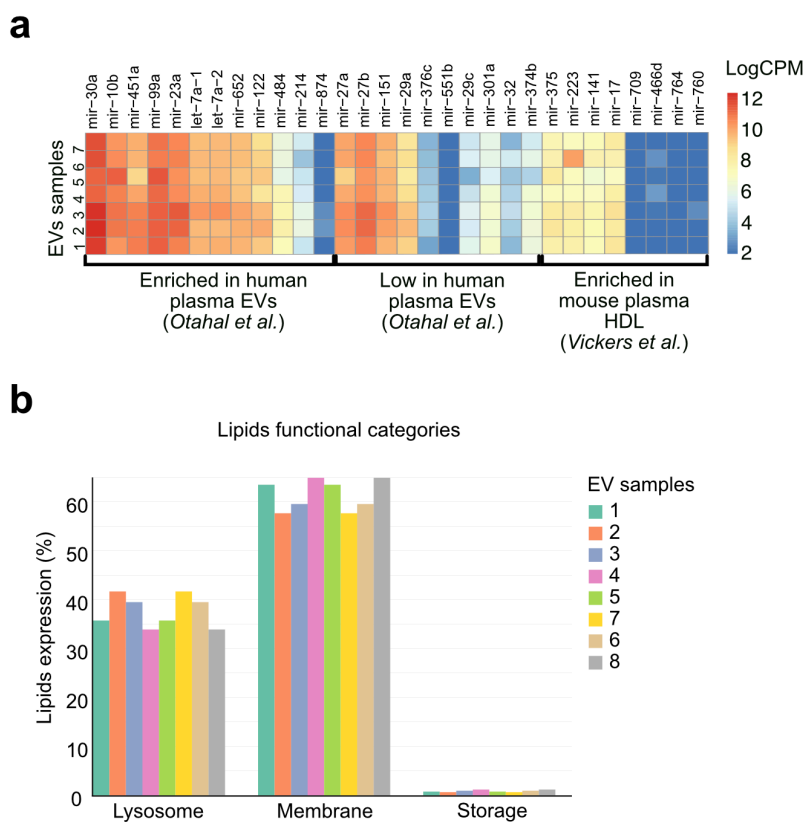
A.A and I.M. conceived and designed the experiments. A.A., L.S., A.O. performed the experiments. L.S. prepared sperm RNA-seq libraries. A.O. performed

metabolomics and lipidomics experiments. A.A performed the rest of molecular experiments and animal experiments. F.M. assisted with animal experiments planning and execution. A.A., A.O. analyzed the data and A.A. prepared the figures with the input from R.G.A.-M and I.M. A.A and I.M. wrote the paper.

2.8 Conflict of interest

The authors declare no conflicts of interest.

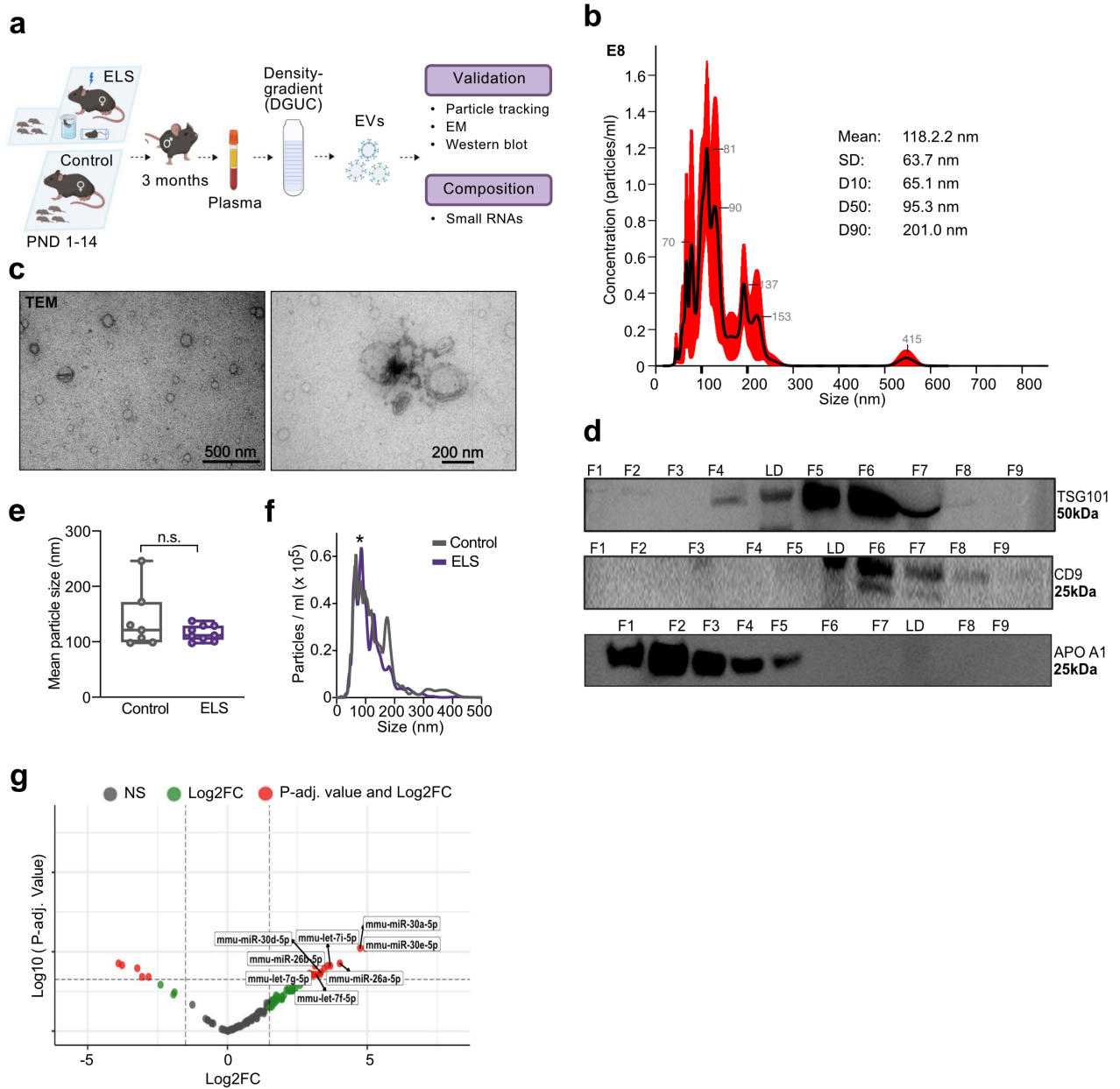
2.9 Supplementary Figures



Supplementary Figure 2-1. Expression of EVs-specific and HDL-specific miRNAs and functional lipids categories in human and mouse plasma EVs.

a. Heatmap of the expression of EV-specific and HDL-specific miRNAs plasma EVs isolated by size-exclusion chromatography.

b. Functional categories of lipids in our plasma EVs preparations.



Supplementary Figure 2-2. Isolation and characterization of ELS plasma EVs by density-gradient ultracentrifugation.

a. Experimental design. Plasma EVs are isolated from ELS and Controls by density-gradient ultracentrifugation, and analyzed by small RNA-sequencing. Created using *Biorender.com*.

b. Concentration of plasma EVs (particles/ml) by size (nm) obtained by nanoparticle tracking. SD (Standard Deviation), D10-50-90 (points at which 10%, 50% and 90% of the sample is contained).

c. Electron microscopy images of EVs from size-exclusion chromatography F4-5. Arrows point to individual EVs.

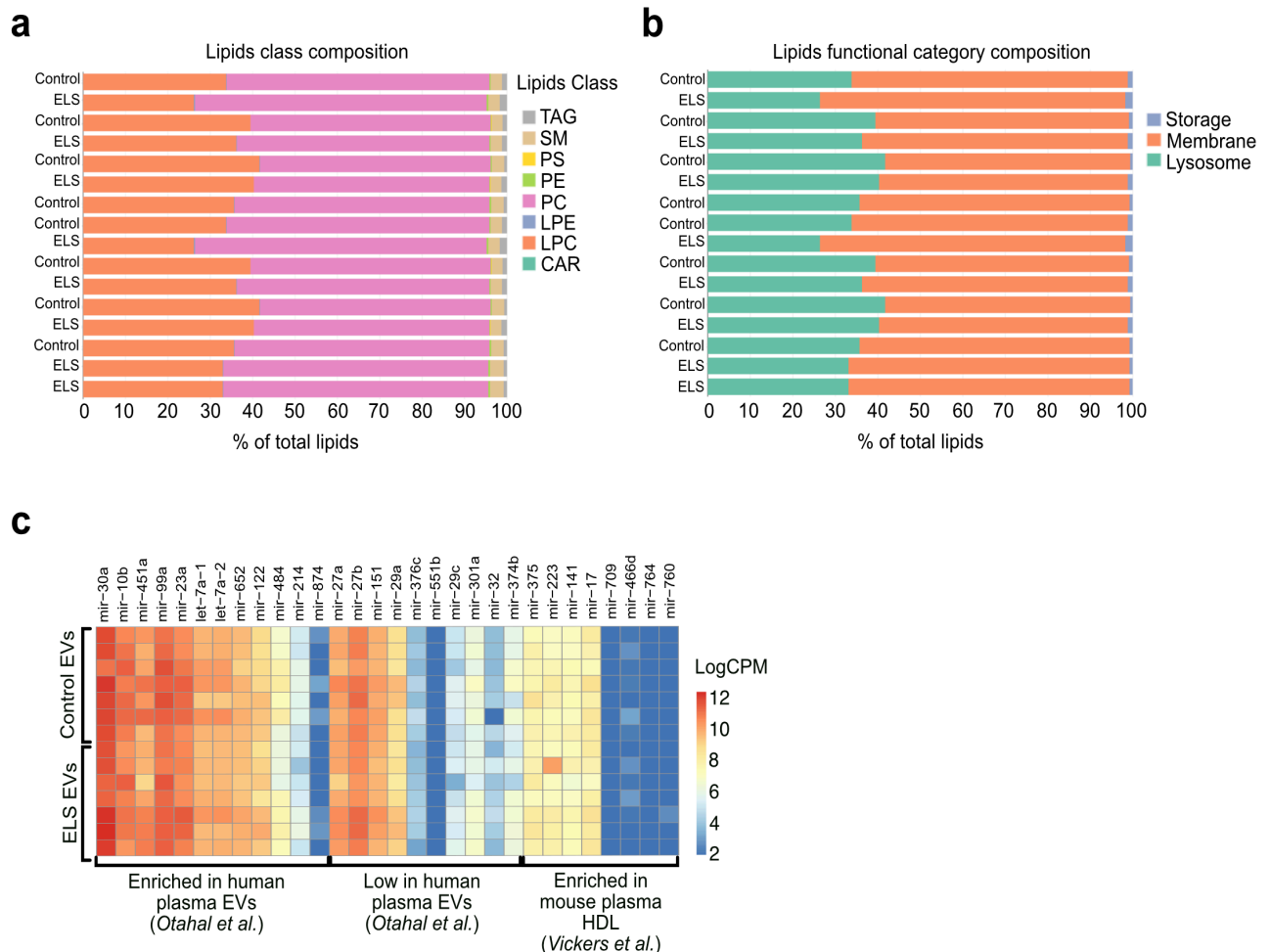
d. Protein levels of extracellular vesicle markers transmembrane protein associated to plasma membrane (CD9) and cytosolic protein (TSG 101), and high-density lipoprotein

marker (ApoA1). C+ (positive control), C- (negative control), M (Molecular weight marker) in the different fractions of size-exclusion chromatography. F 1-9 (fractions 1-9) of the density gradient.

e. Mean particle size of plasma EVs from ELS and Controls (two-tailed unpaired Student's t-test, ns=non-significant, $n=8$ biologically independent samples/group). Error bars are SEM.

f. Concentration of plasma EVs in ELS and Controls ($n=8$ biologically independent samples/group, $*P < 0.05$).

g. Volcano plot of differentially-expressed small RNAs in ELS plasma EVs compared to Controls, isolated by density-gradient. ($n=7$ biologically independent samples/group for small RNAs). Corrected for multiple testing with Benjamini-Hochberg test. Significance: $P_{adj.} < 0.05$.



Supplementary Figure 2-3. Lipid and microRNA profiles of ELS and control plasma EVs.

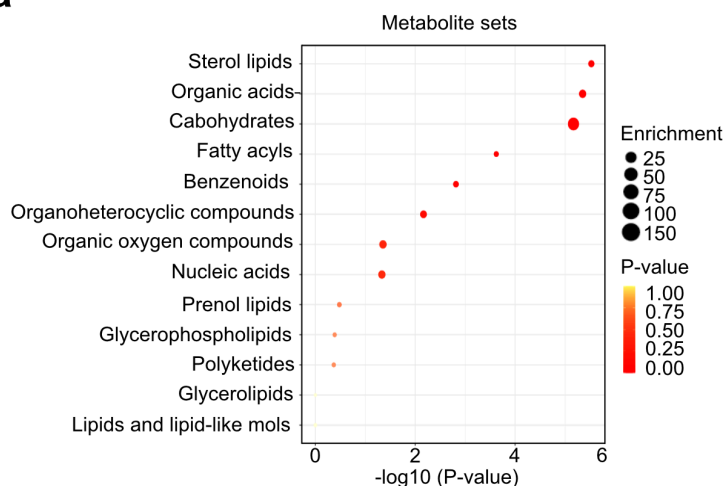
a. Distribution of lipid classes in plasma EVs from ELS and Controls, isolated with size-exclusion chromatography F4-5. $n=8$ biologically independent samples. PC (Phosphatidylcholine), LPC (Lysophosphatidylcholine), SM (Sphingomyelin), TAG

(Triglyceride), PE (Phosphatidylethanolamine), LPE (Lysophosphatidylethanolamine), PS (Phosphatidylserine), CAR (Acylcarnitine). *n*=6 biologically independent samples.

b. Distribution of lipid functional categories in plasma EVs from ELS and Controls, isolated with size-exclusion chromatography F4-5.

c. Heatmap of the expression of EV-specific and HDL-specific miRNAs in ELS and Control plasma EVs.

a

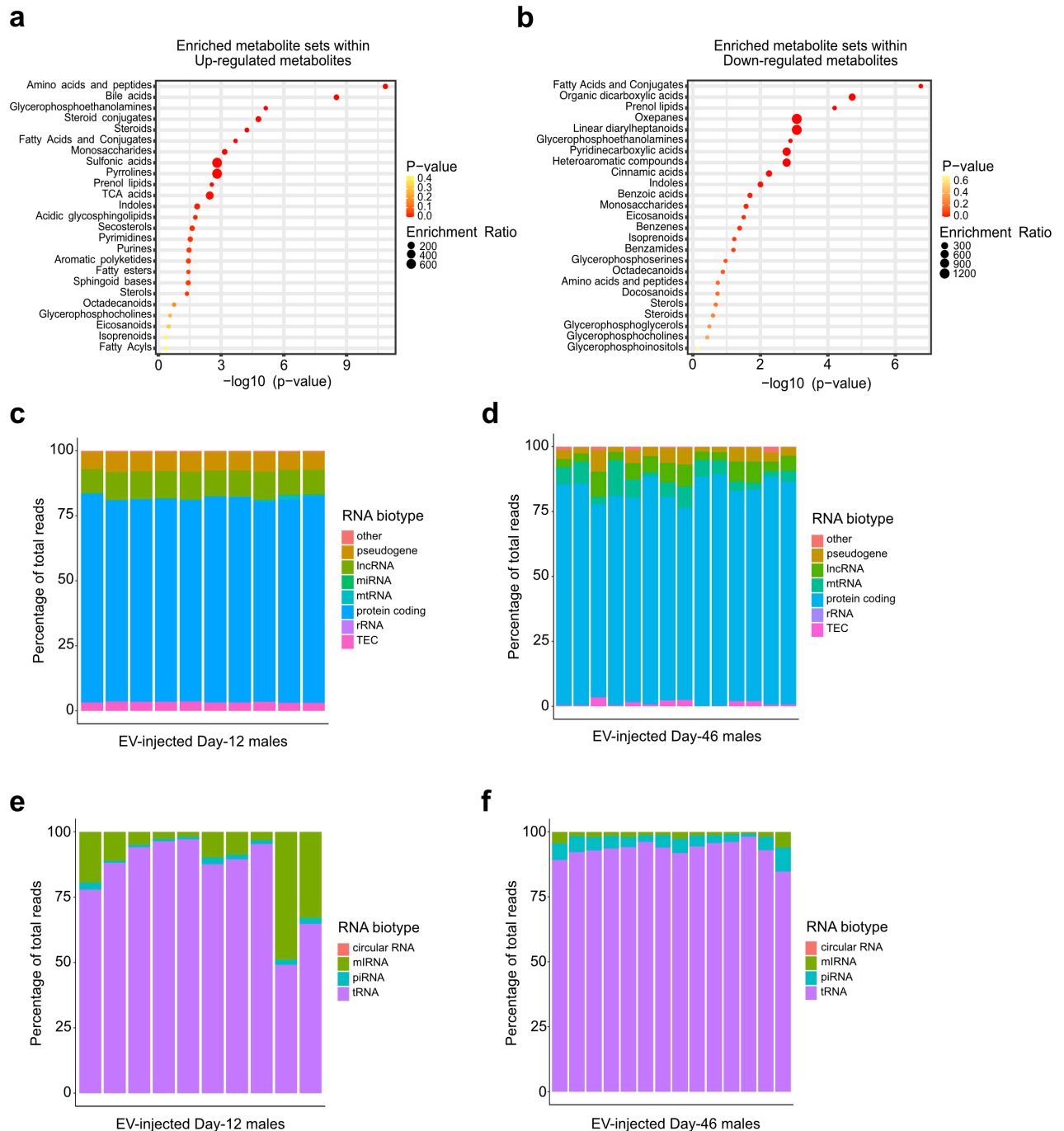


b

Metabolite sets	Total	Expected	Hits	Raw p	Holm p	FDR
Sterol Lipids	2380	0.624	7	2.97E-06	8.02E-05	5.99E-05
Organic acids	914	0.239	5	4.44E-06	0.000115	5.99E-05
Carbohydrates	136	0.0356	3	6.77E-06	0.000169	6.10E-05
Fatty Acyls	8120	2.13	9	0.000238	0.00571	0.00161
Benzenoids	1890	0.494	4	0.00153	0.0352	0.00827
Organoheterocyclic compounds	469	0.123	2	0.00683	0.15	0.0307
Organic oxygen compounds	173	0.0453	1	0.0443	0.931	0.157
Nucleic acids	182	0.0477	1	0.0466	0.931	0.157
Prenol Lipids	1530	0.4	1	0.331	1	0.992
Glycerophospholipids	27000	7.06	8	0.411	1	1
Polyketides	5540	1.45	2	0.428	1	1
Glycerolipids	41500	10.9	2	1	1	1
Lipids and lipid-like molecules	83000	21.7	8	1	1	1

Supplementary Figure 2-4. Metabolite functional analysis of ELS and Control plasma EVs.

a-b. Metabolite sets enriched in plasma EVs isolated by size-exclusion chromatography. Functional analysis of plasma EV metabolites was performed using MetaboAnalyst tool, by looking at the enriched sets of functionally related metabolites. Enrichment ratio was computed as Hits/Expected, where Hits = observed hits, and Expected = expected hits.



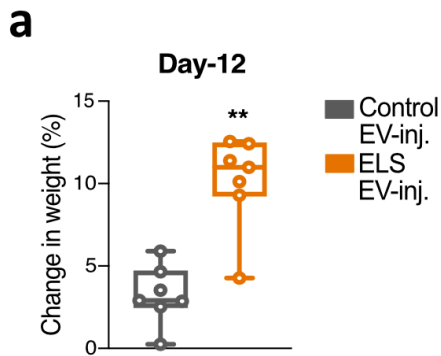
Supplementary Figure 2-5.

a-b. Metabolite sets enriched within differentially up-regulated (a) and down-regulated (b) metabolites in plasma of ELS EV-injected males compared to Controls. $n=7$ biologically independent samples/group. Corrected for multiple testing with Benjamini-Hochberg test. Significance: $P_{adj.} < 0.05$. Metabolites with $P_{adj.} < 0.05$ were selected as input for Metaboanalyst tool to look at compound enrichment.

c-d. Distribution of RNA biotypes as % of total reads in sperm long RNA-sequencing of ELS and Control EV-injected males 12 days (Distribution of RNA biotypes as % of total reads in plasma EVs from size-exclusion chromatography F4-5. $n=6$ biologically independent

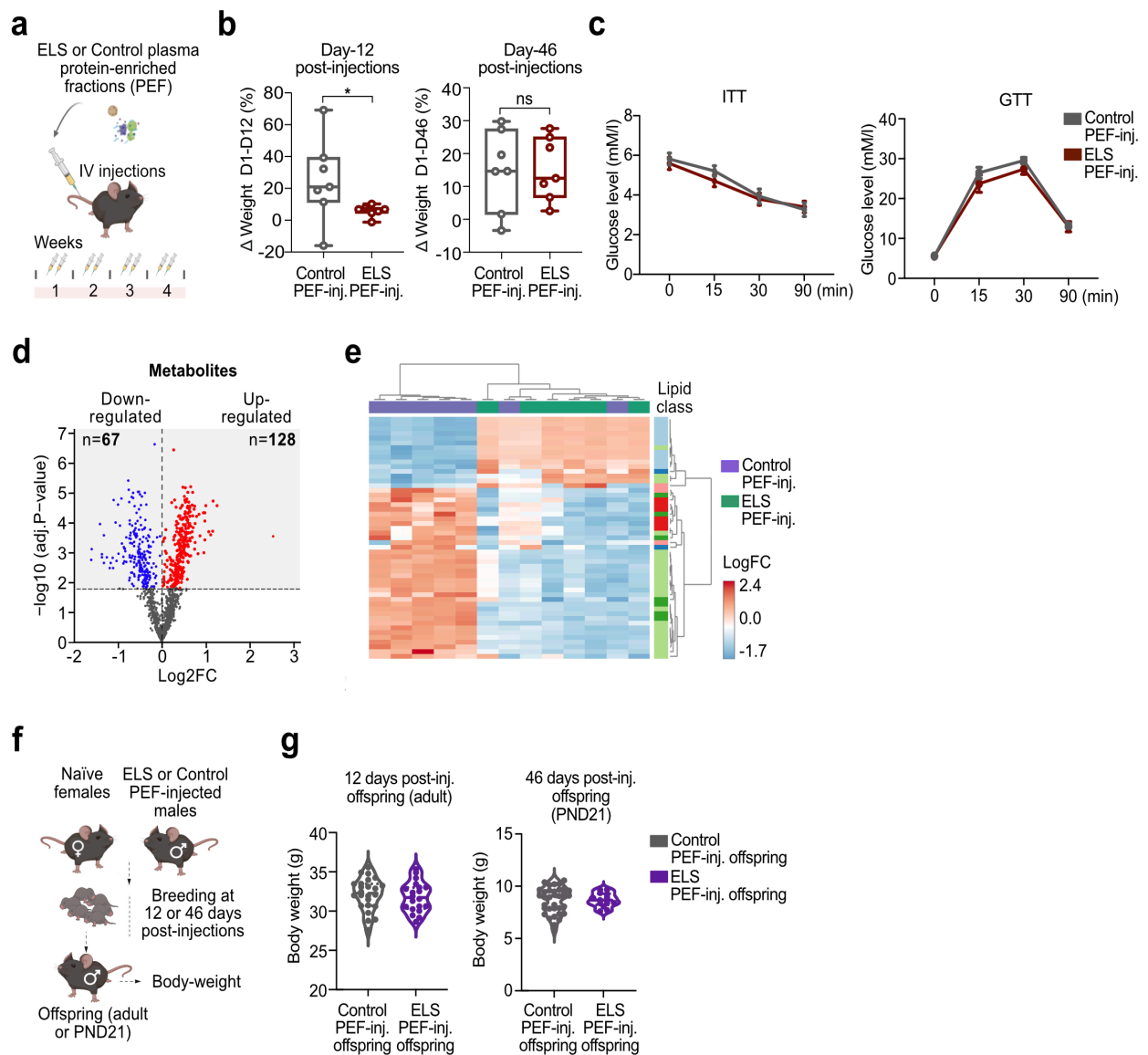
samples (c) or 46 days (d) post-injections. $n=6$ biologically independent samples.

e-f. Distribution of RNA biotypes as % of total reads in sperm small RNA -sequencing of ELS and Control EV-injected males 12 days (Distribution of RNA biotypes as % of total reads in plasma EVs from size-exclusion chromatography F4-5. $n=6$ biologically independent samples (e) or 46 days (f) post-injections. $n=6$ biologically independent samples.



Supplementary Figure 2-6. Change in body weight of ELS EV-injected males.

a. Change in body weight (%) of the ELS or Control EV-injected males at 12 day post-injections compared to 1 day post-injections. Two-tailed unpaired Student's t-test, ns=non-significant.



Supplementary Figure 2-7.

a. Experimental design. Plasma protein-enriched fractions (PEF) from ELS or Controls were intravenously injected into naïve mice for 4 weeks, 2 times per week ($n=7$ biologically independent samples/group). Created using *Biorender.com*.

b. Body weight of the ELS or Control PEF-injected males at 12 day post-injections (Day-12) and % change in body weight at 46 days post-injections (Day-46). Two-tailed unpaired Student's t-test, ns=non-significant, $P_{adj} < 0.05$.

c. Glucose tolerance test (GTT) and insulin tolerance test (ITT) of ELS or Control PEF-injected males.

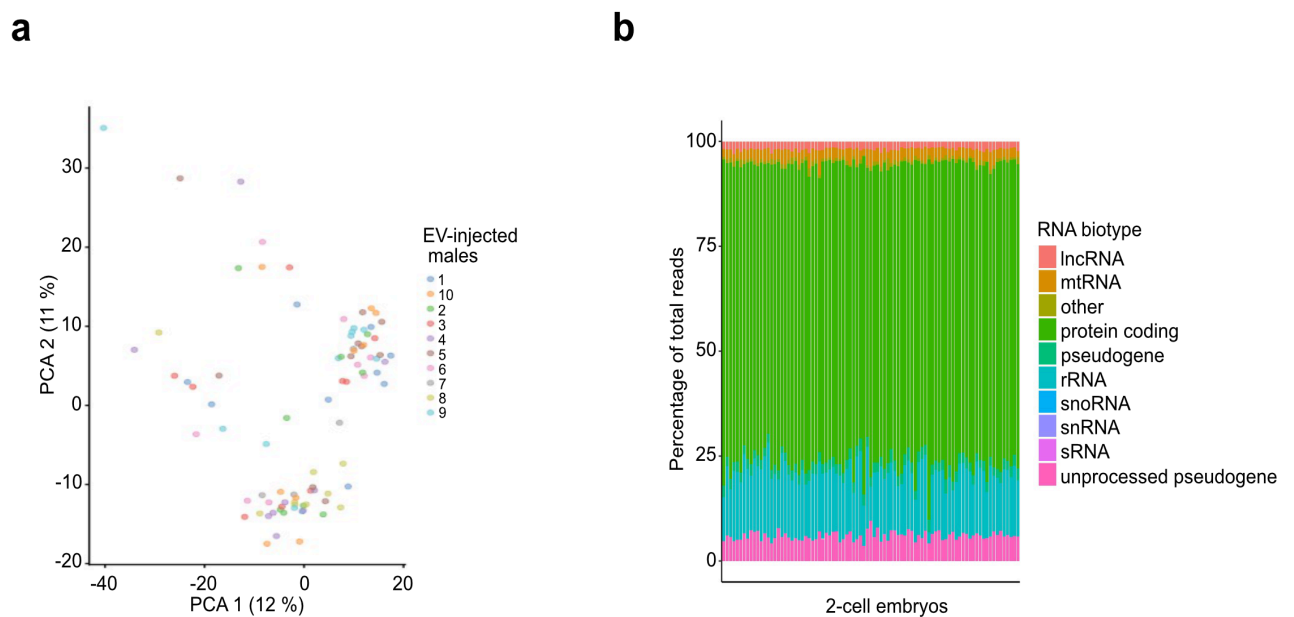
d. Changes in circulating metabolites in plasma of ELS PEF-injected males at 46 days post-injections ($n=7$ biologically independent samples/group). Corrected for multiple testing with Benjamini-Hochberg test. Significance: $P_{adj} < 0.05$. Metabolites with $P_{adj} < 0.05$ were

selected as input for Metaboanalyst tool to look at compound enrichment.

e. Heatmap of significantly changed ($P_{adj.} < 0.05$) plasma lipids in ELS PEF-injected males at 46 days post-injections compared to controls ($n=7$ biologically independent samples/group).

f. Experimental design. ELS or Control PEF-injected males were paired with a naïve female at 12 days and 46 days post-injections to obtain offspring. Created using *Biorender.com*.

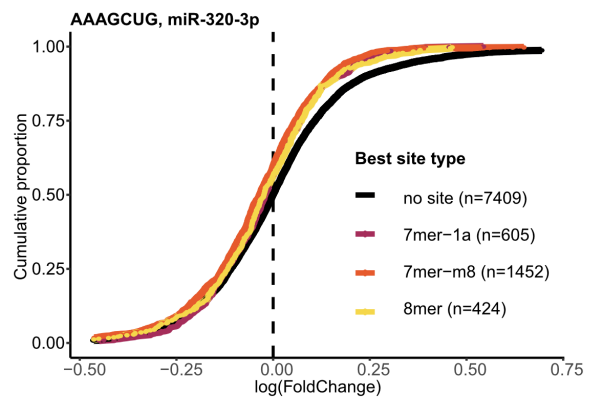
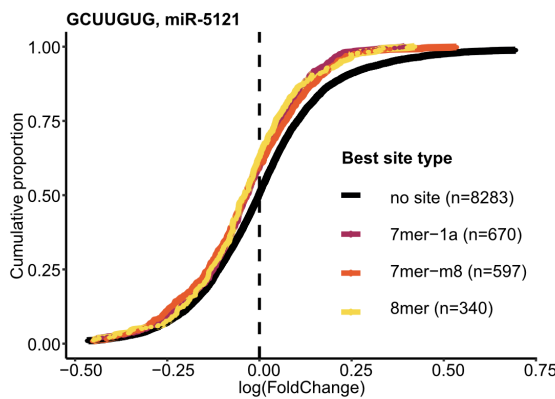
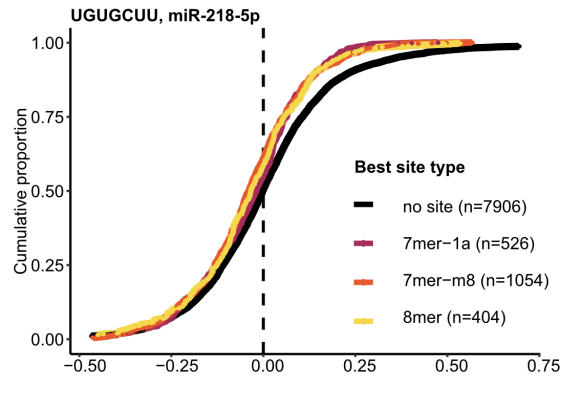
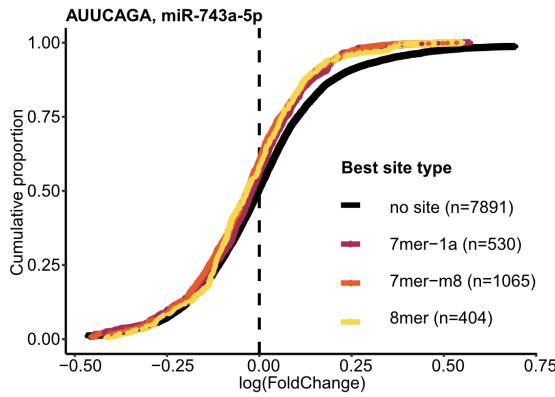
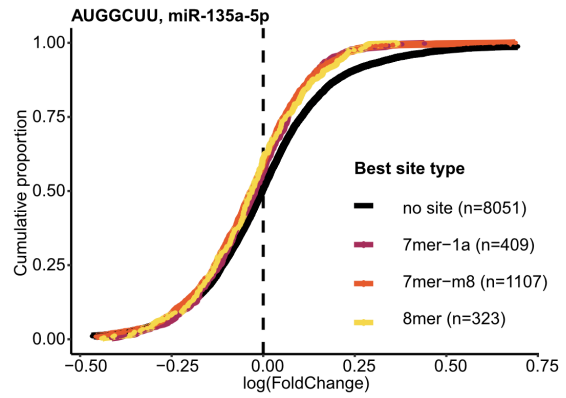
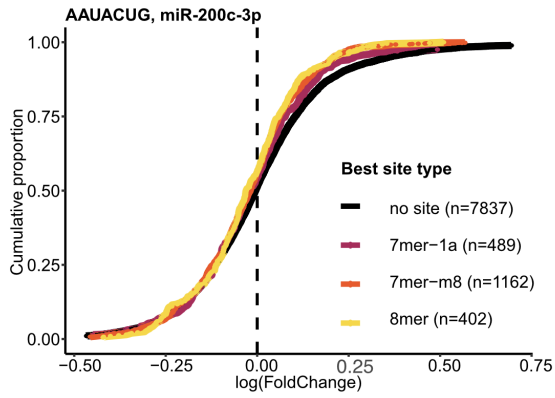
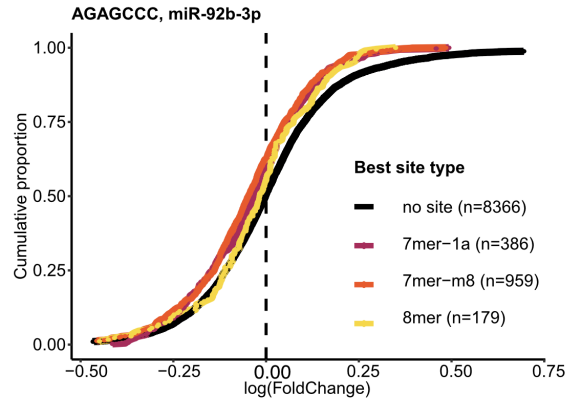
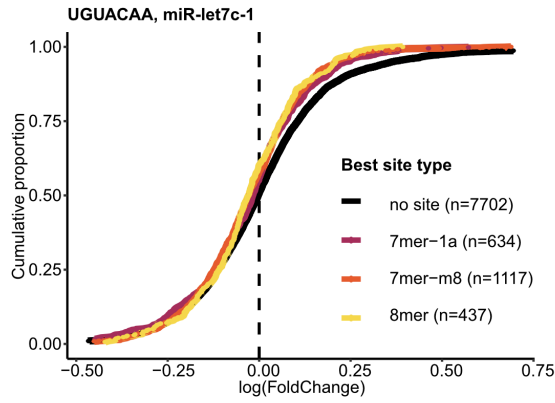
g. Body weight of ELS and Control PEF-injected males' offspring obtained 12 days and 46 days post-injections. Postnatal day 21 (PND21). Two-tailed Student's t- test, treatment effect * $P < 0.05$, ** $P < 0.01$, *** $P < 0.001$, **** $P < 0.0001$. ns=non-significant.



Supplementary Figure 2-8.

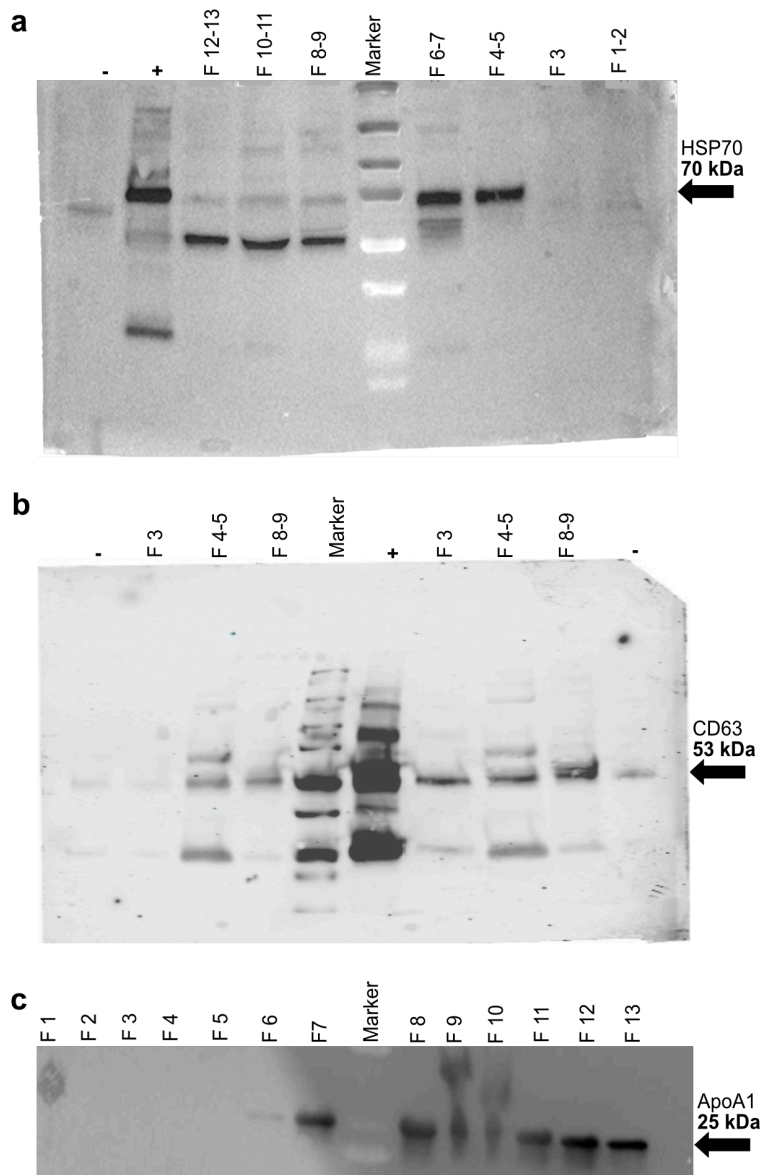
a. Plot of 2 main principal components in the embryo RNA-sequencing data. Colour coding: EV-injected male.

b. Distribution of RNA biotypes as % of total reads in embryos obtained from ELS or Control EV-injected males 12 days post-injections. $n=92$ embryos.



Supplementary Figure 2-9.

a-h. Cumulative distribution plots of all genes in embryos and genes that have different amounts of binding sites to differentially expressed sperm microRNAs in the sperm of ELS EV-injected males 12 days post-injections.



Supplementary Figure 2-10. Full immunoblot images.

a, b. Full immunoblot images of plasma size-exclusion fractions for EV-specific markers HSP70 (a) and CD63 (b).

c. Immunoblot image of plasma size-exclusion fractions for high-density lipoprotein-specific marker ApoA1.

3. Early life stress affects the miRNA cargo of epididymal extracellular vesicles in mouse

Anar Alshanbayeva^{1,2,3}, Deepak K. Tanwar^{1,2,3}, Martin Roszkowski^{1,2,3}, Francesca Manuella^{1,2,3}, Isabelle M. Mansuy^{1,2,3*}

Affiliations:

¹Laboratory of Neuroepigenetics, Brain Research Institute at the Medical Faculty of the University of Zurich

²Institute for Neuroscience of the Department of Health Sciences and Technology, ETH Zurich, Zurich, Switzerland

³Zurich Neuroscience Center, ETH and University of Zurich, Zurich, Switzerland

Corresponding author: Isabelle M. Mansuy; E-mail: mansuy@hifo.uzh.ch

*Published in **Biology of Reproduction**, September 2021;
<https://doi.org/10.1093/biolre/ioab156>*

Description of the contributions to the manuscript.

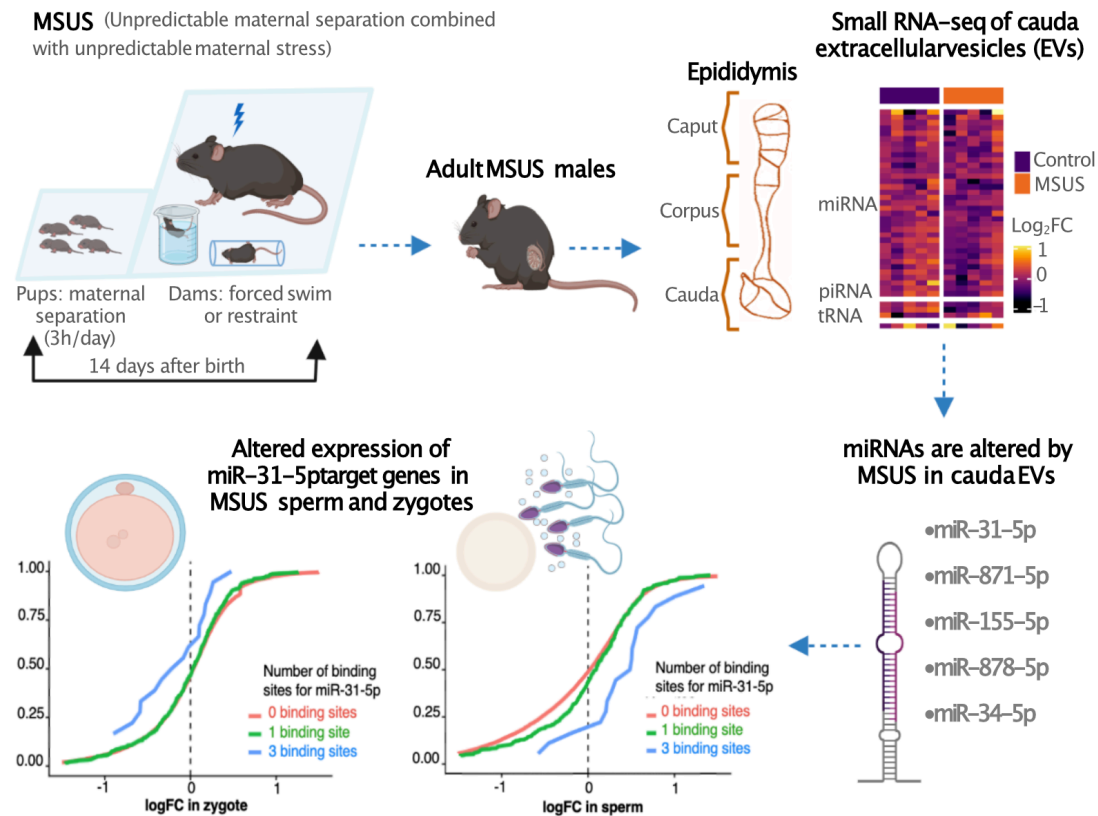
Contributions of Anar Alshanbayeva:

- i. Processed samples, isolated epididymosomes by ultracentrifugation and confirmed their properties by electron microscopy, nanoparticle-tracking analysis and immunoblotting.
- ii. Isolated RNA from epididymosomes and prepared small RNA-sequencing libraries.
- iii. Performed RT-qPCR of caput epididymis samples.
- iv. Analyzed small RNA-sequencing data, with the help of Deepak K. Tanwar.
- v. Processed samples for cholesterol measurements.
- vi. Prepared the figures together with Deepak K. Tanwar.
- vii. Designed the study and interpreted the data together with Isabelle M. Mansuy.
- viii. Wrote the Manuscript together with Isabelle M. Mansuy and Deepak K. Tanwar.

Contribution of the other authors:

- i. Deepak K. Tanwar assisted in the analysis of epididymosomal small RNA-sequencing, preparation of the figures related to epididymosomal small RNA-sequencing and writing of the Manuscript.
- ii. Francesca Manuella and Martin Roszkowski performed the MSUS breeding and collected tissue samples.
- iii. Isabelle M. Mansuy designed, coordinated and funded the study, performed data interpretation and wrote the Manuscript together with Anar Alshanbayeva.

3.1 Graphical Abstract



3.2 Abstract

Sperm RNA can be modified by environmental factors and has been implicated in communicating signals about changes in a father's environment to the offspring. The small RNA composition of sperm could be changed during its final stage of maturation in the epididymis by extracellular vesicles released by epididymal cells. We studied the effect of exposure to stress in early postnatal life on the transcriptome of epididymal extracellular vesicles using a mouse model of transgenerational transmission. We found that the small RNA signature of epididymal extracellular vesicles, particularly miRNAs, is altered in adult males exposed to postnatal stress. In some cases, these miRNA changes correlate with differences in the expression of their target genes in sperm and zygotes generated from that sperm. These results suggest that stressful experiences in early life can have persistent biological effects on the male reproductive tract that may in part be responsible for the transmission of the effects of exposure to the offspring.

Keywords: epigenetics, epididymis, miRNAs, epididymosomes, early life stress, sperm, extracellular vesicles.

3.3 Introduction

Post-testicular maturation of spermatozoa in the epididymis is an elaborate process that involves modifications of sperm RNA, protein and lipid content (Tamessar et al. 2021; Sharma et al. 2016; Nixon et al. 2015; Rejraji et al. 2006; Skerget et al. 2015). The epididymis is segmented into different parts, including the initial segment, caput, corpus and cauda. Each segment has a distinct gene expression profile, and different protein and lipid composition. Some modifications in epididymal spermatozoa are conserved across species (Sellem et al. 2020). For example, approximately 50% of miRNAs, a class of small RNAs that are modified during caput to cauda epididymis transit, is identical in mouse and bovine spermatozoa (Sellem et al. 2020). One mechanism by which small RNA load in spermatozoa is modified along the epididymis is by uptake of extracellular vesicles (EVs), also known as epididymosomes, which are produced by epididymal epithelial cells (Reilly et al. 2011). Studies have shown that epididymosomes can be taken up by maturing sperm through proteins present on the sperm head such as dynamin in mice and tetraspanins or syntenins in humans (Reilly et al. 2011; Cabarello et al. 2013; Thimon et al. 2008; Zhou et al. 2019). Co-incubation experiments provided evidence for epididymosome-mediated transfer of miRNAs to spermatozoa (Reilly et al. 2011). Exogenous DNA and RNA can also be directly taken up by spermatozoa via artificial liposomes (Bachiller et al. 1991).

However, it is still not clear if changes in small RNA composition of spermatozoa occurring during epididymal transit are required for embryonic development, and studies on the subject have been conflicting (Suganuma et al. 2005; Conine et al. 2018). Changes in sperm small RNA have nevertheless been suggested to play a role in the transmission of information about paternal experiences to the progeny and can influence their developmental trajectory (Sharma et al. 2016; Chan et al. 2020; Gapp et al. 2014). Epididymosomal small RNA content can also be altered by exposure, for instance, to dietary insult and stress (Sharma et al. 2016; Chan et al. 2020). For instance, epididymosomal miRNAs are changed by exposure to chronic stress (Chan et al. 2020) and low-protein diet in mice (Sharma et al. 2016).

Transmission of information about paternal exposure to the offspring depends on the type of exposure, its duration and the developmental window at which it is applied. To date, little is known about the long-term effects of early life stress, particularly stress experienced after birth, on epididymosomal small RNA composition

in adulthood, and whether any changes to this composition can influence gene expression in sperm and in zygotes generated from that sperm. Using a transgenerational mouse model of postnatal stress induced by unpredictable maternal separation combined with unpredictable maternal stress, MSUS (Franklin et al. 2010), we show that the miRNA signature of cauda epididymosomes in adult males is altered by exposure, and that this alteration correlates with changes in the expression of their target genes in sperm and in zygotes.

3.4 Results

3.4.1 Isolation of cauda epididymosomes confirmed by several methods

To characterize the RNA composition of cauda epididymosomes, epididymosomes were isolated by high-speed ultracentrifugation from adult control males and males exposed to MSUS (**Fig. 3-1a**). MSUS consists of exposing newborn pups to unpredictable maternal separation for 3 hours daily and subjecting dams to unpredictable maternal stress during separation (Franklin et al. 2010). Adult MSUS-exposed and control males were euthanized and cauda epididymis was collected. Successful isolation of cauda epididymosomes was confirmed by electron microscopy, immunoblotting and nanoparticle-tracking analyses (**Fig. 3-1**). The presence and purity of epididymosomes was further validated by staining with the EV-specific marker CD9 and confirming the absence of the cellular marker GAPDH (**Fig. 3-1b**). Size analysis by nanoparticle-tracking indicated that the collected particles are 50-300 nm in diameter (**Fig. 3-1d**), and imaging by transmission electron microscopy showed the typical cup-shaped structures of epididymosomes (**Fig. 3-1c; Supplementary Fig. 3-1a**) (Choi et al. 2017). RNA profiling by high-resolution automated electrophoresis showed enrichment for small RNAs of different length, similar to previous studies on cauda epididymosomal RNA content (**Supplementary Fig. 3-1b**) (Sharma et al. 2016; Conine et al. 2018).

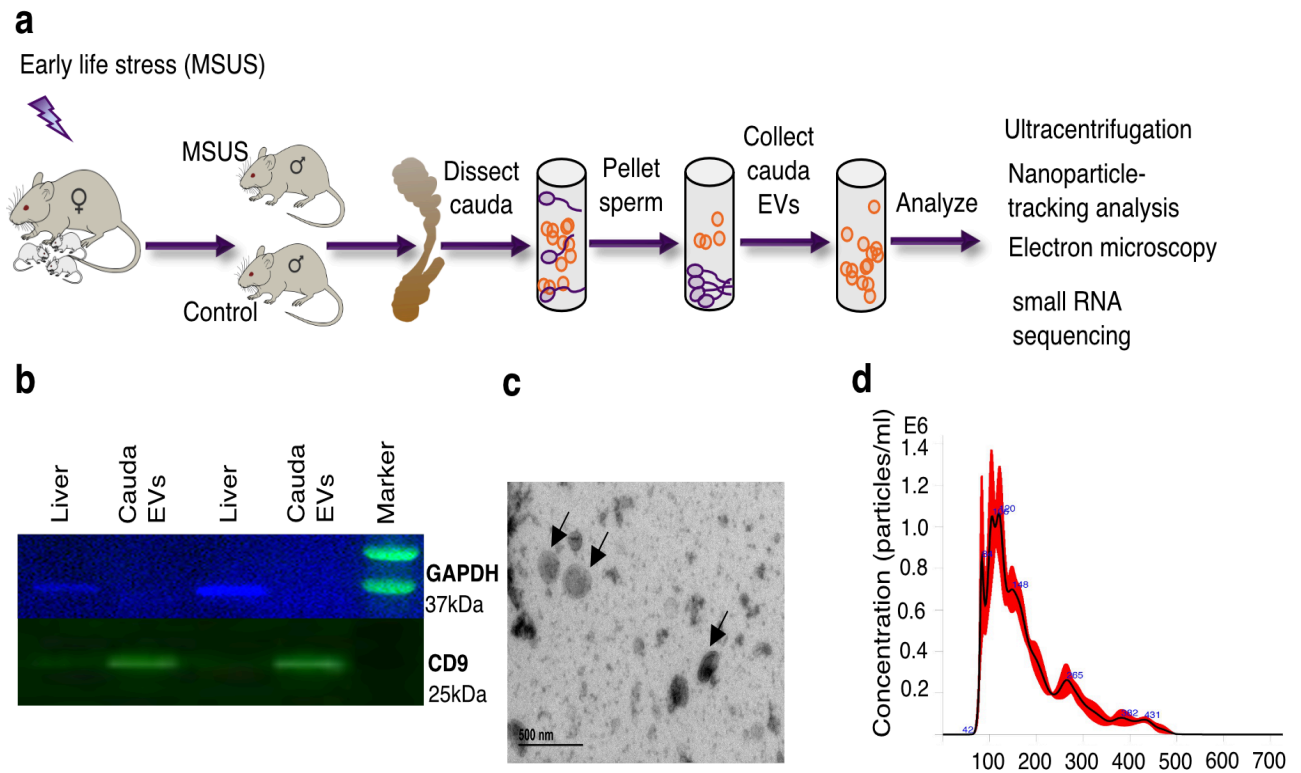


Figure 3-1. Isolation and characterization of cauda epididymosomes.

a. Schematic representation of cauda epididymosomes preparation.

b. Immunoblot analysis was used to confirm the purity of isolation by staining with epididymosomal marker CD9 and absence of cellular marker GAPDH in the ultracentrifuged pellet.

c. Electron microscopy images of the preparations were used to assess the size and heterogeneity of the isolated populations. Arrows indicate cauda epididymosomes.

d. Nanoparticle-tracking analysis by dynamic light scattering showed particles of expected size of 50-300 nm.

3.4.2 The number and size of epididymosomes in adult males are not altered by postnatal stress

We next examined the number and size of cauda epididymosomes in adult MSUS and control males by dynamic light scattering. No significant difference could be detected between MSUS and control males (**Fig. 3-2a, 2b**). Since most epididymosomal production occurs via apocrine secretion from principal cells located in caput epididymis, we also examined the expression of genes involved in extracellular vesicles exocytosis. We chose Ras-related protein Rab-5A (*Rab5*) and

Ras-related protein Rab-7A (*Rab7*), which are involved in vesicle trafficking, the SNARE family protein vesicle-associated membrane protein 7 (*Vamp7*) and SNARE recognition molecule synaptobrevin homolog YKT6 (*Ykt6*), involved in vesicle fusion. No significant change in the expression of these genes could be detected in caput epididymis between MSUS and control adult males (**Fig. 3-2c**). However, we observed a consistent trend (not statistically significant) for decreased expression of all genes involved in extracellular vesicles secretion in caput epididymis of MSUS mice (**Fig. 3-2c**).

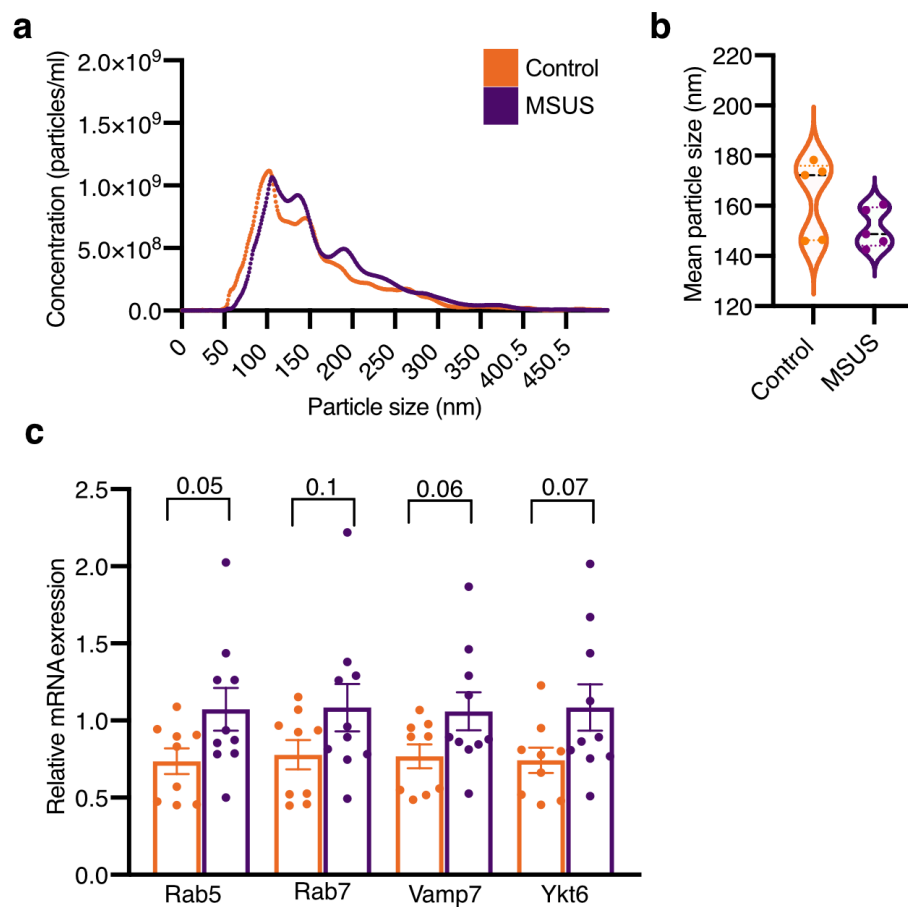


Figure 3-2. Comparison of epididymosomal number, size and release machinery in adult MSUS and control males.

a. Nanoparticle-tracking analysis showed no difference in the number of cauda epididymosomes between MSUS and control males. The plots were generated from average values across replicates (N = 5 animals/group). Data are presented as mean \pm standard error of the mean (SEM). $P < 0.05$.

b. Quantification of nanoparticle-tracking analysis showed the mean size of cauda epididymosomes was not changed between the two groups (N = 5 animals/group). Data are presented as mean \pm SEM. $P < 0.05$.

c. Expression of genes involved in vesicular secretion in the caput epididymis from adult males measured by qRT-PCR. The experiments were performed in triplicates without pooling (N = 8 animals/group). Expression of Gapdh was used as endogenous control to normalize the expression level of the target genes. Data are presented as mean \pm SEM. $P < 0.05$.

3.4.3 miRNAs are persistently altered by postnatal stress in cauda epididymosomes

Epididymosomal small RNAs are known to be affected by changing environmental conditions in rodents. Small RNAs, like tRNA-derived fragments (tRFs), miRNAs and more recently rRNA-derived small RNA fragments are believed to act as messengers of a father's experiences that can be transferred to the offspring (Sharma et al. 2016; Chan et al. 2020; Wang et al. 2021; Zhang et al. 2018). Our previous work showed that early postnatal stress alters small and long RNA content in sperm of adult males (Gapp et al. 2014; Gapp et al. 2020). Since caudal sperm and epididymosomal small RNA profiles are highly similar (Sharma et al. 2016), we examined whether small RNA content of cauda epididymosomes is also altered by postnatal stress. We extracted RNA from cauda epididymosomes of adult MSUS and control males and prepared small RNA-seq (sRNA-seq) libraries. RNAs of different size were observed in cauda epididymosomes, with the majority of small RNA reads mapping to tRNAs as previously observed (**Fig. 3-3a**) (Sharma et al. 2016). When plotting the results of differential expression analysis of small RNAs ($P < 0.05$) between MSUS and control sample, the majority of nonsignificant differences in small RNAs appeared to be in miRNAs, although some differences in tRNAs and piRNAs were also detected (**Fig. 3-3b**). We next performed size-selection on the same libraries to enrich for miRNAs and then, we re-sequenced the libraries (**Supplementary Fig. 3-2a, 2c**). As expected, size-selection did not alter the abundance of miRNAs and uniformly enriched the miRNA fraction in all samples (**Supplementary Fig. 3-2b, 2d**). Differential expression analysis of miRNAs biotypes from the combined sequencing datasets after batch effect correction revealed changes in several miRNAs in MSUS cauda epididymosomes (**Supplementary Table 3-1**). These include upregulation of miR-878-5p, miR34c-5p, miR-881-3p and downregulation of miR-31-5p and miR-155-5p (adjusted $P \leq 0.1$). Differential expression analysis on all small RNA biotypes from the combined datasets showed that 70% of all significantly altered small RNAs correspond to miRNAs, 15% to tRNAs, 15% to piRNAs and snoRNAs, while rRNAs are not

changed (**Supplementary Table 3-4**). Pathway analysis of top candidate RNAs from miRNA-based analysis after size-selection revealed that the most up- and down-regulated miRNAs ($P < 0.05$) have target mRNAs that encode proteins involved in fatty acid metabolism, steroid biosynthesis, lysine degradation and thyroid hormone signaling (**Fig. 3-3c**). Notably, similar pathways are altered in plasma of MSUS males during postnatal life and adulthood as shown by metabolomic analysis (van Steenwyk et al. 2020). In particular, metabolites implicated in polyunsaturated fatty acid biogenesis were up-regulated, whereas steroidogenesis and the steroidogenic ligand aldosterone were down-regulated (van Steenwyk et al. 2020). Steroidogenesis was already altered at postnatal day 28 in MSUS males, with total cholesterol significantly decreased in testis (**Fig. 3-3d**) and HDL cholesterol significantly increased in liver (**Fig. 3-3f**). Since the primary role of HDL cholesterol in blood is to transport excess cholesterol from peripheral tissues to liver, an increase in HDL in liver is consistent with a decrease in testis. However, cholesterol was no longer altered in testis of adult MSUS males (**Fig. 3-3e**), suggesting a transient alteration. The androgen receptor, which the cholesterol derivatives, androgens bind to, was decreased in adult caput epididymis (**Fig. 3-3g**), suggesting potential secondary effects of lower cholesterol in testis when occurring in early postnatal life.

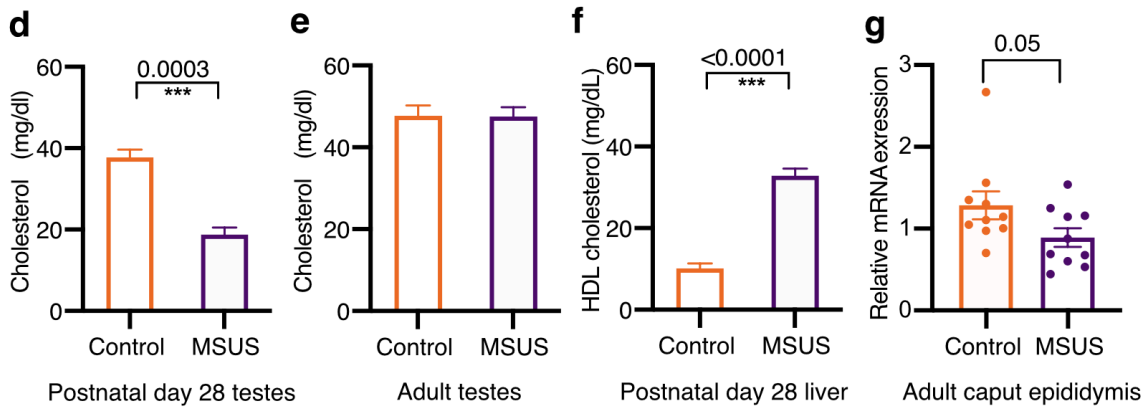
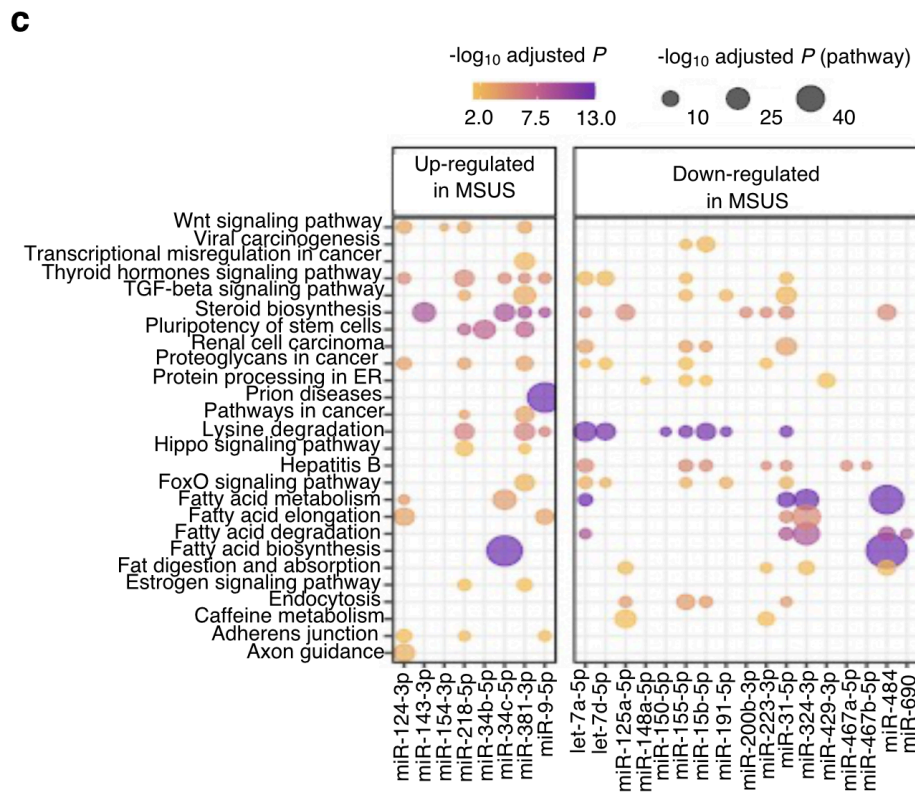
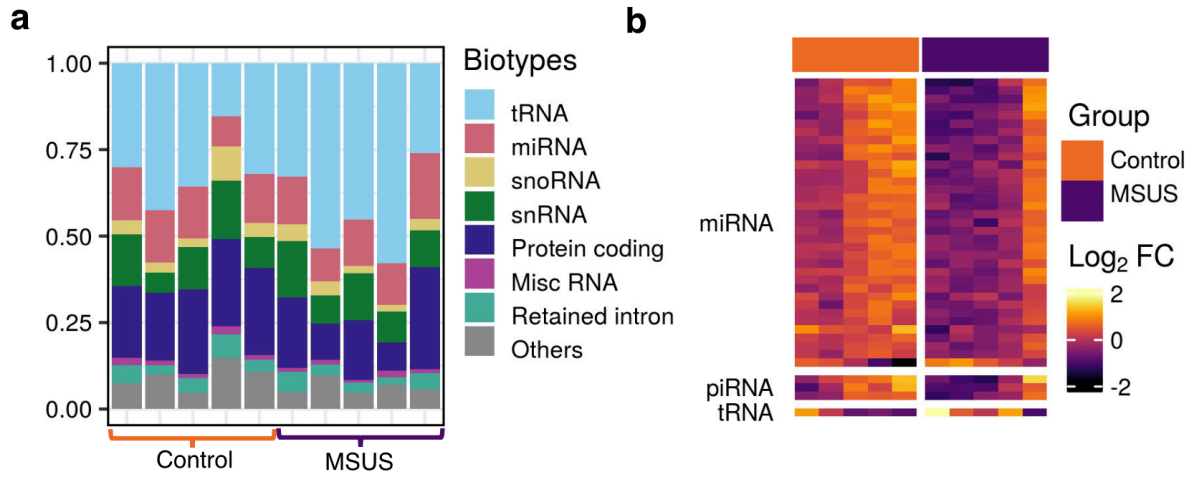


Figure 3-3. Target pathways of up- and down-regulated miRNAs in adult MSUS cauda epididymosomes and alterations in steroidogenesis in postnatal and adult MSUS males.

a. Representative distribution of RNA biotypes from cauda epididymosomal sequencing (N = 10 animals, 5 animals/group).

b. Heatmap of the most abundant small RNAs (n = 39). Expression fold-change (\log_2 FC) was calculated by subtracting \log_2 counts per million (CPM) of MSUS from controls. Each row depicts a small RNA and each column depicts a sample. Samples and RNAs are ordered by “PCA” method using seriation (R package).

c-e. Dot plot of miRNAs and pathways. Color-scale of the dot represents $-\log_{10}$ adjusted *P* of miRNA in a pathway and size of the dot represents $-\log_{10}$ adjusted *P* of the pathway. Total cholesterol measurements in whole testes of males at postnatal day 28 (N = 4 males/group) (**d**) and adulthood (N = 10 Controls, N = 7 MSUS) (**e**).

f. HDL cholesterol level in the liver of males at postnatal day 28 (N = 6 males/group).

g. Relative expression level of the androgen receptor in adult caput epididymis measured by qRT-PCR. qRT-PCR experiments were performed in triplicates, without pooling (N = 10 animals/group). (**d-g**) Data are presented as mean \pm standard error of the mean (SEM). *P* < 0.05.

3.4.4 mRNA targets of miRNAs from cauda epididymosomes are altered by postnatal stress in sperm and in zygotes

The relative abundance of miRNAs in cauda epididymosomes and mature sperm significantly correlated (**Fig. 3-4c**), consistent with prior findings (Sharma et al. 2016; Chan et al. 2020). Since cauda epididymosomes carry small RNA payloads matching those of mature sperm and are part of the ejaculate (Frenette et al. 2005; Belleannée et al. 2013), they may contribute to the information delivered to the oocyte upon fertilization. Therefore, we looked at the mRNA targets of miRNAs significantly changed in MSUS cauda epididymosomes in 2 previously published analysis of genes identified in MSUS sperm and in zygotes derived from MSUS males (*P* < 0.05) (Gapp et al. 2020). For this, we plotted the cumulative log fold-change distribution of all genes from differential expression analysis of sperm or zygotes versus the number of conserved binding sites for miRNAs significantly changed by MSUS in cauda epididymosomes (**Fig. 3-4a, 4b; Supplementary Fig. 3-5**). Target genes with 3 binding sites for miR-31-5p, a miRNA differentially expressed in MSUS cauda epididymosomes, had increased expression in sperm and decreased expression in

zygotes from MSUS males (**Fig. 3-4a, 4b; Supplementary Table 3-2, 3**). However, not all targets of miRNAs significantly altered in MSUS cauda epididymosomes showed corresponding changes in expression in sperm and zygotes (**Supplementary Fig. 3-5**). We then conducted miRNA-gene interaction analysis based on experimentally validated data from Tarbase (Vlachos et al. 2017). This analysis showed that, overall, the 5 miRNAs significantly changed in MSUS cauda epididymosomes target genes that are part of pathways involved in steroid biosynthesis, ECM-receptor interaction and cell adhesion molecules (**Fig. 3-4d**).

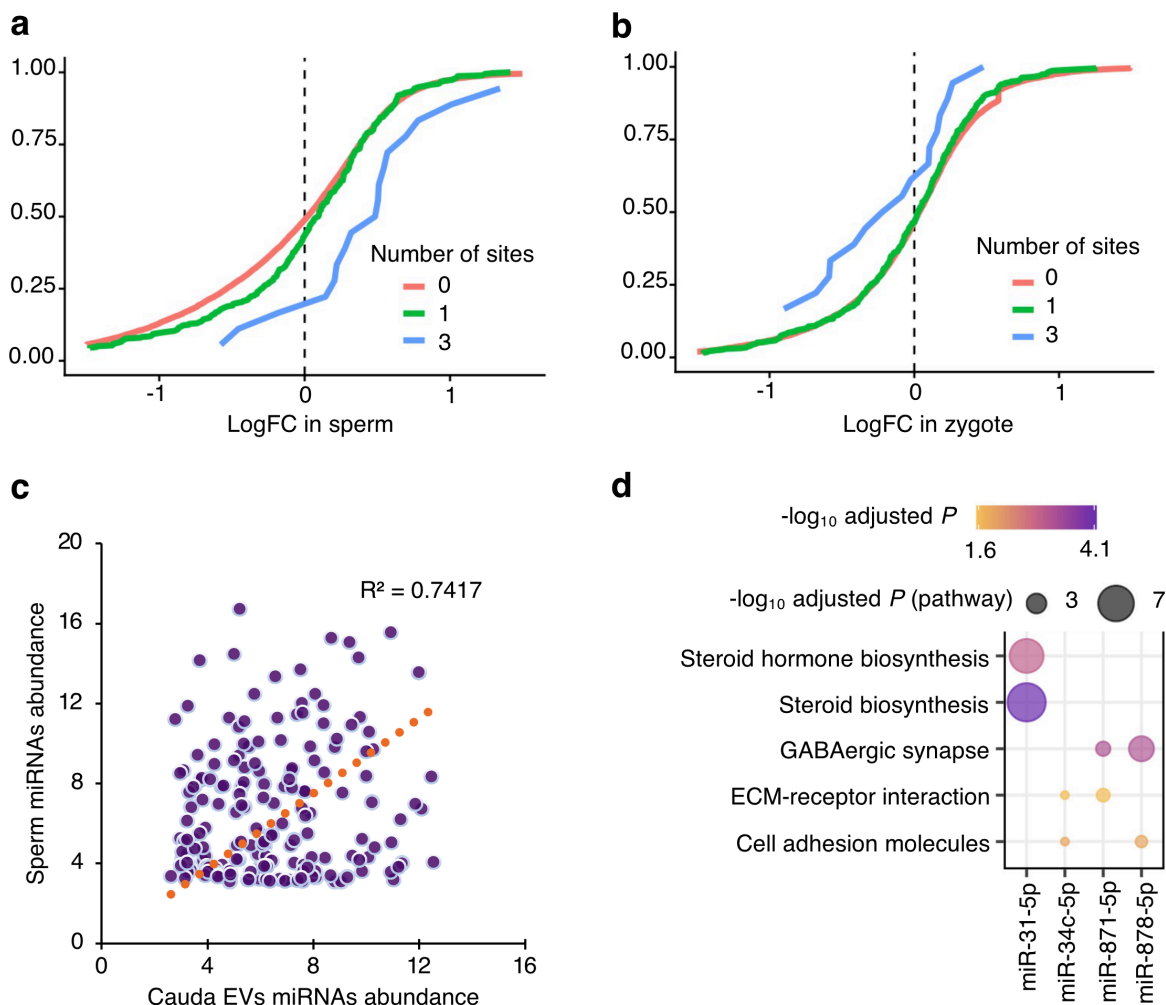


Figure 3-4. Targets of miRNAs from cauda epididymosomes are altered by MSUS in sperm and zygotes.

a-b. Cumulative distribution plots of miR-31-5p targets from 5 months old MSUS and control caudal sperm RNA-seq (**a**) and from RNA-seq of zygotes originating from 3 months old MSUS and control males (**b**).

c. miRNA abundance of sperm plotted against abundance in cauda epididymosomes. Coefficient of determination (R^2) = 0.74.

d. Dot plot of the top target pathways (adjusted $P < 0.05$) of miRNAs differentially expressed (adjusted $P \leq 0.1$) in adult MSUS cauda epididymosomes. Color-scale of the dot represents $-\log_{10}$ adjusted P of miRNA in a pathway and size of the dot represents $-\log_{10}$ adjusted P of the pathway.

3.5 Discussions

The effects of environmental factors on RNA in the male reproductive tract, in particular, the epididymis have been examined in rodent models. Until now, most models have used invasive exposure such as dietary insult or injection of endocrine disruptors, applied prenatally and sometimes before conception. Few studies have examined the effects of non-invasive psychological/emotional exposure such as stress in early life and the effects on epididymal RNA in adulthood (Chan et al. 2020). This study examines if postnatal stress affects RNAs in EVs released from the cauda epididymis and whether this has consequences for mature sperm and zygotes generated from that sperm.

Using a transgenerational mouse model of early postnatal stress, we show that several miRNAs, including miR-871-3p, miR-31-5p, miR-155-5p, miR-878-5p and miR-34c-5p are altered in cauda epididymosomes in adult males exposed to postnatal stress, and that the targets of some of these miRNAs are affected in mature sperm and zygotes. Particularly, miR-31-5p is significantly decreased in cauda epididymosomes and its target genes are up-regulated in sperm but down-regulated in zygotes generated from that sperm, suggesting an over-compensation during early development. This may also be due to the heterogeneity of epididymosomes which have different size, biogenesis and cellular targeting (Sullivan et al. 2015), leading to a dissociation between the RNA content of epididymosomes and transcriptional changes in zygotes. It has been suggested that different subsets of epididymosomes have different roles. While a subset communicates with spermatozoa during sperm epididymal transit (Sharma et al. 2016; Reilly et al. 2016), another subset serves in the communication within epididymal epithelial cells (Belleannée et al. 2013), and a third one is delivered as part of seminal fluid during fertilization (Frenette et al. 2005; Belleannée et al. 2013). Thus owing to their heterogeneity, not all cauda epididymosomes or their cargo are delivered to the oocyte upon fertilization, which may explain the differences in miRNAs targets that are affected in sperm and zygotes.

Several of the differentially expressed miRNAs in MSUS cauda epididymosomes play a role in metabolic processes and early development (Reza et al. 2019). For instance, miR-31-5p is involved in glucose metabolism and fatty acid oxidation (Reza et al. 2019). In humans, its target complement C1q Tumor Necrosis Factor-Related Protein 9A (*CTRP9*) protein is negatively correlated with the amount of visceral fat and positively associated with a beneficial glucose and metabolic phenotype (Shao et al. 2017). This is consistent with the observation that glucose and insulin metabolism are also affected by MSUS (Gapp et al. 2014; Franklin et al. 2010). The level of other miRNAs is significantly increased or decreased in MSUS epididymosomes, such as miR-155-5p, which facilitates differentiation of mouse embryonic stem cells, or miR-34c-5p which initiates the first embryonic cleavage in mice (Reza et al. 2019).

The first days after birth are a sensitive period for the development and the establishment of cellular niches in tissues. Epithelial cells in the epididymis, which are the source of epididymosomes, undergo differentiation and expansion postnatally until puberty (Robaire et al. 2002). Once their expansion is completed, epididymal epithelial cells remain at a nearly constant number in adulthood. If they can be modified by prior exposure, they may therefore carry a memory of exposure into adulthood. The postnatal development and differentiation of epididymal epithelial cells primarily depend on testicular signals (Robaire et al. 2002; Robaire et al. 2011; Zhu et al. 2000; Bilińska et al. 2006). Since chronic stress affects the coupling of the hypothalamus-pituitary and hypothalamus-gonadal axes, stress-related decrease in steroidogenesis can profoundly affect the differentiation and expansion of epididymal epithelial cells in early postnatal life. A number of studies have shown the importance of the abundance of androgens during postnatal life for epididymal development (Robaire et al. 2002). Thus, the availability of testicular cholesterol during epididymal cells differentiation has implications for these cells. Systemic alteration in cholesterol metabolism seen in young MSUS males (decreased total cholesterol in testis and increased HDL cholesterol in liver) may contribute to metabolic changes seen in adult animals, for instance in plasma steroidogenesis and fatty acid pathways, and to alterations in glucose and insulin metabolism in adult MSUS males. Moreover, androgen-dependent miRNAs miR-878-5p and miR-871-3p are significantly increased in cauda epididymosomes in MSUS.

In conclusion, our results provide evidence that chronic stress in early postnatal life alters miRNAs in extracellular vesicles of the male reproductive tract in adulthood, with effects in mature sperm and zygotes. These persistent and intergenerational effects *in vivo* point to the sensitivity of the reproductive system to stress exposure and the detrimental consequences for descendants. These consequences may differ depending on the time window and severity of paternal stress exposure. Further studies are necessary to more precisely define these effects and the source of vesicles and their cargo miRNAs.

3.6 Materials and Methods

3.6.1 Animals

Animal experiments were conducted according to the Swiss Law for Animal Protection and were approved by the cantonal veterinary office in Zürich under license number 83/2018. C57Bl/6J mice were obtained from Janvier (France) and bred in-house to generate animals for the experiments. Animals were maintained under a reverse light-dark cycle in a temperature and humidity-controlled environment with constant access to food and water. 9 months old age-matched MSUS and control males were used for small RNA-sequencing (sRNA-seq) of cauda epididymosomes, tissue collection for RT-qPCR, nanoparticle-tracking analysis and total cholesterol measurements. HDL cholesterol and total cholesterol measurements were performed on MSUS and control males at postnatal day 28. Datasets from previous publication (Gapp et al. 2020) : caudal sperm RNA-seq was performed on 5 months old males, and zygote RNA-seq was performed on zygotes from 3 months old males.

3.6.2 MSUS

To obtain MSUS mice, 3 months old C57Bl/6J females and their litters were subjected to daily 3 hour separation unpredictably and females were exposed to an unpredictable stressor during separation as previously described (Franklin et al. 2010). Control dams and pups were left undisturbed. After weaning at postnatal day 21, pups from different litters were randomly assigned to cages of 4-5 mice, in corresponding treatment groups to avoid litter effects.

3.6.3 Tissue collection

After decapitation and blood collection, mice were pinned on a dissection board and cleaned with alcohol. Epididymis and testis were carefully excised and separated from surrounding adipose tissue. The epididymis was further separated into caput, corpus and cauda. Cauda was excised with several incisions and sperm collected with a swim-up protocol. The supernatant was collected to isolate epididymosomes. The whole testis and caput epididymis were crushed with stainless steel beads in a tissue crusher in cold PBS, centrifuged at 3'000 rcf for 10 min to pellet the tissue and cells and used for total cholesterol and HDL cholesterol measurements.

3.6.4 Electron microscopy images

Negative staining of cauda epididymosomes was performed with methylcellulose. Briefly, the carrier grid was glow-discharged in plasma for 10 min and washed with a drop of PBS, then incubated in 1% glutaraldehyde (GA) in water for 5 min and washed with water 5 times for 2 min each. Afterwards the grid was incubated in 1% UAc (uranyl acetate) for 5 min and then kept on ice in Methylcellulose/UAc (900 ul Methylcellulose 2 % and 100 ul 3 % UAc) solution. After incubation with Methylcellulose/UAc, the excess liquid was removed by dipping onto a filter paper. The grid was air-dried on ice for 5 min. Imaging was performed with a Transmission Electron Microscope.

3.6.5 Epididymosomes isolation by ultracentrifugation

After pelleting sperm following the sperm swim-up protocol in M2 medium (Sigma, M7167), the supernatant was centrifuged at 2'000 rcf for 10 min, 10'000 rcf for 30 min and then ultracentrifuged at 120'000 rcf at 4 °C for 2 h (TH 64.1 rotor, Thermo Fisher Scientific). The epididymosomal pellet was then washed in PBS at 4 °C and ultracentrifuged at 120'000 rcf at 4 °C for 2 h. The resulting pellet was resuspended in 60 µl of PBS for all downstream analysis.

3.6.6 Immunoblotting

PBS-resuspended pellet containing epididymosomes was lysed in 10x RIPA buffer for 5 min at 4 °C. Equal amounts of protein were mixed with 4x Laemmli Sample Buffer (Bio-Rad Laboratories, USA) and loaded on 4-20% Tris-Glycine polyacrylamide gels

(Bio-Rad Laboratories, USA). The membranes were blocked in 5% SureBlock (in Tris-buffer with 0.05% Tween-20) for 1 h at room temperature and incubated with primary antibodies overnight at 4 °C with anti-*Cd9* [1:3000; System Biosciences, Palo Alto, CA, USA] and anti-*Gapdh* [1:5000; Cell Signaling, Davers, MA, USA; 14C10]).

3.6.7 Nanoparticle tracking analysis

Particle number and size of epididymosomes were measured using a Nanosight NS300 (Malvern, UK) at 20 °C, according to the manufacturer's instructions and lots were generated using a published method (Dragovic et al. 2011). The following parameters were kept constant for all samples: "Camera level" = 14 and "Detection threshold" = 7. For measurements with Nanosight, the resuspended pellet from ultracentrifugation was diluted to a 1:1000 concentration.

3.6.8 RNA isolation and epididymosomes profiling

To lyse purified epididymosomes, 33 µl of lysis buffer (6.4 M guanidine HCl, 5 % Tween 20, 5 % Triton, 120 mM EDTA, and 120 mM Tris pH 8.0) per every 60 µl of PBS resuspended pellet was added to each sample, together with 3.3 µl ProteinaseK and 3.3 µl of water. Samples were incubated at 60 °C for 15 min with shaking. 40 µl of water was added and RNA was extracted using the Trizol LS protocol, according to the manufacturer's instructions. Profiling of the extracted RNA was performed using high-resolution automated electrophoresis on a 2100 Bioanalyzer (Agilent, G2939BA), according to instructions for the RNA 6000 Pico Kit (Agilent, 5067-1513) reagent.

3.6.9 Preparation and sequencing of sRNA-seq libraries from epididymosomes

sRNA-seq libraries were prepared using the NEB Next Small RNA-sequencing kit (NEB #E7300, New England BioLabs), according to the manufacturer's instructions. 80-90 ng of total RNA per sample was used to prepare the libraries. The same libraries were sequenced before and after size-selection (target peak 150bp) with the BluePippin System. 200 million reads were obtained for 10 samples, with 125bp single-stranded read-length on a HiSeq2500 sequencer.

3.6.10 RT-qPCR

For gene expression analysis in caput epididymis, RNA was extracted using the phenol/chloroform extraction method (TRIzol; Thermo Fisher Scientific). Reverse transcription was performed using miScript II RT reagents (Qiagen) - HiFlex buffer, and RT qPCR was performed with QuantiTect SYBR (Qiagen) on the Light-Cycler II 480 (Roche). All samples were run in cycles as follows: 95 °C for 15 min, 45 cycles of 15 sec at 94 °C, 30 sec at 55 °C and 30 sec at 70°C, followed by gradual increase of temperature to 95 °C. The endogenous control *Gapdh* was used for normalization. The expression level of genes was analysed using two-tailed Student's t-test.

3.6.11 Cholesterol measurements

Testicular and epididymal total cholesterol and HDL cholesterol levels were measured using the CHOL reagent, in conjunction with SYNCHRON LX® System(s), UniCel® DxC 600/800 System(s) and Synchron® Systems Multi Calibrator (Beckman Coulter), according to the manufacturer's instructions at the Zurich Integrative Rodent Physiology (ZIRP) facility of the University of Zurich.

3.6.12 Bioinformatics data analysis

sRNA-sequencing FASTQ files were processed using the ExceRpt pipeline, a previously established pipeline for extracellular vesicle small RNA data analysis (Rozowsky et al. 2019). Briefly, ExceRpt first automatically identifies and removes known 3' adapter sequences. Afterwards the pipeline aligns against known spike-in sequences used for library construction, filters low-quality reads and aligns them to annotated sequences in the UniVec database. Reads that were not filtered out in the pre-processing steps are then aligned to the mouse genome and transcriptome using STAR aligner (Dobin et al. 2013). The annotations were performed in the following order: miRbase, tRNAscan, piRNA, GENCODE and circRNA. rRNA counts were obtained using Oasis 2 tool. Reads mapped to miRNAs were combined from sequencing obtained before and after size-selection and were corrected for batch effect using RUVSeq (Leek et al. 2014). Normalization factors were calculated using the TMM (Robinson et al. 2010) method and differential expression was performed using the edgeR package in R (Robinson et al. 2010).

For cumulative distribution plots, miRNA targets (all and conserved) were downloaded from TargetScan release 7.2 (Agarwal et al. 2015). When using the context++ scores, targets were split into 3 same-frequency groups according to their scores. *P*-values were calculated using a Kolmogorov-Smirnov test between the first and the last groups (i.e., strongest and weakest targets). The miRNA pathway analysis was conducted using a web-server tool DIANA-miRPath (Vlachos et al. 2017), where targets were predicted-derived from DIANA-TarBase v6.0, a database of experimentally validated miRNA targets. The adjusted *P* cutoff value of 0.05 was used for the identification of expressed pathways. The miRNAs and their corresponding target pathways information was extracted and plots were generated in R. ggplot2 (Wickham et al. 2016) and ComplexHeatmap R packages (Gu et al. 2016) were used for generation of figures.

3.7 Data availability

The datasets collected for this study are available as follows:

- sRNA-seq dataset of cauda epididymosomes before and after size-selection : NCBI GEO under accession number GSE175976.
- Codes for bioinformatics analysis of RNA-sequencing datasets and all corresponding differential expression analyses: Github repository https://github.com/mansuylab/alshanbayeva_et_al_2021.
- Sperm and zygote sequencing datasets from previous publications can be found in ArrayExpress database at EMBL-EBI (www.ebi.ac.uk/arrayexpress) with the accession number E-MTAB-5834 (sperm) and E-MTAB-6589 (zygotes).

3.8 Acknowledgements

We thank Pierre-Luc Germain for advice on data analysis and for generating cumulative distribution plots, Irina Lazar-Contes for help with MSUS breeding, Silvia Schelbert for work on the animal license, Emilio Yandez at Function Genomics Center Zurich (FGCZ) for advice on the sRNA sequencing, Alekhya Mazumkhar for help with nanoparticle-tracking analysis, Yvonne Zipfel for animal care, Zurich Integrative Rodent Physiology facility for performing cholesterol measurements. We also thank Eloise Kremer, Ali Jawaid and Mea Holmes for their initial contributions to the project.

The Mansuy lab is funded by the University Zürich, the Swiss Federal Institute of Technology, the Swiss National Science Foundation (31003A-135715), ETH grants (ETH-10 15-2 and ETH-17 13-2), the Slack-Gyr foundation, the Escher Foundation. Deepak K. Tanwar is supported by the Swiss Government Excellence Scholarship. Martin Roszkowski was funded by the ETH Zurich Fellowship (ETH-10 15-2).

3.9 Authors contributions

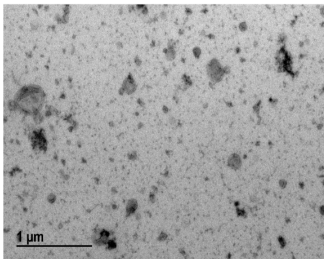
AA and IMM conceived and designed the study. FM and MR performed the MSUS breeding and collected tissue samples. AA and DKT performed data analysis and generated figures. AA wrote the manuscript with input from DKT and IMM. AA performed all experiments for RNA sequencing and all molecular analyses. IMM supervised the project and raised funds.

3.10 Conflict of interest

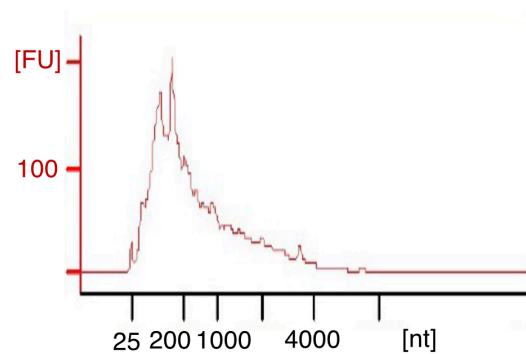
The authors declare no conflict of interest.

3.11 Supplementary Figures

a



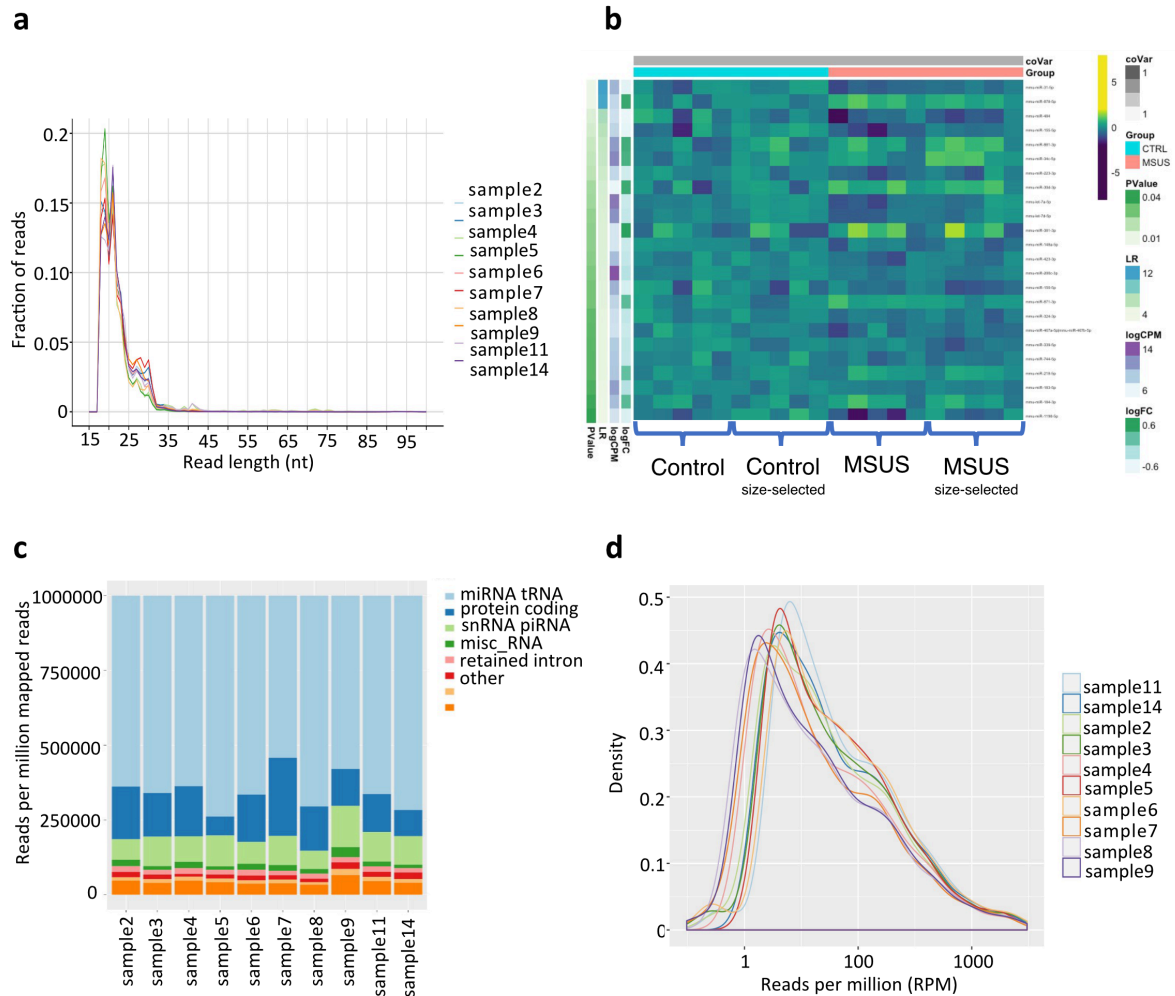
b



Supplementary Figure 3-1.

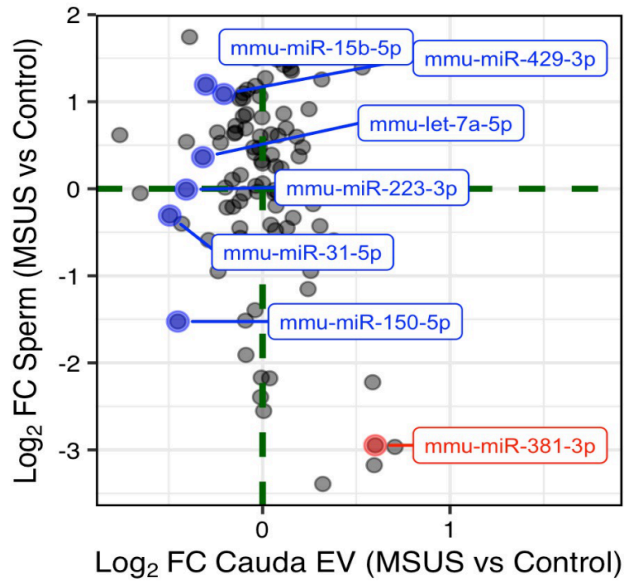
a. Electron microscopy images of the preparations used to assess the size and heterogeneity of the isolated populations.

b. The RNA amount of epididymosomes preparations was assessed by high-resolution automated electrophoresis.



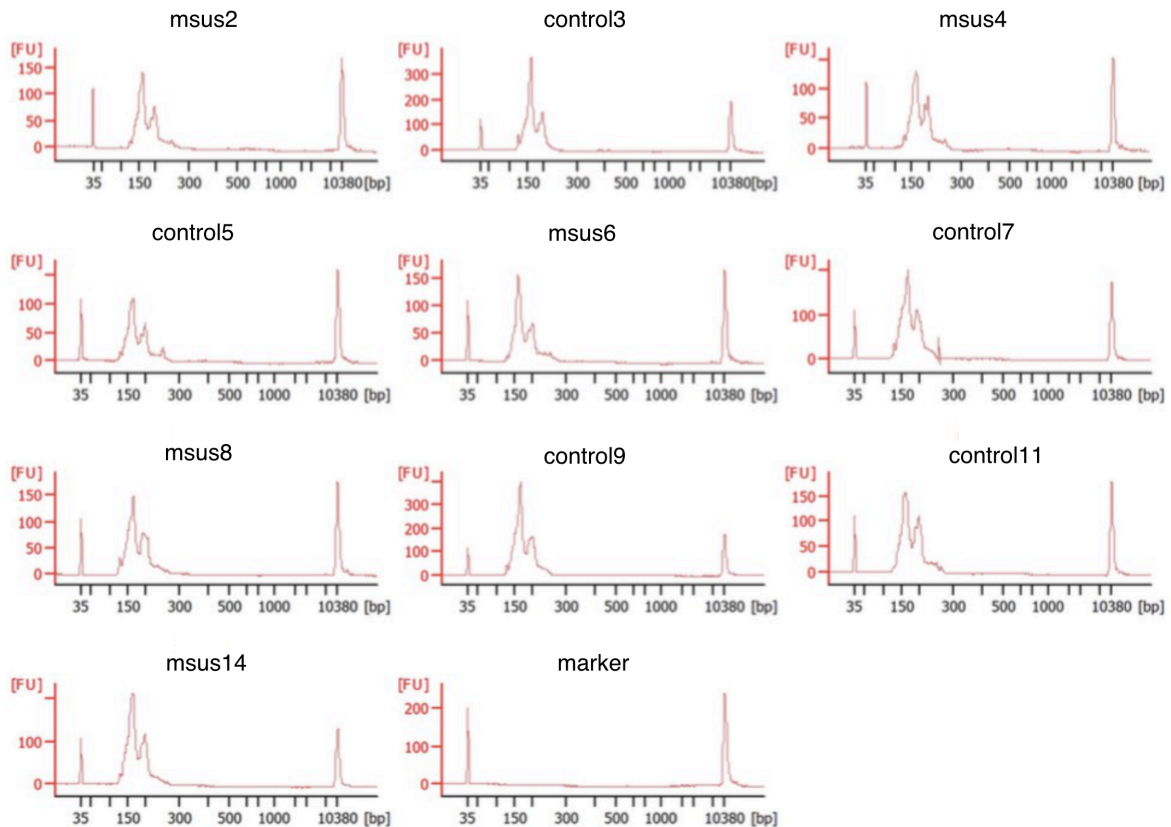
Supplementary Figure 3-2.

- a.** RNA read-length distribution of cauda epididymosomal small RNAs after size-selection.
- b.** Heatmap of top miRNAs of cauda epididymosomal small RNA-seq before and after size-selection. Each row depicts a miRNA and each column depicts a sample. (N= 10 Controls, N=10 MSUS).
- c.** Representative distribution of RNA biotypes from cauda epididymosomal sRNA-seq after size-selection. (N = 5 Controls, N = 5 MSUS).
- d.** miRNA abundance distributions plot of cauda epididymosomal sRNA-seq. (N = 10 Controls, N = 10 MSUS)



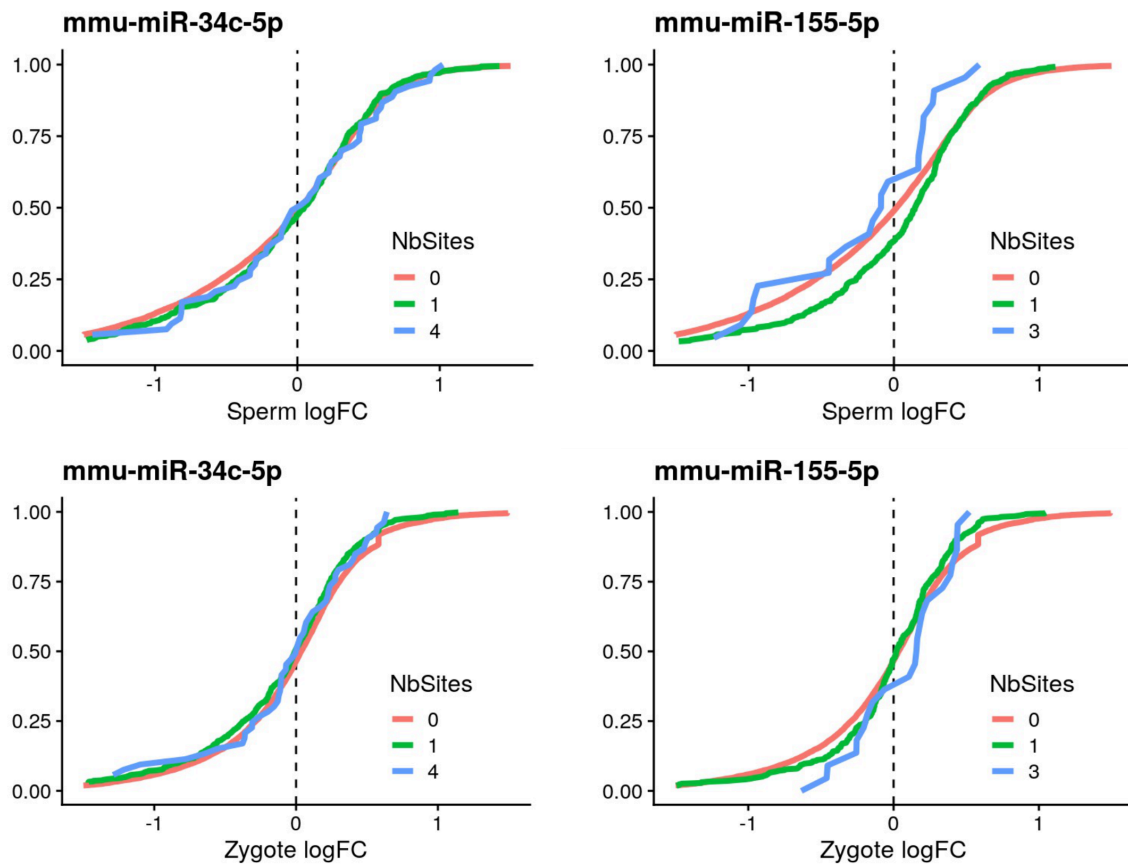
Supplementary Figure 3-3.

Scatterplot of log fold-change of miRNAs in sperm and cauda epididymosomes. miRNAs down-regulated (blue) and up-regulated (red) in MSUS cauda epididymosomes.



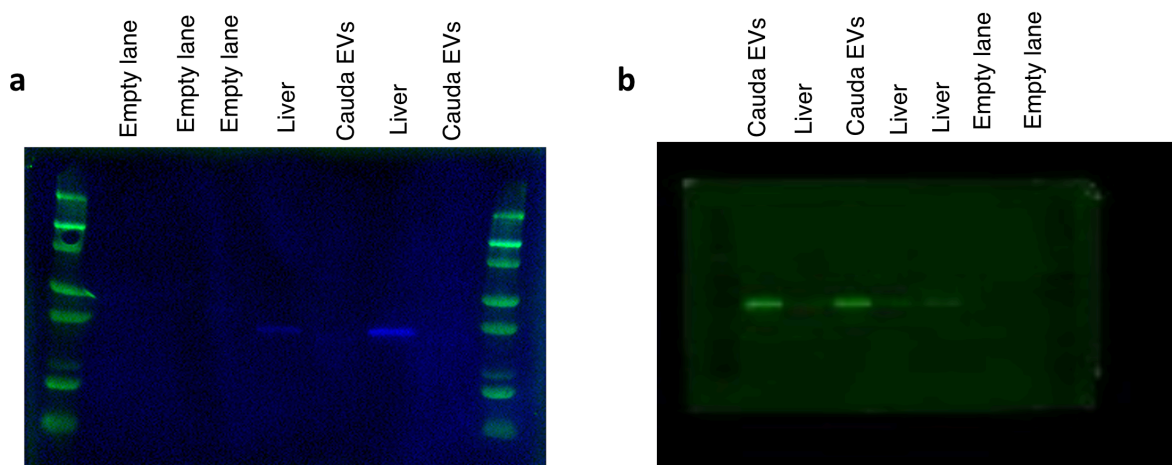
Supplementary Figure 3-4.

Profiles of cauda epididymosomal small RNAs by high-resolution automated electrophoresis. (N = 10 Controls, N = 10 MSUS).



Supplementary Figure 3-5.

Cumulative distribution plots of miR-34c-5p, miR-155-5p targets in differentially expressed genes ($P < 0.05$) from 5 months old MSUS sperm and RNA-sequencing of zygotes from 3 months old control and MSUS males.



Supplementary Figure 3-6.

a-b. Immunoblot images of cauda epididymosomes and liver cell lysate, stained with cellular marker GAPDH (37kDa) (**a**) and extracellular vesicle marker CD9 (25kDa) (**b**). Same membrane was incubated and imaged separately.

microRNA	logFC	logCPM	LR	PValue	FDR
mmu-miR-871-3p	0.422444517	7.865089889	11.91735299	5.56E-04	0.072125889
mmu-miR-31-5p	-0.387636483	9.998798838	11.06785143	8.78E-04	0.072125889
mmu-miR-155-5p	-0.450978421	7.903016039	10.27041439	0.001351804	0.072125889
mmu-miR-881-3p	0.289881511	11.46562387	9.94702628	0.001611094	0.072125889
mmu-miR-878-5p	0.45177335	7.616360458	9.829571964	0.001717283	0.072125889
mmu-let-7f-5p	-0.253942019	15.09468443	8.265117988	0.004041403	0.141449121
mmu-let-7a-5p	-0.325256599	13.37869938	7.854572769	0.005069233	0.150794548
mmu-miR-34c-5p	0.369976432	12.49081551	7.628736184	0.005744554	0.150794548
mmu-let-7c-5p	-0.266068404	14.17072394	6.590840952	0.010250474	0.239177725
mmu-let-7d-5p	-0.295724455	12.06052526	6.254406671	0.012388474	0.251473433
mmu-miR-148a-5p	-0.386049823	6.58277579	6.099744235	0.013520145	0.251473433
mmu-miR-486a-5p mmu-miR-486b-5p	0.42423281	9.175211467	5.992121421	0.01436991	0.251473433
mmu-miR-223-3p	-0.391855135	7.62759898	5.758552047	0.016408589	0.265061814
mmu-miR-142a-5p	-0.33881759	7.860398876	5.331804116	0.020939699	0.299518558
mmu-miR-484	-0.446451895	7.035886557	5.294393265	0.021394183	0.299518558
mmu-miR-182-5p	-0.18588054	11.5375818	5.084665409	0.024138334	0.316815633
mmu-miR-183-5p	-0.210626504	11.35664904	4.759218654	0.029141774	0.339567889
mmu-let-7g-5p	-0.176927466	14.49917081	4.704359966	0.030086202	0.339567889
mmu-miR-181d-5p	0.272998777	7.492399346	4.642132182	0.03119622	0.339567889
mmu-miR-467a-5p mmu-miR-467b-5p	-0.339190729	6.822511268	4.509472306	0.033707638	0.339567889

Supplementary Table 3-1.

Differential expression analysis of miRNAs from the combined and batch-corrected reads of the two sequencing runs.

gene_name	logFC	meanExpr	Pvalue	FDR	sites	targetscan.score	conserved.sites
Glu1	1.00	7.7	2.40E-06	0.0042	2	-0.60	1
Pik3c2a	1.00	4.2	3.00E-06	0.0048	2	-0.36	2
Trank1	0.93	4.7	6.90E-05	0.0240	3	-0.53	1
Wdr5	1.00	1.8	2.10E-03	0.1000	2	-0.65	1
Eif5	0.93	5.2	8.40E-05	0.0260	1	-0.39	1
Bicd1	1.10	3.7	1.10E-04	0.0280	2	-0.23	1

Supplementary Table 3-2.

miR-31-5p target genes in RNA-seq dataset from MSUS sperm.

gene_name	logFC	meanExpr	Pvalue	FDR	sites	targetscan.score	conserved.sites
Hsf2bp	-2.30	-1.60	0.0300	0.12	1	-0.460	1
Satb2	-1.90	-1.60	0.0110	0.12	2	-0.380	2
Dpep3	-2.50	-2.90	0.0029	0.12	1	-0.019	1
Jazf1	-1.20	-0.23	0.0015	0.12	2	-0.640	1
Ret	-1.90	-1.80	0.0100	0.12	2	-0.250	1
Wdr5	-0.93	2.50	0.0360	0.12	2	-0.650	1
Snx22	-1.70	-1.30	0.0067	0.12	2	-0.250	2
Rab9b	-1.20	-4.30	0.0380	0.12	2	-0.490	1
Nr5a2	-1.50	1.30	0.0140	0.12	1	-0.320	1
Plin1	-2.70	-0.62	0.0290	0.12	1	-0.210	0

Supplementary Table 3-3.

miR-31-5p target genes in RNA-seq dataset from MSUS zygote.

RNA	logFC	logCPM	LR	PValue	FDR
Prr15:protein coding	-0.7873999	4.547372	30.18055	0	0.0001084
Gm15806:processed pseudogene	-0.6498672	6.510597	25.26703	0.0000005	0.0006874
mmu-miR-34c-5p	0.7802879	11.007007	17.68464	0.0000261	0.0184327
mmu_piR_004086	0.97693	6.282539	17.63425	0.0000268	0.0184327
Gm42427:TEC	-0.6134632	8.60391	16.67736	0.0000443	0.0244041
Gata3:protein coding	-0.4928509	6.189582	16.11356	0.0000597	0.0273818
mmu-miR-878-5p	0.8891784	6.148635	15.77038	0.0000715	0.0281354
Hpgd:protein coding	-0.5320409	8.066485	15.16616	0.0000985	0.0338922
Ccdc136:protein coding	0.6987606	4.387168	14.00494	0.0001823	0.0472578
mmu-miR-181d-5p	0.6157888	5.694342	13.85633	0.0001973	0.0472578
Tacc2:protein coding	-0.5657623	4.398129	13.6902	0.0002156	0.0472578
mmu-miR-871-3p	0.6763168	6.446751	13.66182	0.0002189	0.0472578
mmu-miR-9-5p	0.7204504	6.140215	13.49688	0.000239	0.0472578
Gm26168:misc RNA	0.6325019	4.872739	13.22844	0.0002757	0.0472578
Gm23921:misc RNA	0.5727151	6.650877	13.21883	0.0002772	0.0472578
Abcg2:nonsense mediated decay	-0.5214647	6.63881	13.19591	0.0002806	0.0472578
Hipk3:protein coding	-0.4861401	4.791792	12.68259	0.0003691	0.0472578
Odf1:protein coding	0.5552237	6.042366	12.63222	0.0003792	0.0472578
mmu-miR-881-3p	0.8813852	10.06467	12.60867	0.000384	0.0472578
mmu-miR-455-5p	0.6872305	5.255313	12.60016	0.0003857	0.0472578
Snord88a:snoRNA	0.6180176	5.030322	12.50995	0.0004048	0.0472578
His	1.1442782	10.636565	12.47395	0.0004127	0.0472578
Rnf2:protein coding	-0.4823013	4.596362	12.32996	0.0004457	0.0472578
Gm10524:TEC	-0.494331	5.296549	12.29409	0.0004544	0.0472578
Ptgr1:protein coding	-0.4927718	6.068551	12.28196	0.0004574	0.0472578
Abcg2:protein coding	-0.5283684	7.721448	12.26538	0.0004614	0.0472578
mmu-miR-218-5p	0.659141	7.439262	12.23378	0.0004693	0.0472578
iMet	0.8698821	9.497592	12.18997	0.0004805	0.0472578

Supplementary Table 3-4.

Differential expression analysis of all RNA biotypes from the combined and batch-corrected reads of the two sequencing runs (adjusted $P \leq 0.05$).

4. Conclusions and Outlook

We previously showed that injections of whole serum from mice exposed to early life stress into naïve males cause metabolic alterations in the offspring of the naïve males (van Steenwyk et al., 2020). To gain a better understanding of the different circulating components involved in passing stress-related information to the injected males and their offspring, we divided blood components into EV-enriched and protein-enriched fractions with size-exclusion chromatography, and injected these fractions from ELS mice or controls to naïve animals. We proceeded to characterize the effect of chronic ELS EV injections on the naïve males, their sperm, embryos and offspring. This thesis provides evidence that, when injected chronically, circulating EVs from mice exposed to ELS can cause several alterations in naïve unexposed mice and their offspring. These alterations include changes in circulating metabolites, lipids, and sperm RNA of the injected males, gene expression changes in early embryos and metabolic alterations in the offspring.

In the section below, I will summarize our findings from **Chapter 2** and **Chapter 3** and explain the basis for our experimental approaches. I will then discuss the challenges and limitations of the current work that are caused by the chosen methods or time restrictions. I will then describe further experimental suggestions that will help to dissect the mechanism of action of EVs on male germ cells and to understand the establishment of changes in EV cargo due to the environmental exposure. Finally, I will discuss the contribution of this thesis work on the current state of knowledge on circulating factors' role in communicating information on life experiences to the germ cells in males.

4.1 Summary of research questions and major findings

Early life experience can have an effect on the physical and mental development of an organism during adolescence and adulthood. In addition, parental early life exposure to environmental stressors can affect the unexposed offspring intergenerationally and sometimes transgenerationally. Impact of stressors to the exposed organism and offspring was demonstrated from *C.elegans*, rodents to humans (Conine et al. 2022). The effects observed in the offspring of parents subjected to an environmental insult vary depending on different parameters, such as exposure time, severity, the age of the exposed generation and many others. The

mechanisms of this effect are not single-fold and were suggested to involve a number of potential factors, such as RNAs, proteins, histone modifications and DNA methylation (Conine et al. 2022). Even though studies of the direct or indirect mechanisms of epigenetic inheritance often focused on deciphering the information carried in sperm or seminal fluid delivered to females upon fertilization, how those changes in the sperm or seminal fluid arise is less known. More specifically, the question of by which intermediaries the periphery can communicate with the germ cells to inform on changes in the environmental conditions is not well addressed. These intermediaries include a number of factors, such as factors in the blood, factors in the lymphatic system, the somatic cells that have direct or indirect contact with the germ cells in testis and epididymal tract, the nerve innervations to the testis and epididymis.

This research work attempts to address one of the potential intermediaries in this gap by tackling the question whether the body can communicate to sperm through circulating factors and alter information carried by sperm to the offspring. It executes this attempt by using a mouse model of ELS, which was shown to alter metabolic and behavioral phenotype of the exposed and unexposed generations (van Steenwyk et al. 2018). ELS is used as a model due to the developmental time point it targets and its relevance to studies in humans (Eachus et al. 2021, Smith et al. 2020, Brenhouse et al. 2018, Murphy et al. 2017).

As we previously showed that chronic serum-injections can recapitulate some of the metabolic phenotype of ELS in naïve animals, we concentrated on dissecting the contribution of different circulating factors in this phenomena (Chapter 2). To do that, we performed a series of experiments. First, since circulating EVs are involved in long-distance interorgan communication, we tested whether ELS can alter the circulating EV components in adult animals. In particular, we looked at EV RNA, lipids and metabolites. We next examined if chronic exposure to circulating EVs from males exposed to ELS can have an effect in the naïve males as well as their offspring, by chronically injecting ELS or control EVs into naïve males and breeding at different time-points. In addition to metabolism of the EVs injected males, we looked at both sperm small and long RNAs, as well as mRNAs of their embryos generated by IVF. IVF was the method of choice, since it allows one to differentiate between the factors that arrive from male upon fertilization into sperm-factors and non-sperm factors, such as seminal vesicles and other components of seminal fluid. Furthermore, in order to understand if the effect we observe in the offspring of EV-injected males is dependent

on the presence of EVs or other plasma components, we have chronically injected plasma protein-enriched fractions from mice exposed to ELS into naïve males to examine the offspring phenotype. Since germ cells in males are modified in their RNA, protein and lipidic content throughout the transit in the epididymal tract, in addition to characterizing circulating EV RNA components in ELS and control mice, we looked at the small RNA content of ELS epididymal EVs (Chapter 3). We found that ELS alters the epididymal EV small RNA content, and for some of the differentially expressed small RNAs, such as miRNAs, the upregulation in miRNAs is correlated with the downregulation of their target genes in sperm and zygotes, generated from ELS sperm (Chapter 3).

4.2 Novelty of the research

In addition to providing information about the different tissue states and informing on the cellular damages or disease states, circulating EVs can also transfer messages among cells or tissues across the body. Examples of these processes include, but are not limited to, targeting of immune cells by tumor cell EVs, communication between damaged liver hepatocytes and macrophages, secretion of modulating EVs from adipocytes in obesity. However, the potential of circulating EVs signaling to germ cells in males has not been extensively researched.

A few studies attempted to address this potential role of circulating EVs or other circulating factors by either introducing changes into environmental conditions or by introducing exogenous systems into animals. For example, Cossetti et al. xenografted human melanoma cells expressing EGFP plasmid in mice and observed the EGFP-specific RNA in the circulating vesicles and sperm, whereas O'Brien et al. stereotactically injected AAV expressing human pre-miR-491 in mice striatum and detected presence of the human pre-miR-491 in epididymis, lymph nodes and blood (O'Brien et al. 2020, Cossetti et al. 2014).

The ability of blood factors in altering physiological states has been undeniable - the rejuvenating effect of blood transfer from young to old mice, together with parabiosis experiments put circulating factors into perspective (Gonzalez-Armenta et al. 2020, Gan et al. 2019, Villeda et al. 2014). The active circulating components responsible for such effects were suggested to be proteins (Zeybel et al. 2014) and metabolites (van Steenwyk et al. 2020). Here we show that EVs enriched blood fractions alone can cause metabolic alterations, changes in sperm small and long

RNAs and furthermore, affect the early embryo development and offspring metabolism. Waiting 12 and 46 days after injecting naïve males with ELS and control EVs before obtaining offspring allowed us to distinguish the time-dependent impact of the ELS EVs on naïve males' metabolism, sperm and offspring. Metabolic alterations in the injected males 46 days after injections and their offspring, demonstrates that ELS EVs can (i) have long-lasting effects in the naïve males; (ii) can directly or indirectly affect the mature male germ cells; (iii) can alter developmental trajectory of early embryos generated from that sperm. These findings demonstrate that, in addition to metabolites and proteins, circulating EVs can act as messengers of life experiences to germ cells in males and influence offspring phenotype.

4.3 Challenges and limitations

This work contains several limitations, which could be divided into practical limitations (such as methodological, time-dependent, resource-dependent and other similar constraints) and theoretical limitations (such as the choice of the experimental designs in addressing the hypotheses and the type of hypotheses that were addressed). In the section below we will cover both types of limitations and their impact on the results and interpretations of the findings.

Undoubtedly, SEC, as the main method of EVs isolation from circulation used in our study, is limited due to concentrating on one property of particles in a biofluid - the size. Circulating EVs are known to be of different sizes; in addition, they are known to overlap in size and sometimes in density with other components in the blood, such as lipoproteins and apoptotic bodies. Although we showed enrichment of small EVs in our preparations from plasma and demonstrated comparable purity from HDL particles, the presence and potential contribution of other lipoproteins such as LDL and vLDL, or other blood components that overlap with small EVs in size cannot be excluded from our preparations. Moreover, since circulating EVs vary in size, with our method, we could only concentrate on small EVs, due to the higher overlap in size of large EVs with other circulating components, mentioned above.

In addition to the functional RNA and lipid content, circulating EVs are known to carry proteins inside and on the surface of their membrane. Even though EV surface proteins were originally thought to be assembled before the release of EVs from a parent cell, emerging evidence suggests that EV proteins are also taken up while EVs are in the extracellular milieu and assist in circulating EVs' roles in immune response,

coagulation, complement pathway activation and others (Ramos et al. 2022). In the current study, we did not examine how and if the proteins in circulating EVs are altered by ELS. This stems partially due to the limits in the amount of accessible material (plasma from mice subjected to ELS) and prioritization of small RNAs, metabolites and lipids due to previous research findings in ELS. These findings include but are not limited to the changes of circulating metabolites in adult ELS males, alterations in the sperm small and long RNAs and changes in the offspring body weight as well as glucose metabolism (Gapp et al. 2014, Gapp et al. 2020, van Steenwyk et al. 2020, van Steenwyk et al. 2018).

Another challenge is the choice of cells that were used to study the uptake of circulating EVs by male germ cells in mice, particularly the GC-1 cell line. According to previous knowledge in the field and history of usage, GC-1 cells display characteristics of cells that are between type B spermatogonia and primary spermatocytes (Wang et al. 2019, Godmann et al. 2010). However, other evidence based on transcriptomic profiling of GC-1 cells suggests that these cells could be similar to somatic cells in the testis than germ cells (Normal et al. 2021). Evidently, this is not the only possible limitation of using GC-1 cells to address the question of circulating EVs uptake by male germ cells. Employing such an *in vitro* system to model complex *in vivo* processes in the testis limits the extent of possible interpretations, due to: (i) the absence of neighboring supporting, cells such as macrophages, Leydig cells and Sertoli cells; (ii) the inability of GC-1 cells to mimic germ cells at different stages of differentiation; (iii) lack of communicating signals among all different types of germ and somatic cells in the testis.

Although we showed that circulating EVs can transfer some of the stress-induced metabolic phenotype to naïve males and their offspring, the mechanism by which EVs are able to communicate the information on the exposure to the germ cells is yet to be understood. This mechanism could include either a direct uptake by crossing blood-testis or blood-epididymal barriers or an indirect communication by contacting the somatic cells in the testis and epididymis.

Another important question to address is how the changes in the gene expression profile of the 2-cell embryos obtained from ELS EV-injected naïve males initiate altered developmental processes that result in metabolic changes in adult offspring.

We showed that both the RNA and lipid content of circulating EVs is altered by

ELS; however, we did not casually link the phenotype we see in the injected males or their offspring to specific RNAs or lipids. Although not the main part of our work, it is also compelling to draw on the origins of those lipids and RNAs that are differentially present in the circulating EVs of ELS males.

Blood possesses a heterogeneous mixture of EVs. This heterogeneity cannot be eliminated by a size-based isolation method, such as size-exclusion chromatography, which was the main method used for our EV isolations. Therefore, although we succeed in enriching small EVs from mice plasma, the heterogeneity of these EVs is still present. This heterogeneity makes it more difficult to understand which specific cells and organs ELS or control EVs target when injected in naïve mice.

Injections of ELS sperm long RNAs were shown to contribute to the inheritance of some of the stress symptoms observed in adult ELS mice (Gapp et al. 2018); in particular, inheritance of glucose response to insulin, risk-taking behavior and changes in the food intake behavior were demonstrated. Whereas ELS sperm small RNAs altered offspring body weight and stress-induced behaviors (Gapp et al. 2018). Through *in vitro* fertilization experiments with the sperm of ELS EV-injected males, we demonstrated the effect of ELS EVs to the transcriptional changes in early embryos; however, we failed to demonstrate whether and how the altered transcriptional patterns in early embryos lead to the metabolic phenotype we observe in the adult offspring of the ELS EV-injected males.

Another important aspect that should be considered while interpreting the findings in this work is the dosage of EVs and the timing of injections relative to the differentiation of germ cells in male mice. Our injections last for four weeks and repeat two times per week to have the property of chronicity and to mimic our previous serum injection experiments. When analyzing the effect of EV injections, we look at the EV-injected males at 12 and 46 days after injections as well as their offspring generated at these two timepoints. These are important timepoints, since 12 days after injections, the mature sperm at fertilization has a possibility to be exposed to the injected material during its latest stages of testicular maturation and during epididymal transit; however, with this time-point, one cannot distinguish if the male germ cells are also potentially susceptible to the injected material at the earlier stages of maturation, such as spermatogonium or preleptotene spermatocyte, which take place outside the BTB. This is partially answered by waiting 46 days post-injections before breeding, which provided enough time for a complete spermatogenesis cycle and clearance of mature

sperm from cauda by spontaneous ejaculation. Nevertheless, none of these two time-points eliminate another important parameter – the effect of adapted long-term metabolic alterations in the injected animals. As the ELS EV-injected males had extensive alterations in circulating metabolites and lipids, the possibility of the small and long RNA changes we observe in the mature sperm of these animals originating due to those alterations cannot be eliminated. Therefore, the effect of shorter or longer injection periods, higher amounts of EVs injected more acutely or injecting at different developmental time points throughout an animal's life, are all possible ways to address further the questions on the effect of time, dosage and period of EV injections.

Although we are using ELS EVs, the effect of the injections on the naïve animals cannot be directly compared to the effect ELS has on the adult animals, since any epigenetic changes in ELS sperm encompasses a merged effect of the ELS, combination of constant signals through somatic cells in the testis, possible effect of the ELS on the differentiation of somatic cells and establishment of germ stem cell pool. Therefore, this work can be recognized as a tool to understand how circulating factors such as EVs can signal to germ cells in males, using a mouse model with known impacts on mature germ cells, rather than explaining the effect of ELS in adulthood through circulating EVs.

4.4 Recommendations for implementation of future research

To address the heterogeneity of EVs in blood and dissect the diversity of EV-secreting sources that are contributing to our findings, one could involve high-resolution flow cytometry to characterize the circulating EVs in ELS and control mice on their surface markers and therefore deduce the cells or tissues of origin. This could be combined with proteomics of EVs. In addition to these experiments, dissection of the role of ELS EV small RNAs and lipids in the metabolic effect we observe in the injected animals could be performed by enriching the EV lipid bilayer in the ELS EV-enriched PC or PE lipids, or by electroporating a cocktail of synthetic miRNAs of interest into plasma EVs and observing the effect in naïve males with *in vivo* injections of either.

Tracking EVs to the tissue and cells of uptake is another experiment that would help us understand our findings. The uptake tissue could be tracked by labeling EVs with a lipophilic fluorescent membrane dye and performing imaging of the different tissues. Understanding the target organs of the injected EVs is important, since some

extracellular EVs were shown to possess organ or cell specificity. For example, tumor cell-derived EVs exhibited preferential targeting of organs involved in immune response, with the underlying effect of immunosuppression for tumor progression; on the other hand, intestinal epithelial cell-derived EVs favorably targeted liver, with some also reaching adipose and muscle tissue.

Since our EV injections are repeated two times per week for four weeks, a very interesting experiment, that would give an extensive overview of the processes altered during the injections, is looking at several time-points during and post-injections into different tissues with multi-omics approaches. The major interests for such an experiment would be liver, epididymal epithelial cells and testicular somatic cells, as well as the germ cells in the testis and epididymis.

Some other experiments to understand different aspects of our findings would be: (i) understanding the sources of circulating EVs in ELS and characterizing lipids and RNAs by the EV type (EV surface marker); (ii) culturing cells from the EV source tissue in ELS and using EVs secreted by them into the cell culture media for injection into naïve animals to test for any metabolic abnormalities; (iii) blocking cell-specific secretion of small EV production in culture by adding IFN and examining the role other secreted components have.

Looking at the effect of EV injections on the cells residing in the testis is another unexplored area. It was demonstrated that testicular EVs are secreted mainly from Leydig cells and testicular macrophages (Choy et al. 2022). Whether the amount of EVs, their cargo or size is altered by environmental exposures is not known and whether circulating EVs can impact testicular resident cells is, to our best knowledge, has not been studied. Sertoli cells, that play the role of nurture cells to the testicular germ cells, providing lactate and main energy support to them, were shown to alter spermatogenesis due to exposure to a high-fat diet. Lipotoxicity increases glycolysis and lactate production, affects energy metabolism in Sertoli cells, which in turns impairs spermatogenesis. In addition, lipotoxicity can lead to the impairment of the BTB. As we have seen differences in EV lipid cargo, once again, looking at the changes of testicular and epididymal cells due to increase in EV PC and PE lipids would be important.

The role of different EV components

The lipid composition of EVs can be affected in pathological states (Kumar et al. 2022, Lam et al. 2021). We showed that ELS significantly increases circulating EV

lipids, namely 3 PC lipids, 1 PE and 1 TAG lipid. The majority of significantly increased EV lipids in ELS plasma are PC lipids, that are a major component of biological membranes. Biological functionality and uptake properties of PC lipids was shown to be dependent on the form of the PC lipid. For example, in their free form PC lipids have no targeting specificity, whereas as a part of EVs, they are taken up more efficiently and can increase the uptake efficiency of EVs (Kumar et al. 2022). Kumar et al. demonstrated that high-fat diet increased the amount of PC lipids in EVs secreted by intestinal epithelial cells, which in turn improved the uptake of these EVs by liver hepatocytes and macrophages, causing suppression of genes involved in insulin activation pathway and inhibition of insulin response in animals fed with high-fat diet (Kumar et al. 2021). According to Kumar et al., the PC-driven effect of HFD EVs is caused by the inhibition of insulin response via binding of these EV-PCs to the Aryl hydrocarbon receptor (AhR) in hepatocytes. Binding of a ligand to AhR causes translocation of the ligand-receptor complex into the nucleus and activation of the AhR pathway. This in turn causes suppression of genes involved in the insulin activation pathway, such as IRS-1, IRS-2 and PPAR and creates insulin resistance. Overall, mice fed with HFD have increased body weight, epididymal white adipose tissue and circulating triglycerides and are glucose-intolerant and insulin-resistant. Interestingly, ELS EV-injected males are also insulin resistant and have an increased body weight. If a similar mechanism takes place in our EV-injected mice due to the higher amount of PC lipids in circulating EVs from ELS mice, the apparent metabolic changes in the ELS and ELS EV-injected mice could be explained by comparable gut-liver-muscle tissue axes metabolic syndrome observed in HFD mice. Injecting PC-depleted ELS EVs into naïve males, incubating PC-depleted or PC-enriched EVs with primary SCs and somatic cells of epididymis and testis, estimating the expression of genes involved in insulin activation pathway in hepatocytes in ELS and ELS EV-injected animals are a few of the ways to address the relevance of increased PC amount in ELS circulating EVs to their functionality.

PCs in EVs do not only alter uptake of EVs, but they were also shown to directly bind transcription factors, such as AhR. Lipids are known to function as ligands to lipid-activated receptors that play roles in metabolic diseases. For example, lipid-activated nuclear receptors, such as liver X-receptor (LXR), pregnane X-receptor (PXR) and peroxisome proliferator-activated receptor alpha (PPAR alpha) control expression of genes involved in bile acid homeostasis in the liver (Barbier et al. 2009). Therefore,

the presence of various lipids in not only ELS circulating EVs, but also in epididymis, testis and seminal fluid of the EV-injected males should be determined.

We showed that circulating EV RNAs were significantly altered by ELS. There are many reasons to consider EV RNAs as potential candidates that could be at least partially responsible for the EV-induced phenotypes we observe in naïve males: (i) RNAs in EVs are protected from degradation in extracellular environments, including circulation (Arroyo et al., 2011; Shurtleff et al., 2017; Pua et al., 2019); (ii) in some cases, RNAs in EVs can be used as a readout of the biological state of the secreting cell or tissue (Konstantinidou et al., 2016; Shah et al., 2017b; Murillo et al., 2019; Pua et al., 2019); (iii) RNAs in EVs can be transferred between cells and alter cellular states or functions (Mathieu et al., 2019; Stahl and Raposo, 2019). In our findings, we observed that most of the differentially-expressed small RNAs in ELS EVs are up-regulated miRNAs. Among these miRNAs, the miRNA families miR-30, let-7 and miR-26 are the most recurrent, regardless of the underlying EV isolation method.

Regardless of the RNA candidates altered by ELS in circulating EVs, one must be cautious in interpreting these findings, without additional *in vitro* and *in vivo* experiments to test the functions of the altered small RNAs in physiologically relevant amounts and while being a part of the EV cargo. This is due to: (i) the low abundance of miRNAs per circulating EV, which is estimated to be approximately 1 miRNA molecule in every 13 EVs (Otahal et al. 2021); (ii) EV RNAs are highly susceptible and carry irreversible alterations due to the storage and handling differences of EVs as well as the blood (Kim et al. 2022); (iii) some studies show that miRNAs in EVs are not accountable for functional roles of EVs (Albanese et al. 2021).

4.5 Concluding summary

To conclude, this work provides a stimulating update on the potential role of circulating factors, such as EVs, as the messenger of an organism's experiences of environmental stressors to the germ cells. It demonstrates that (i) environmental exposures such as early life stress can alter the components of circulating EVs, particularly their small RNAs and lipids contents; (ii) when chronically injected, EVs from animals exposed to early life stress can alter the physiological state of naïve animals long-term; (iii) some of the physiological alterations caused by these EV-injections are transferred to the offspring of those naïve males. These findings pave the way to further understand the overall contribution of blood components in

communicating changes in the periphery to the germ cells and encourage a more in-depth study of blood-testis- and blood-epididymal barriers, permeability of these barriers to circulating factors, alterations to male germ cells during the testicular-epididymal maturation, as well as the role of lipids and metabolic alterations as an overall connecting element of many models of environmental exposures.

References

Abey, S. K., Yuana, Y., Joseph, P. V., Grootemaat, A. E., & Leroyer, A. S. (2017). Lysozyme association with circulating RNA, extracellular vesicles, and chronic stress. *BBA Clinical*, 7, 23-35.

Agarwal, V., Bell, G. W., Nam, J. W., & Bartel, D. P. (2015). Predicting effective microRNA target sites in mammalian mRNAs. *eLife*, 4, e05005.

Albanese, M., Chen, Y. F. A., Hüls, C., Gärtner, K., Tagawa, T., Kopp-Schneider, A., Seimiya, M., Walter, J., Tamura, T., Hatakeyama, S., & Kinoshita, T. (2021). MicroRNAs are minor constituents of extracellular vesicles that are rarely delivered to target cells. *PLoS Genetics*, 17(12), e1009951.

Alshanbayeva, A., Tanwar, D. K., Roszkowski, M., Manuella, F., & Mansuy, I. M. (2021). Early life stress affects the miRNA cargo of epididymal extracellular vesicles in mouse. *Biology of Reproduction*, 105(3), 593-602.

Anway, M. D., Cupp, A. S., Uzumcu, M., & Skinner, M. K. (2005). Epigenetic transgenerational actions of endocrine disruptors and male fertility. *Science*, 308(5727), 1466-1469.

Armingol, E., Officer, A., Harismendy, O., & Lewis, N. E. (2021). Deciphering cell-cell interactions and communication from gene expression. *Nature Reviews Genetics*, 22, 71-88.

Arroyo, J. D., Chevillet, J. R., Kroh, E. M., Ruf, I. K., Pritchard, C. C., Gibson, D. F., Mitchell, P. S., Bennett, C. F., Pogosova-Agadjanyan, E. L., Stirewalt, D. L., & Tait, J. F. (2011). Argonaute2 complexes carry a population of circulating microRNAs independent of vesicles in human plasma. *Proceedings of the National Academy of Sciences*, 108(12), 5003-5008.

Bachiller, D., Schellander, K., Peli, J., & Rüther, U. (1991). Liposome-mediated DNA uptake by sperm cells. *Molecular Reproduction and Development*, 30, 194-200.

Barbier, O., Trottier, J., Kaeding, J., Caron, P., & Verreault, M. (2009). Lipid-activated transcription factors control bile acid glucuronidation. *Molecular and Cellular Biochemistry*, 326(1-2), 3-8.

Bazzan, E., Tinè, M., Casara, A., et al. (2021). Critical review of the evolution of extracellular vesicles' knowledge: from 1946 to today. *International Journal of Molecular Sciences*, 22(12), 6475.

Belleannée, C., Calvo, É., Caballero, J., & Sullivan, R. (2013). Epididymosomes convey different repertoires of microRNAs throughout the bovine epididymis. *Biology of Reproduction*, 89, 30.

Belleannée, C., Légaré, C., Calvo, E., Thimon, V., & Sullivan, R. (2013). microRNA signature is altered in both human epididymis and seminal microvesicles following vasectomy. *Human Reproduction*, 28, 1455-1467.

- Berumen Sánchez, G., Bunn, K. E., Pua, H. H., & Rafat, M. (2021). Extracellular vesicles: mediators of intercellular communication in tissue injury and disease. *Cellular Communication and Signaling*, 19(1), 104.
- Bilińska, B., Wiszniewska, B., Kosiniak-Kamysz, K., Kotula-Balak, M., Gancarczyk, M., Hejmej, A., Sadowska, J., Marchlewicz, M., Kolasa, A., & Wenda-Rózewicka, L. (2006). Hormonal status of male reproductive system: androgens and estrogens in the testis and epididymis. In vivo and in vitro approaches. *Reproductive Biology*, 6(Suppl 1), 43-58.
- Bohacek, J., & Mansuy, I. M. (2015). Molecular insights into transgenerational non-genetic inheritance of acquired behaviours. *Nature Reviews Genetics*, 16(11), 641-652.
- Bond, S. T., Calkin, A. C., & Drew, B. G. (2022). Adipose-Derived Extracellular Vesicles: Systemic Messengers and Metabolic Regulators in Health and Disease. *Frontiers in Physiology*, 13, 837001.
- Brenhouse, H. C., Danese, A., & Grassi-Oliveira, R. (2018). Neuroimmune impacts of early-life stress on development and psychopathology. *Current Topics in Behavioral Neurosciences*.
- Buzas, E. I. (2022). The roles of extracellular vesicles in the immune system. *Nature Reviews Immunology*, 1-15.
- Caballero, J. N., Frenette, G., Belleannée, C., & Sullivan, R. (2013). CD9-positive microvesicles mediate the transfer of molecules to Bovine Spermatozoa during epididymal maturation. *PLoS ONE*, 8, e65364.
- Cajka, T., & Fiehn, O. (2016). Increasing lipidomic coverage by selecting optimal mobile-phase modifiers in LC-MS of blood plasma. *Metabolomics*, 12(2), 34.
- Castaño, C., Kalko, S., Novials, A., & Párrizas, M. (2018). Obesity-associated exosomal miRNAs modulate glucose and lipid metabolism in mice. *Proceedings of the National Academy of Sciences of the United States of America*, 115(48), 12158-12163.
- Chan, J. C., Lai, C. Y., Remmelzwaal, S., Jongen-Lavrencic, M., Coenen-Stass, A. M., van der Meijden, W. A., Broekmans, M., Böttcher, R., de Haan, G., van der Schoot, C. E., Fuchs, E., Pospisilik, J. A., de Winther, M. P. J., Mokry, M., Théry, C., Giepmans, B. N. G., & van der Vlag, J. (2020). Reproductive tract extracellular vesicles are sufficient to transmit intergenerational stress and program neurodevelopment. *Nature Communications*, 11, 1499.
- Chargaff, E., & West, R. (1946). The biological significance of the thromboplastic protein of blood. *The Journal of Biological Chemistry*, 166(1), 189-197.
- Chen, Q., Yan, M., Cao, Z., Li, X., Zhang, Y., Shi, J., Feng, G. H., Peng, H., Zhang, X., Zhang, Y., Qian, J., Duan, E., & Zhai, Q. (2016). Sperm tsRNAs contribute to

intergenerational inheritance of an acquired metabolic disorder. *Science*, 351(6271), 397-400.

Cheng, C. Y., & Mruk, D. D. (2012). The blood-testis barrier and its implications for male contraception. *Pharmacological Reviews*, 64(1), 16-64.

Choi, H., & Mun, J. Y. (2017). Structural analysis of exosomes using different types of electron microscopy. *Analytical and Bioanalytical Chemistry*, 47, 171-175.

Choy, K. H. K., Chan, S. Y., Lam, W., et al. (2022). The repertoire of testicular extracellular vesicle cargoes and their involvement in inter-compartmental communication associated with spermatogenesis. *BMC Biology*, 20(1), 78.

Chua, E. C.-P., Shui, G., Cazenave-Gassiot, A., Wenk, M. R., & Gooley, J. J. (2015). Changes in plasma lipids during exposure to total sleep deprivation. *Sleep*, 38(11), 1683-1691.

Chuo, S. T.-Y., Chien, J. C.-Y., & Lai, C. P.-K. (2018). Imaging extracellular vesicles: current and emerging methods. *Journal of Biomedical Science*, 25(1), 91.

Conine, C. C., & Rando, O. J. (2022). Soma-to-germline RNA communication. *Nature Reviews Genetics*, 23(2), 73-88.

Conine, C. C., Sun, F., Song, L., Rivera-Pérez, J. A., & Rando, O. J. (2018). Small RNAs gained during epididymal transit of sperm are essential for embryonic development in mice. *Developmental Cell*, 46, 470-480.e3.

Coolbaugh, C. L., Damon, B. M., Bush, E. C., Welch, E. B., & Towse, T. F. (2019). Cold exposure induces dynamic, heterogeneous alterations in human brown adipose tissue lipid content. *Scientific Reports*, 9(1), 13600.

Cossetti, C., Smith, J. A., Iraci, N., et al. (2014). Soma-to-germline transmission of RNA in mice xenografted with human tumour cells: possible transport by exosomes. *PLoS ONE*, 9, e101629.

Cuomo-Haymour, N., Dallari, G., Farzam-Kia, N., et al. (2022). Evidence for effects of extracellular vesicles on physical, inflammatory, transcriptome and reward behaviour status in mice. *International Journal of Molecular Sciences*, 23.

Dadoune, J. P. & Alfonsi, M. F. (1984). Autoradiographic investigation of sperm transit through the male mouse genital tract after tritiated thymidine incorporation. *Reprod. Nutr. Dev.* 24, 927–935.

Dardet JP, Serrano N, Andrés IE, Toborek M. (2022). Overcoming Blood-Brain Barrier Resistance: Implications for Extracellular Vesicle-Mediated Drug Brain Delivery. *Front Drug Deliv* 2.

Dean, L. (2005). Blood and the cells it contains.

- Dehghani, M., & Gaborski, T. R. (2020). Fluorescent labeling of extracellular vesicles. *Meth Enzymol*, 645, 15–42.
- Delabriere, A., Warmer, P., Brennsteiner, V., & Zamboni, N. (2021). SLAW: A Scalable and Self-Optimizing Processing Workflow for Untargeted LC-MS. *Anal Chem*.
- Deng, Q., Ramsköld, D., Reinius, B., & Sandberg, R. (2014). Single-cell RNA-seq reveals dynamic, random monoallelic gene expression in mammalian cells. *Science*, 343, 193–196.
- Di Fiore, P. P., & De Camilli, P. (2001). Endocytosis and signaling: An inseparable partnership. *Cell*, 106, 1–4.
- Dobin, A., Davis, C. A., Schlesinger, F., Drenkow, J., Zaleski, C., Jha, S., Batut, P., Chaisson, M., & Gingeras, T. R. (2013). STAR: Ultrafast universal RNA-seq aligner. *Bioinformatics*, 29, 15–21.
- Doyle, L. M., & Wang, M. Z. (2019). Overview of extracellular vesicles, their origin, composition, purpose, and methods for exosome isolation and analysis. *Cells*, 8(7).
- Dragovic, R. A., Gardiner, C., Brooks, A. S., Tannetta, D. S., Ferguson, D. J. P., Hole, P., Carr, B., Redman, C. W. G., Harris, A. L., Dobson, P. J., Harrison, P., & Sargent, I. L. (2011). Sizing and phenotyping of cellular vesicles using Nanoparticle Tracking Analysis. *Nanomedicine*, 7, 780-788.
- Driedonks, T. A. P., & Nolte-'t Hoen, E. N. M. (2018). Circulating Y-RNAs in Extracellular Vesicles and Ribonucleoprotein Complexes; Implications for the Immune System. *Frontiers in Immunology*, 9, 3164.
- Durairajanayagam, D., Rengan, A. K., Sharma, R. K., & Agarwal, A. (2015). Sperm Biology from Production to Ejaculation. In G. L. Schattman, S. C. Esteves, & A. Agarwal (Eds.), *Unexplained Infertility* (pp. 29-42). Springer New York.
- Eachus, H., Choi, M. K., & Ryu, S. (2021). The effects of early life stress on the brain and behaviour: insights from zebrafish models. *Frontiers in Cell and Developmental Biology*, 9, 657591.
- Ferrero, G., Carpi, S., Polini, B., et al. (2020). Intake of Natural Compounds and Circulating microRNA Expression Levels: Their Relationship Investigated in Healthy Subjects With Different Dietary Habits. *Frontiers in Pharmacology*, 11, 619200.
- Franklin, T. B., Russig, H., Weiss, I. C., Gräff, J., Linder, N., Michalon, A., Vizi, S., Mansuy, I. M. (2010). Epigenetic transmission of the impact of early stress across generations. *Biological Psychiatry*, 68(5), 408-415.
- Frenette, G., Légaré, C., Saez, F., & Sullivan, R. (2005). Macrophage migration inhibitory factor in the human epididymis and semen. *Molecular Human Reproduction*, 11, 575-582.

Fuhrer, T., Heer, D., Begemann, B., & Zamboni, N. (2011). High-throughput, accurate mass metabolome profiling of cellular extracts by flow injection-time-of-flight mass spectrometry. *Analytical Chemistry*, 83(18), 7074-7080.

Fullston, T., Ohlsson Teague, E. M. C., Palmer, N. O., et al. (2013). Paternal obesity initiates metabolic disturbances in two generations of mice with incomplete penetrance to the F2 generation and alters the transcriptional profile of testis and sperm microRNA content. *The FASEB Journal*, 27(10), 4226-4243.

Gan, K. J., & Südhof, T. C. (2019). Specific factors in blood from young but not old mice directly promote synapse formation and NMDA-receptor recruitment. *Proceedings of the National Academy of Sciences of the United States of America*, 116(25), 12524–12533.

Gapp, K., Parada, G. E., Gross, F., et al. (2021). Single paternal dexamethasone challenge programs offspring metabolism and reveals multiple candidates in RNA-mediated inheritance. *iScience*, 24(8), 102870.

Gapp, K., et al. (2020). Alterations in sperm long RNA contribute to the epigenetic inheritance of the effects of postnatal trauma. *Molecular Psychiatry*, 25, 2162–2174.

Gapp, K., et al. (2014). Implication of sperm RNAs in transgenerational inheritance of the effects of early trauma in mice. *Nature Neuroscience*, 17, 667–669.

Ghanam, J., Chetty, V. K., Barthel, L., Reinhardt, D., Hoyer, P.-F., & Thakur, B. K. (2022). DNA in extracellular vesicles: from evolution to its current application in health and disease. *Cellular Bioscience*, 12(1), 37.

Giardina, S., Hernández-Alonso, P., Díaz-López, A., Salas-Huetos, A., Salas-Salvadó, J., & Bulló, M. (2019). Changes in circulating miRNAs in healthy overweight and obese subjects: Effect of diet composition and weight loss. *Clinical Nutrition*, 38(1), 438–443.

Ginsburg, M., Snow, M. H., & McLaren, A. (1990). Primordial germ cells in the mouse embryo during gastrulation. *Development*, 110(2), 521–528.

Godmann, M., May, E., & Kimmins, S. (2010). Epigenetic mechanisms regulate stem cell expressed genes *Pou5f1* and *Gfra1* in a male germ cell line. *PLoS ONE*, 5(9), e12727.

Gonzalez-Armenta, J. L., Li, N., Lee, R.-L., Lu, B., & Molina, A. J. A. (2020). Heterochronic parabiosis: old blood induces changes in mitochondrial structure and function of young mice. *The Journals of Gerontology. Series A, Biological Sciences and Medical Sciences*.

Grandjean, V., Fourné, S., De Abreu, D. A. F., Derieppe, M.-A., Remy, J.-J., & Rassoulzadegan, M. (2015). RNA-mediated paternal heredity of diet-induced obesity and metabolic disorders. *Scientific Reports*, 5, 18193.

- Gu, Z., Eils, R., & Schlesner, M. (2016). Complex heatmaps reveal patterns and correlations in multidimensional genomic data. *Bioinformatics*, 32, 2847–2849.
- Guelfi, G., Iaboni, M., Sansone, A., Capaccia, C., Santoro, M. M., & Diverio, S. (2022). Extracellular circulating miRNAs as stress-related signature to search and rescue dogs. *Scientific Reports*, 12(1), 3213.
- Gur, Y., & Breitbart, H. (2006). Mammalian sperm translate nuclear-encoded proteins by mitochondrial-type ribosomes. *Genes & Development*, 20(4), 411–416.
- Harmati, M., Bukva, M., Böröczky, T., Buzás, K., & Gyukity-Sebestyén, E. (2021). The role of the metabolite cargo of extracellular vesicles in tumor progression. *Cancer Metastasis Reviews*, 40(4), 1203–1221.
- Huber, M. H. R., & Bronson, F. H. (1980). Social modulation of spontaneous ejaculation in the mouse. *Behavioral and Neural Biology*, 29, 390–393.
- Jain, R., Wade, G., Ong, I., Chaurasia, B., & Simcox, J. (2022). Determination of tissue contributions to the circulating lipid pool in cold exposure via systematic assessment of lipid profiles. *Journal of Lipid Research*, 63(7), 100197.
- Jelonek, K., Widlak, P., & Pietrowska, M. (2016). The Influence of Ionizing Radiation on Exosome Composition, Secretion and Intercellular Communication. *Protein & Peptide Letters*, 23(7), 656–663.
- Jung, Y. H., Lee, E. S., Kim, H. S., Lee, Y. J., Cho, Y. S., Lee, J., Kim, M. Y., Kim, S. H., Lee, S., Lee, H., Lee, S., & Choi, Y. C. (2020). Transgenerational inheritance of BPA-induced obesity correlates with transmission of new CTCF sites in the *Fto* gene. *BioRxiv*. <https://doi.org/10.1101/2020.11.20.391672>
- Kaati, G., Bygren, L. O., & Edvinsson, S. (2002). Cardiovascular and diabetes mortality determined by nutrition during parents' and grandparents' slow growth period. *European Journal of Human Genetics*, 10(11), 682–688.
- Karimi, N., Cvjetkovic, A., Jang, S. C., et al. (2018). Detailed analysis of the plasma extracellular vesicle proteome after separation from lipoproteins. *Cell Mol Life Sci*, 75(15), 2873–86.
- Kiani, J., Grandjean, V., Liebers, R., et al. (2013). RNA-mediated epigenetic heredity requires the cytosine methyltransferase *Dnmt2*. *PLoS Genet*, 9(5), e1003498.
- Kim, H. J., Rames, M. J., Tassi Yunga, S., et al. (2022). Irreversible alteration of extracellular vesicle and cell-free messenger RNA profiles in human plasma associated with blood processing and storage. *Sci Rep*, 12(1), 2099.
- Kim, J., Lee, S. K., Jeong, S.-Y., et al. (2021). Cargo proteins in extracellular vesicles: potential for novel therapeutics in non-alcoholic steatohepatitis. *J Nanobiotechnology*, 19(1), 372.

Komarova, E. Y., et al. (2021). Hsp70-containing extracellular vesicles are capable of activating of adaptive immunity in models of mouse melanoma and colon carcinoma. *Sci. Rep.*, 11, 21314.

Konstantinidou, A., Mougios, V., Sidossis, L. S. (2016). Acute Exercise Alters the Levels of Human Saliva miRNAs Involved in Lipid Metabolism. *Int J Sports Med*, 37(7), 584–8.

Korman, M. (1967). Distribution of injected L-3,4-dihydroxyphenylalanine (L-dopa) in the adult rat testis and epididymis. *Acta Physiol Scand*, 71(1), 125–6.

Kowal, J., Arras, G., Colombo, M., Jouve, M., Morath, J. P., Primdal-Bengtson, B., ... & Théry, C. (2016). Proteomic comparison defines novel markers to characterize heterogeneous populations of extracellular vesicle subtypes. *Proceedings of the National Academy of Sciences*, 113(E968-E977).

Krawetz, S. A. (2005). Paternal contribution: new insights and future challenges. *Nature Reviews Genetics*, 6(8), 633-642.

Kumar, A., Sundaram, K., Mu, J., Cui, L., Lee, M., Lee, Y., ... & Jung, T. W. (2021). High-fat diet-induced upregulation of exosomal phosphatidylcholine contributes to insulin resistance. *Nature Communications*, 12(1), 213.

Lam, S. M., Zhang, C., Wang, Z., Zhang, J., Su, W., Tan, C. H., ... & Shui, G. (2021). A multi-omics investigation of the composition and function of extracellular vesicles along the temporal trajectory of COVID-19. *Nature Metabolism*, 3(7), 909-922.

Leek, J. T. (2014). svaseq: removing batch effects and other unwanted noise from sequencing data. *Nucleic Acids Research*, 42.

Robinson, M. D., & Oshlack, A. (2010). A scaling normalization method for differential expression analysis of RNA-seq data. *Genome Biology*, 11(3), R25.

Leung, A. K. L., & Sharp, P. A. (2010). MicroRNA functions in stress responses. *Molecular Cell*, 40(2), 205-215.

Li, W., Sun, H., Xu, X., Zhao, J., Zhao, Y., Wang, M., ... & Chen, X. (2022). Endothelial cells regulate astrocyte to neural progenitor cell trans-differentiation in a mouse model of stroke. *Nature Communications*, 13(1), 7812.

Mathieu, M., Martin-Jaular, L., Lavieu, G., & Théry, C. (2019). Specificities of secretion and uptake of exosomes and other extracellular vesicles for cell-to-cell communication. *Nature Cell Biology*, 21(1), 9-17.

McDonald, S. W., & Scothorne, R. J. (1988). The lymphatic drainage of the epididymis and of the ductus deferens of the rat, with reference to the immune response to vasectomy. *J. Anat.*, 158, 57–64.

Meistrich, M. L., Hughes, T. H., & Bruce, W. R. (1975). Alteration of epididymal sperm transport and maturation in mice by oestrogen and testosterone. *Nature*, 258, 145–147.

Mital, P., Hinton, B. T., & Dufour, J. M. (2011). The blood-testis and blood-epididymis barriers are more than just their tight junctions. *Biol Reprod*, 84(5), 851–8.

Morales-Prieto, D. M., et al. (2022). Small Extracellular Vesicles from Peripheral Blood of Aged Mice Pass the Blood-Brain Barrier and Induce Glial Cell Activation. *Cells*, 11.

Morgan, H. D., Sutherland, H. G., Martin, D. I., & Whitelaw, E. (1999). Epigenetic inheritance at the agouti locus in the mouse. *Nat Genet*, 23(3), 314–8.

Muñoz, E. L., Fuentes, F. B., Felmer, R. N., Yeste, M., & Arias, M. E. (2022). Extracellular vesicles in mammalian reproduction: a review. *Zygote*, 30(4), 440–63.

Murillo, O. D., Thistlethwaite, W., Rozowsky, J., et al. (2019). exRNA Atlas Analysis Reveals Distinct Extracellular RNA Cargo Types and Their Carriers Present across Human Biofluids. *Cell*, 177(2), 463-477.e15.

Murphy, M. O., Cohn, D. M., & Loria, A. S. (2017). Developmental origins of cardiovascular disease: Impact of early life stress in humans and rodents. *Neurosci Biobehav Rev*, 74(Pt B), 453–65.

Nixon, B., Stanger, S. J., Mihalas, B. P., Reilly, J. N., Anderson, A. L., Tyagi, S., Holt, J. E., & McLaughlin, E. A. (2015). The microRNA signature of mouse spermatozoa is substantially modified during epididymal maturation. *Biol Reprod*, 93, 91.

Norman, A. R., Byrnes, L., & Reiter, J. F. (2021). GC-1 spg cells are most similar to Leydig cells, a testis somatic cell-type, and not germ cells. *BioRxiv*.

O'Brien, E. A., Ensbey, K. S., Day, B. W., Baldock, P. A., & Barry, G. (2020). Direct evidence for transport of RNA from the mouse brain to the germline and offspring. *BMC Biology*, 18(1), 45.

O'Brien, K., Breyne, K., Ughetto, S., Laurent, L. C., & Breakefield, X. O. (2020). RNA delivery by extracellular vesicles in mammalian cells and its applications. *Nature Reviews Molecular Cell Biology*, 21(10), 585–606.

O'Donnell, L., Nicholls, P. K., O'Bryan, M. K., McLachlan, R. I., & Stanton, P. G. (2011). Spermiation: The process of sperm release. *Spermatogenesis*, 1(1), 14–35.

Oatley, J. M., & Brinster, R. L. (2006). Spermatogonial stem cells. *Methods in Enzymology*, 419, 259–282.

Odaka, H., Hiemori, K., Shimoda, A., Akiyoshi, K., & Tateno, H. (2022). CD63-positive extracellular vesicles are potential diagnostic biomarkers of pancreatic ductal adenocarcinoma. *BMC Gastroenterology*, 22, 153.

Onódi, Z., Pelyhe, C., Terézia Nagy, C., Brenner, G. B., Almási, L., Kittel, Á., & Buzás, E. I. (2018). Isolation of High-Purity Extracellular Vesicles by the Combination of Iodixanol Density Gradient Ultracentrifugation and Bind-Elute Chromatography From Blood Plasma. *Frontiers in Physiology*, 9, 1479.

Ostermeier, G. C., Miller, D., Huntriss, J. D., Diamond, M. P., & Krawetz, S. A. (2004). Reproductive biology: delivering spermatozoan RNA to the oocyte. *Nature*, 429(6988), 154.

Otahal, A., Kuten-Pella, O., Kramer, K., & Thery, C. (2021). Functional repertoire of EV-associated miRNA profiles after lipoprotein depletion via ultracentrifugation and size exclusion chromatography from autologous blood products. *Scientific Reports*, 11(1), 5823.

Palena, A., et al. (2000). E2F transcription factors are differentially expressed in murine gametes and early embryos. *Mech. Dev.*, 97, 211–215.

Palviainen, M., Saari, H., Kärkkäinen, O., et al. (2019). Metabolic signature of extracellular vesicles depends on the cell culture conditions. *J Extracell Vesicles*, 8(1), 1596669.

Pellegrino, R. M., Di Veroli, A., Valeri, A., Goracci, L., & Cruciani, G. (2014). LC/MS lipid profiling from human serum: a new method for global lipid extraction. *Anal Bioanal Chem*, 406(30), 7937–7948.

Pembrey, M. E., Bygren, L. O., Kaati, G., et al. (2006). Sex-specific, male-line transgenerational responses in humans. *Eur J Hum Genet*, 14(2), 159–166.

Penell, J., Lind, L., Salihovic, S., van Bavel, B., & Lind, P. M. (2014). Persistent organic pollutants are related to the change in circulating lipid levels during a 5 year follow-up. *Environ Res*, 134, 190–197.

Pua, H. H., Happ, H. C., Gray, C. J., et al. (2019). Increased Hematopoietic Extracellular RNAs and Vesicles in the Lung during Allergic Airway Responses. *Cell Rep*, 26(4), 933-944.e4.

Rakyan, V. K., Chong, S., Champ, M. E., et al. (2003). Transgenerational inheritance of epigenetic states at the murine Axin(Fu) allele occurs after maternal and paternal transmission. *Proc Natl Acad Sci USA*, 100(5), 2538–2543.

Ramos, A. P., Sebinelli, H. G., Ciancaglini, P., et al. (2022). The functional role of soluble proteins acquired by extracellular vesicles. *J of Extracellular Bio*, 1(1).

Ramos-Zaldívar, H. M., Polakovicova, I., Salas-Huenuleo, E., et al. (2022). Extracellular vesicles through the blood-brain barrier: a review. *Fluids Barriers CNS*, 19(1), 60.

Raposo, G., & Stahl, P. D. (2019). Extracellular vesicles: A new communication paradigm? *Nat Rev Mol Cell Biol*, 20, 509-510.

Rejraji, H., Sion, B., Prensier, G., Carreras, M., Motta, C., Frenoux, J. M., Vericel, E., Grizard, G., Vernet, P., & Drevet, J. R. (2006). Lipid remodeling of murine epididymosomes and spermatozoa during epididymal maturation. *Biol Reprod*, 74, 1104-1113.

Ren, X., Chen, X., Wang, Z., & Wang, D. (2017). Is transcription in sperm stationary or dynamic? *J Reprod Dev*, 63(5), 439-443.

Reza, A. M. M. T., Choi, Y. J., Han, S. G., Song, H., Park, C., Hong, K., & Kim, J. H. (2019). Roles of microRNAs in mammalian reproduction: From the commitment of germ cells to peri-implantation embryos. *Biol Rev Camb Philos Soc*, 94, 415-438.

Richardson, B. E., & Lehmann, R. (2010). Mechanisms guiding primordial germ cell migration: Strategies from different organisms. *Nat Rev Mol Cell Biol*, 11(1), 37-49.

Rinaldi, V., Messemer, K., Desevin, K., et al. (2022). Evidence for RNA or protein transport from somatic tissues to the male reproductive tract in mouse. *BioRxiv*.

Rinaldi, V. D., Donnard, E., Gellatly, K., et al. (2020). An atlas of cell types in the mouse epididymis and vas deferens. *eLife*, 9.

Robaire, B., & Hamzeh, M. (2011). Androgen action in the epididymis. *J Androl*, 32, 592-599.

Robaire, B., Hinton, B. T., & Orgebin-Crist, M. (2006). CHAPTER 22 – The Epididymis | Semantic Scholar.

Robaire, B., & Hinton, B. T. (Eds.). (2002). *The epididymis: From molecules to clinical practice*. Springer US.

Robinson, M. D., McCarthy, D. J., & Smyth, G. K. (2010). edgeR: a Bioconductor package for differential expression analysis of digital gene expression data. *Bioinformatics*, 26, 139–140.

Rodgers, A. B., Morgan, C. P., Leu, N. A., & Bale, T. L. (2015). Transgenerational epigenetic programming via sperm microRNA recapitulates effects of paternal stress. *Proceedings of the National Academy of Sciences of the United States of America*, 112(44), 13699–13704.

Roefs, M. T., Sluijter, J. P. G., & Vader, P. (2020). Extracellular vesicle-associated proteins in tissue repair. *Trends in Cell Biology*, 30(12), 990–1013.

Rokad, D., Jin, H., Anantharam, V., Kanthasamy, A., & Kanthasamy, A. G. (2019). Exosomes as Mediators of Chemical-Induced Toxicity. *Current Environmental Health Reports*, 6(3), 73–79.

Rozowsky, J., Kitchen, R. R., Park, J. J., Galeev, T. R., Diao, J., Warrell, J., Thistlethwaite, W., Subramanian, S. L., Milosavljevic, A., & Gerstein, M. (2019). exceRpt: A Comprehensive Analytic Platform for Extracellular RNA Profiling. *Cell Systems*, 8, 352-357.e3.

- Saitou, M., & Yamaji, M. (2012). Primordial germ cells in mice. *Cold Spring Harbor Perspectives in Biology*, 4(11).
- Samanta, S., Rajasingh, S., Drosos, N., Zhou, Z., Dawn, B., & Rajasingh, J. (2018). Exosomes: new molecular targets of diseases. *Acta Pharmacologica Sinica*, 39(4), 501–513.
- Sellem, E., Marthey, S., Rau, A., Jouneau, L., Bonnet, A., Perrier, J. P., ... & Schibler, L. (2020). A comprehensive overview of bull sperm-borne small non-coding RNAs and their diversity across breeds. *Epigenetics & Chromatin*, 13, 19.
- Reilly, J. N., McLaughlin, E. A., Stanger, S. J., Anderson, A. L., Hutcheon, K., Church, K., ... & Nixon, B. (2016). Characterisation of mouse epididymosomes reveals a complex profile of microRNAs and a potential mechanism for modification of the sperm epigenome. *Scientific Reports*, 6, 31794.
- Setchell, B. P., Voglmayr, J. K., & Waites, G. M. (1969). A blood-testis barrier restricting passage from blood into rete testis fluid but not into lymph. *The Journal of Physiology*, 200(1), 73–85.
- Shah, R., Yeri, A., Das, A., et al. (2017). Small RNA-seq during acute maximal exercise reveal RNAs involved in vascular inflammation and cardiometabolic health: brief report. *American Journal of Physiology-Heart and Circulatory Physiology*, 313(6), H1162–H1167.
- Shao, Y., Li, C., Xu, W., Zhang, P., Zhang, W., & Zhao, X. (2017). miR-31 Links Lipid Metabolism and Cell Apoptosis in Bacteria-Challenged *Apostichopus japonicus* via Targeting CTRP9. *Frontiers in Immunology*, 8, 263.
- Sharma, U., Conine, C. C., Shea, J. M., Boskovic, A., Derr, A. G., Bing, X. Y., ... & Sharp, P. A. (2016). Biogenesis and function of tRNA fragments during sperm maturation and fertilization in mammals. *Science*, 351(6271), 391–396.
- Shurtleff, M. J., Yao, J., Qin, Y., et al. (2017). Broad role for YBX1 in defining the small noncoding RNA composition of exosomes. *Proceedings of the National Academy of Sciences of the United States of America*, 114(43), E8987–E8995.
- Sidhom, K., Obi, P. O., & Saleem, A. (2020). A review of exosomal isolation methods: is size exclusion chromatography the best option? *International Journal of Molecular Sciences*, 21.
- Skerget, S., Rosenow, M. A., Petritis, K., & Karr, T. L. (2015). Sperm proteome maturation in the mouse epididymis. *PLoS ONE*, 10, e0140650.
- Skotland, T., Sagini, K., Sandvig, K., & Llorente, A. (2020). An emerging focus on lipids in extracellular vesicles. *Advanced Drug Delivery Reviews*, 159, 308-321.

- Smith, K. E., & Pollak, S. D. (2020). Early life stress and development: potential mechanisms for adverse outcomes. *Journal of Neurodevelopmental Disorders*, 12(1), 34.
- Stahl, P. D., & Raposo, G. (2019). Extracellular vesicles: exosomes and microvesicles, integrators of homeostasis. *Physiology*, 34(3), 169-177.
- Suganuma, R., Yanagimachi, R., & Meistrich, M. L. (2005). Decline in fertility of mouse sperm with abnormal chromatin during epididymal passage as revealed by ICSI. *Human Reproduction*, 20, 3101-3108.
- Sullivan, R. (2015). Epididymosomes: a heterogeneous population of microvesicles with multiple functions in sperm maturation and storage. *Asian Journal of Andrology*, 17, 726-729.
- Tamessar, C. T., Trigg, N. A., Nixon, B., Skerrett-Byrne, D. A., Sharkey, D. J., Robertson, S. A., Bromfield, E. G., & Schjenken, J. E. (n.d.). Roles of male reproductive tract extracellular vesicles in reproduction. *American Journal of Reproductive Immunology*, 85, e13338.
- Théry, C., Witwer, K. W., Aikawa, E., et al. (2018). Minimal information for studies of extracellular vesicles 2018 (MISEV2018): a position statement of the International Society for Extracellular Vesicles and update of the MISEV2014 guidelines. *Journal of Extracellular Vesicles*, 7(1), 1535750.
- Thimon, V., Frenette, G., Saez, F., Thabet, M., & Sullivan, R. (2008). Protein composition of human epididymosomes collected during surgical vasectomy reversal: a proteomic and genomic approach. *Human Reproduction*, 23, 1698-1707.
- Thomou, T., Mori, M. A., Dreyfuss, J. M., Konishi, M., Sakaguchi, M., Wolfrum, C., ... & Kahn, C. R. (2017). Adipose-derived circulating miRNAs regulate gene expression in other tissues. *Nature*, 542(7642), 450-455.
- Tian, F., Zhang, S., Liu, C., Yu, Y., Chen, Y., & Li, M. (2021). Protein analysis of extracellular vesicles to monitor and predict therapeutic response in metastatic breast cancer. *Nature Communications*, 12(1), 2536.
- Trigg, N. A., Eamens, A. L., Nixon, B., Bromfield, E. G., & Schjenken, J. E. (2021). Acrylamide modulates the mouse epididymal proteome to drive alterations in the sperm small non-coding RNA profile and dysregulate embryo development. *Cell Reports*, 37(11), 109787.
- Tsai, S. Y., Opavsky, R., Sharma, N., Wu, L., & Naidu, S. R. (2008). Mouse development with a single E2F activator. *Nature*, 454(7201), 1137-1141.
- Urabe, F., Patil, K., Ramm, G. A., Ochiya, T., & Soekmadji, C. (2021). Extracellular vesicles in the development of organ-specific metastasis. *Journal of Extracellular Vesicles*, 10(9), e12125.

- van der Pol, E., Böing, A. N., Harrison, P., Sturk, A., & Nieuwland, R. (2012). Classification, functions, and clinical relevance of extracellular vesicles. *Pharmacological Reviews*, 64(3), 676-705.
- van Niel, G., D'Angelo, G., & Raposo, G. (2018). Shedding light on the cell biology of extracellular vesicles. *Nature Reviews Molecular Cell Biology*, 19(4), 213-228.
- van Steenwyk, G., Akhmanova, M., Hoekstra, D., & Kruitwagen, C. L. (2020). Involvement of circulating factors in the transmission of paternal experiences through the germline. *The EMBO Journal*, 39, e104579.
- van Steenwyk, G., Roszkowski, M., Manuella, F., Franklin, T. B., & Mansuy, I. M. (2018). Transgenerational inheritance of behavioral and metabolic effects of paternal exposure to traumatic stress in early postnatal life: evidence in the 4th generation. *Environmental Epigenetics*, 4(2), dvy023.
- Vickers, K. C., Palmisano, B. T., Shoucri, B. M., Shamburek, R. D., & Remaley, A. T. (2011). MicroRNAs are transported in plasma and delivered to recipient cells by high-density lipoproteins. *Nature Cell Biology*, 13(4), 423-433.
- Villeda, S. A., Plambeck, K. E., Middeldorp, J., et al. (2014). Young blood reverses age-related impairments in cognitive function and synaptic plasticity in mice. *Nature Medicine*, 20(6), 659-663.
- Vlachos, I. S., & Hatzigeorgiou, A. G. (2017). Functional analysis of miRNAs using the DIANA tools online suite. *Methods in Molecular Biology*, 1517, 25-50.
- Wang, Y., Chen, Z.-P., Hu, H., Lei, J., Zhou, Z., Yao, B., Chen, L., Liang, G., Zhan, S., Zhu, X., Jin, F., Ma, R., et al. (2021). Sperm microRNAs confer depression susceptibility to offspring. *Science Advances*, 7(2).
- Watkins, A. J., Dias, I., Tsuro, H., Allen, D., Emes, R. D., & Moreton, J. (2018). Paternal diet programs offspring health through sperm- and seminal plasma-specific pathways in mice. *Proceedings of the National Academy of Sciences of the United States of America*, 115(40), 10064-10069.
- Weng, Q., Wang, Y., Xie, Y., et al. (2022). Extracellular vesicles-associated tRNA-derived fragments (tRFs): biogenesis, biological functions, and their role as potential biomarkers in human diseases. *Journal of Molecular Medicine*, 100(1), 63-80.
- Wickham, H. (2016). *ggplot2: Elegant Graphics for Data Analysis*. Springer-Verlag New York.
- Williams, C., Palviainen, M., Reichardt, N.-C., Siljander, P. R.-M., & Falcón-Pérez, J. M. (2019). Metabolomics applied to the study of extracellular vesicles. *Metabolites*, 9(11), 271.
- Yamamoto, H., Zheng, K.-C., & Ariizumi, M. (2003). Influence of heat exposure on serum lipid and lipoprotein cholesterol in young male subjects. *Industrial Health*, 41(1), 1-7.

Maturation of spermatozoa in the epididymis of the Chinese hamster. *American Journal of Anatomy*, 172(4), 317–330.

Yáñez-Mó, M., Siljander, P. R. M., Andreu, Z., et al. (2015). Biological properties of extracellular vesicles and their physiological functions. *Journal of Extracellular Vesicles*, 4, 27066.

Yates, A. G., et al. (2022). In sickness and in health: The functional role of extracellular vesicles in physiology and pathology in vivo: Part I: Health and Normal Physiology. *Journal of Extracellular Vesicles*, 11, e12151.

Yoshida, K., Maekawa, T., Ly, N. H., et al. (2020). ATF7-dependent epigenetic changes are required for the intergenerational effect of a paternal low-protein diet. *Molecular Cell*, 78(3), 445-458.e6.

Zeybel, M., Hardy, T., Robinson, S. M., et al. (2015). Differential DNA methylation of genes involved in fibrosis progression in non-alcoholic fatty liver disease and alcoholic liver disease. *Clinical Epigenetics*, 7, 25.

Zhang, Y., Zhang, X., Shi, J., Tuorto, F., Li, X., Liu, Y., Liebers, R., Zhang, L., Qu, Y., Qian, J., Pahima, M., Liu, Y., et al. (2018). Dnmt2 mediates intergenerational transmission of paternally acquired metabolic disorders through sperm small non-coding RNAs. *Nature Cell Biology*, 20, 535–540.

Zhang, X., et al. (2021). The biology and function of extracellular vesicles in cancer development. *Frontiers in Cell and Developmental Biology*, 9, 777441.

Zhou, W., Stanger, S. J., Anderson, A. L., Bernstein, I. R., De Iuliis, G. N., McCluskey, A., McLaughlin, E. A., Dun, M. D., & Nixon, B. (2019). Mechanisms of tethering and cargo transfer during epididymosome-sperm interactions. *BMC Biology*, 17, 35.

Zhu, L. J., Hardy, M. P., Inigo, I. V., Huhtaniemi, I., Bardin, C. W., & Moo-Young, A. J. (2000). Effects of androgen on androgen receptor expression in rat testicular and epididymal cells: a quantitative immunohistochemical study. *Biology of Reproduction*, 63, 368–376.

5. Annex. Omnisperm: Versatile analyses of sperm and offspring production from a single mouse male

Martin Roszkowski*¹, Leonard C Steg*¹, Irina Lazar-Contes¹, Pierre-Luc Germain^{1,2}, Deepak Tanwar¹, Anara Alshanbayeva¹, Niharika Obrist¹, Ali Jawaid^{1,5,6}, Gretchen van Steenwyk¹, Eloïse Kremer¹, Dalila Korkmaz³, Mark Ormiston³, Francesca Manuella¹, Johannes vom Berg³, Jörg Tost⁴, Johannes Bohacek^{1,7} and Isabelle M Mansuy¹

Affiliations:

¹Laboratory of Neuroepigenetics, Brain Research Institute of the University of Zurich and Institute for Neuroscience of the ETH Zurich, Zurich, Switzerland

²Institute for Neuroscience, ETH Zurich and Department of Molecular Life Sciences of the University Zurich, Switzerland

³Institute of Laboratory Animal Science, University of Zurich, Schlieren, Switzerland

⁴Laboratory for Epigenetics and Environment, Centre National de Génotypage, CEA-Institut de Génomique, Evry, France

⁵BRAIN CITY EMBL-Nencki Center of Excellence for Neural Plasticity and Brain Disorders, Nencki Institute of Experimental Biology, Warsaw, Poland

⁶Department of Neurology, University of Texas Health Science Center, Houston, USA

⁷Laboratory of Molecular and Behavioral Neuroscience, Institute for Neuroscience, ETH Zurich, Zurich, Switzerland

*These authors contributed equally

Corresponding author: Isabelle M. Mansuy; E-mail: mansuy@hifo.uzh.ch

Research Article in Preparation

Description of the contributions to the manuscript.

Contributions of Anar Alshanbayeva:

- i. Pre-processed samples for isolations of epididymosomes together with Martin Roszkowski, isolated epididymosomes by density-gradient ultracentrifugation and characterized them by immunoblotting and nanoparticle-tracking analysis.

Contribution of the other authors:

- i. Martin Roszkowski, Johannes Bohacek and Isabelle M. Mansuy designed the experiments.
- ii. Martin Roszkowski established and performed sperm collection and characterization.
- iii. Martin Roszkowski, Irina Lazar-Contes, Gretchen van Steenwyk and Francesca Manuella performed the animal experiments.
- iv. Martin Roszkowski, Irina Lazar-Contes, Ali Jawaid and Eloïse Kremer collected the sperm.
- v. Martin Roszkowski and Niharika Obrist processed samples and prepared sequencing libraries.
- vi. Leonard C. Steg, Pierre-Luc Germain and Deepak Tanwar performed data processing and bioinformatic analyses.
- vii. Martin Roszkowski, Leonard C. Steg and Pierre-Luc Germain interpreted experimental results.
- viii. Isabelle M. Mansuy, Johannes Bohacek, Johannes vom Berg and Jörg Tost acquired funding for the study.
- ix. Martin Roszkowski, Leonard C. Steg, Johannes Bohacek, Irina Lazar-Contes and Isabelle M. Mansuy wrote the Manuscript.

5.1 Introduction

Sperm cells, the vector of paternal genetic information, have a crucial role in species with sexual reproduction. During spermatogenesis, sperm cells acquire unique cellular traits that enable the fertilization of the oocyte and the undistorted initiation of the embryonic development. These sperm-specific features include the motility apparatus to reach the oocyte and an enzymatic machinery to penetrate the zona pellucida and fuse into the egg [1, 2]. Once the sperm cell enters the oocyte, the sperm-derived phospholipase C, PLC- ζ , initiates the gamete to embryo transition and the paternal genome joins its maternal counterpart for the initiation of the embryonic transcription [3, 4]. To ensure the production of sperm cells capable of all these functions, spermatogenesis involved multiple cell death checkpoints at which erroneous sperm cells undergo apoptosis [5].

Genetic factors, diseases and environmental factors, however, can disrupt spermatogenic mechanisms, potentially resulting in dysfunctional germ cells. Sperm cells without the capacity to move or penetrate the egg, or sperm with defects its proteome or epigenome that will lead to embryonic arrest after a successful fertilization are often the outcome of such dysfunctional spermatogenesis [3, 6, 7]. Recent developments improved the understanding of male reproductive medicine but there is still a large number of idiopathic sperm abnormalities resulting in infertility [8]. As male infertility is becoming an more important issue, with fertility rates in men younger than 30 years decreasing by 15 % over the last decades, there is an growing need to understand pathologies resulting in male infertility [6, 9].

Sperm cells have been further implied to not only deliver DNA to the oocyte, but also to non-genetic factors. Environmentally-induced changes in the sperm epigenome, i.e in small RNA, DNA methylation (DNAm) or histone modifications, have been shown to affect the next generation [10–12]. While the mechanisms behind this epigenetic transmission are not fully understood yet, there are increasing scientific efforts to understand how the somatic cells communicate with sperm and how the alterations in sperm are implanted into the early embryo.

Extracellular vesicles (EVs) have been shown to bear an important role in sperm biology. EVs in the epididymal lumen, where they are called epididymosomes, form a communication route between the epididymis and sperm. The main role of epididymosomes is to transport nutrients from the epididymal epithelium to sperm

where they are needed for the maturation, motility and survival of the germ cells [13, 14]. Additionally, epididymosomes transport small RNA to sperm cells in response to environmental stimuli, where the RNA is eventually transmitted to the embryo [15, 16].

Here we present a method for the simultaneous collection of mature mouse sperm and EVs, Omnisperm, with increased sperm cell yield per male compared to other methods that allows multi-layered analysis of sperm and parallel fertilization of females. We used this approach to study sperm DNAm and RNA from sperm and embryos to identify putative associations of sperm DNAm with transcription in sperm and embryos fertilized by the same sperm samples. The workflow can be easily implemented in any laboratories working with mice and presents a new tool to research sperm biology in the context of in reproduction and development.

5.2 Results

5.2.1 OmniSperm to collect increased numbers of sperm cells for multi-layered analyses

We developed a collection method called OmniSperm to increase the yield of mature sperm cells per individual male. Cauda epididymis and vas deferens were dissected, the luminal fluid of vas deferens was extruded and vas deferens was removed (Figure 1A). Cauda epididymis was cut open, placed, together with the luminal fluid, on a cell strainer and rinsed with M2 medium (Figure 1B). The filtrate was centrifuged to collect sperm cells in the pellet while the supernatant was used for extracellular vesicles collection (Figure 1C and D and Supplementary figure 1). 32-45 million sperm cells per male could be collected, which is $587 \pm 17 \%$ and $173 \pm 18 \%$ more than simple and repeated swim-up methods respectively (Figure 1E). This large number allowed us to use up to 30 million sperm cells for DNA and RNA extraction and, in parallel, fertilize three females per donor male using artificial insemination (AI) with 2 million sperm cells per female (Figure 1F). The nucleic acid extractions resulted in high yields of both DNA and RNA (Figure 1G and H) and the average quantified DNA integrity was 8, indicating good DNA quality (Figure 1G). Sperm RNA quality could not be quantified but was visually assessed using electropherograms which did not show any degradation (Supplementary figure 2). Sperm DNA was used for whole genome bisulfite sequencing (WGBS) to analyse DNAm and RNA for total RNA-sequencing to

analyse the transcriptome. From the AI-fertilized females, we were able to collect preimplantation embryos between 4- and 8-cell stages, which were used for polyA⁺ single-embryo RNA sequencing (Supplementary figure 3A-D).

Epididymosomes were collected from the sperm supernatant using a series of centrifugation and ultracentrifugation steps (Supplementary figure 1A). After confirming their integrity by electron microscopy (Fig. 1C), we measured their size and concentration by nanoparticle tracking analysis. The majority of vesicles were 100-350 nm in diameter and reached a concentration of 2 to 5 million particles/ml (Supplementary figure 1B). We also confirmed the presence of the EV surface marker *Cd9* in the Optiprep gradient fraction between 30 and 35 %, which is expected to contain EVs (Supplementary figure 1C). In summary, Omnisperm can be used for the parallel collection of sperm and epididymosomes, of which sperm yield is high enough for the fertilization of multiple females per male and additional molecular analyses.

5.2.2 Isolation of mature sperm cells confirmed by several methods

To confirm that the collected sperm cells are mature, we employed multiple experimental strategies. First, sperm RNA sequencing data was used to compare the expression of marker genes with RNA sequencing data from testes and somatic tissue (liver) (Figure 2A). Mature sperm marker genes *Prm2* [17] and *Tnp1* [18] were expressed and spermatocyte markers *Piwil3* and *Sycp3* [18] were not transcribed. Further, the histone gene *Hist2h2aa1* was not expressed in sperm but in testes and liver while the liver specific gene *Cyp1a2* [19] was only expressed in liver tissue. We further analysed sperm DNAm at known germline specific imprinted CGs [20] and observed that only paternally imprinted CGs are methylated while maternal imprinted CGs are not. The absence of contaminating somatic cells was additionally confirmed by visually inspecting electropherograms of sperm RNA: The sperm RNA did not have peaks for 18S and 28S ribosomal RNA, which are present whole testis RNA (Supplementary figure 2). Finally, sperm cell structure was assessed using electron microscopy (Figure 1D) and imaging flow cytometry (Supplementary figure 4).

5.2.3 Association of sperm DNAm with RNA expression in sperm and embryos

We then investigated the association between sperm DNAm and RNA expression in sperm and embryos. For each transcript, promoter DNAm was plotted against

transcript expression. First, we examined the effects in the whole datasets, by plotting average promoter DNAm from all sperm samples ($n = 10$) against the median transcript expression in either the same sperm samples ($n = 10$, Figure 2C) or embryos descending from the same sperm samples ($n = 28$, Figure 2D). For sperm RNA, we observed the highest abundance in transcripts with a non-methylated promoter (DNAm < 0.1) but also transcripts with promoter DNAm higher than 0.1 were present, although to a lesser extent (Figure 2C). When analysing the association of sperm DNAm and embryo transcription, we observe a different pattern: Embryo transcripts with promoter methylation > 0.1 in sperm were generally not expressed, and only unmethylated promoters were permissive for transcription in the embryo. To confirm that Omnisperm can be used to generate valuable data from individual males, we conducted the same analyses on sperm from individual males and their respective embryos (Supplementary Figure 5). We observed the same trends as in the cumulated data: In sperm, transcripts are mainly present if their promoter is demethylated but some can be detected with methylated promoters. In embryos, only transcript with unmethylated promoters in sperm are permissive for transcription. In summary, we show that Omnisperm can be used to perform multi-omic analyses in sperm and its derived embryos, in both, cumulated and individual-male data.

5.3 Discussion

As numbers of male infertility are increasing, the understanding of sperm biology in the context of reproduction and development are becoming more relevant for the public. Here we present Omnisperm, an improved method for sperm cell extraction and parallel EV collection, using multiple washes of cauda epididymis. This protocol enables the collection of a large number sperm cells per male to fertilize several females and conduct a versatile analysis of the sperm cells, epididymosomes and offspring.

As example for a multi-layered analysis based on Omnisperm, we collected sperm from several males, fertilized three females per male using AI and generated sperm RNA and DNAm sequencing data. Preimplantation embryos were collected from the females and used for single embryo RNA sequencing.

Most commonly used methods for sperm collection include a swim-up step as a positive selection for motile, and hence mature, sperm. Because this is not the case for Omnisperm, we used multiple experimental approaches to confirm the maturity of

collected sperm. Sperm gene expression showed absence of markers for immature sperm and somatic cells, while mature marker genes were expressed. DNAm at sex- and germline-specific imprinted genes represented the expected pattern of highly methylated paternally imprinted genes and no methylation at maternally imprinted genes. We further compared RNA electropherograms of sperm and whole testis and observed the lack of ribosomal RNA peaks in sperm RNA, indicating absence of somatic cells in our samples. Electron microscopy and flow cytometry imaging were used to assess the cellular structure of collected sperm. Based on these analyses, we are confident that the collected sperm using Omnisperm is mature.

Using the generated sequencing data, we analysed the regulatory connections of sperm DNAm with transcription in sperm and embryos. We observed a general trend of expression of transcripts with a non-methylated promoter, which is in accordance to the general inversed correlation of DNAm and gene expression [21]. In sperm, over half of the transcripts with non-methylated promoters were expressed, but additional transcripts with partial or fully methylated promoters were detected. Sperm cells are thought to be transcriptionally inert and only contain a certain population of RNA retained from spermatogenesis with potential functions for embryo development [3, 22, 23]. This could explain the presence of transcripts with methylated promoters; These transcripts are remaining from earlier spermatogenic stages while the promoters have been methylated during the final differentiation steps. When exploring embryo transcript expression and its relation to sperm DNAm, we observed that generally only transcripts with unmethylated promoters are permissive for transcription in the embryo. Transcripts with partial or fully methylated promoters in sperm, however, are largely not expressed in embryos. Taking these findings together, our data aligns with results of other groups: The role of the sperm epigenome is vastly to constitute a preparation for the zygotic gene regulation but not to control active transcription in sperm cells [3, 24–26]. When performing the analysis using data from individual males and their respective offspring embryos, we were able to observe the same trend. This shows that this sperm DNAm controlled embryo transcription is not an effect of cumulated data but is true within all observed individual males. Since our analysis was based on a small sample size ($n_{\text{sperm}} = 10$, $n_{\text{embryo}} = 28$), these findings should be validated in other experiments and functional experiments are needed to fully understand the impact of the sperm epigenome on the embryo.

The presented analysis strongly focused on the molecular biology of sperm and embryos; however, we envision Omnisperm as a tool for other research fields as well. Omnisperm is also not limited to AI to generate offspring, but other methods, like in-vitro fertilization-based approaches, can be used in the workflow as well. As such, Omnisperm can be used study sperm cells, the generated offspring and epididymosomes, all derived from a single male mouse to improve our understanding in male reproductive biology and its impact on the offspring.

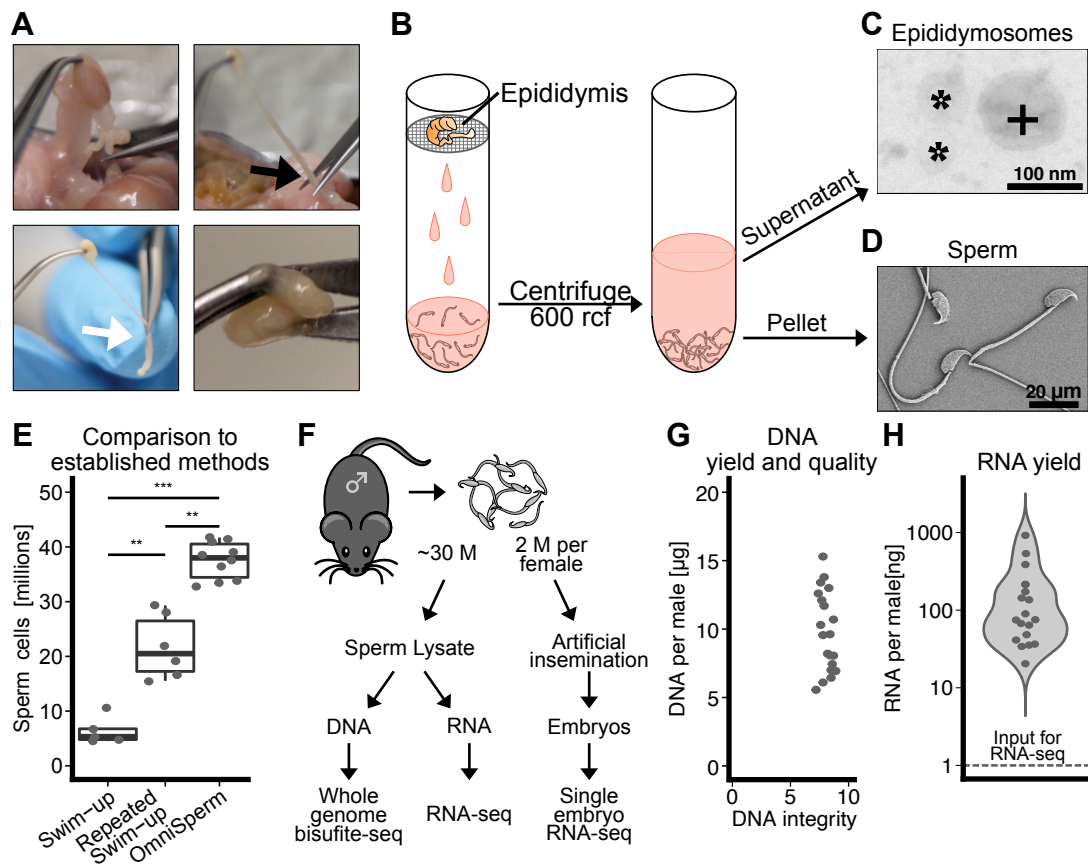


Figure 1. Omnisperm for an increased yield of sperm cells to use for multi-layered sperm and offspring analyses.

A Cauda epididymis and vas deferens are freed and dissected from surrounding tissues (black arrow), luminal fluid from vas deferens is extruded (white arrow) and cauda epididymis is sliced.

B Sliced Cauda epididymis is placed on cell strainer and washed with M2 medium, followed by centrifugation for the separation of the sperm pellet from the epididymosome containing supernatant.

C Transmission electron micrographs showing intact epididymosomes (*) and microvesicles (+).

D Electron micrograph of collected sperm.

E Comparison of the number of collected sperm cells using Omnisperm to the classical collection methods swim-up and repeated swim-up.

F Schematic overview of procedures performed with collected sperm from 10 individual males.

G DNA yield from 50 μ L sperm lysate per male and the respective DNA integrity as a measure for DNA quality.

H RNA yield from 100 μ L sperm lysate per male and the indication how much is needed to generate high-quality total RNA sequencing libraries.

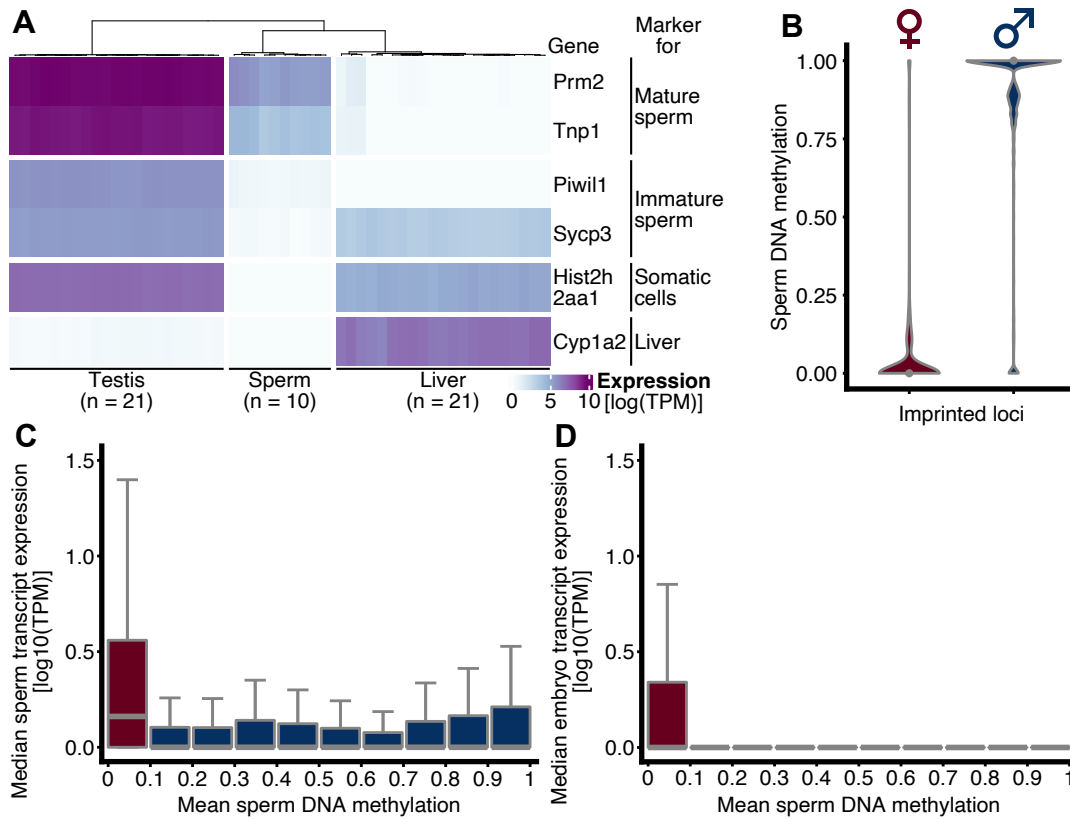


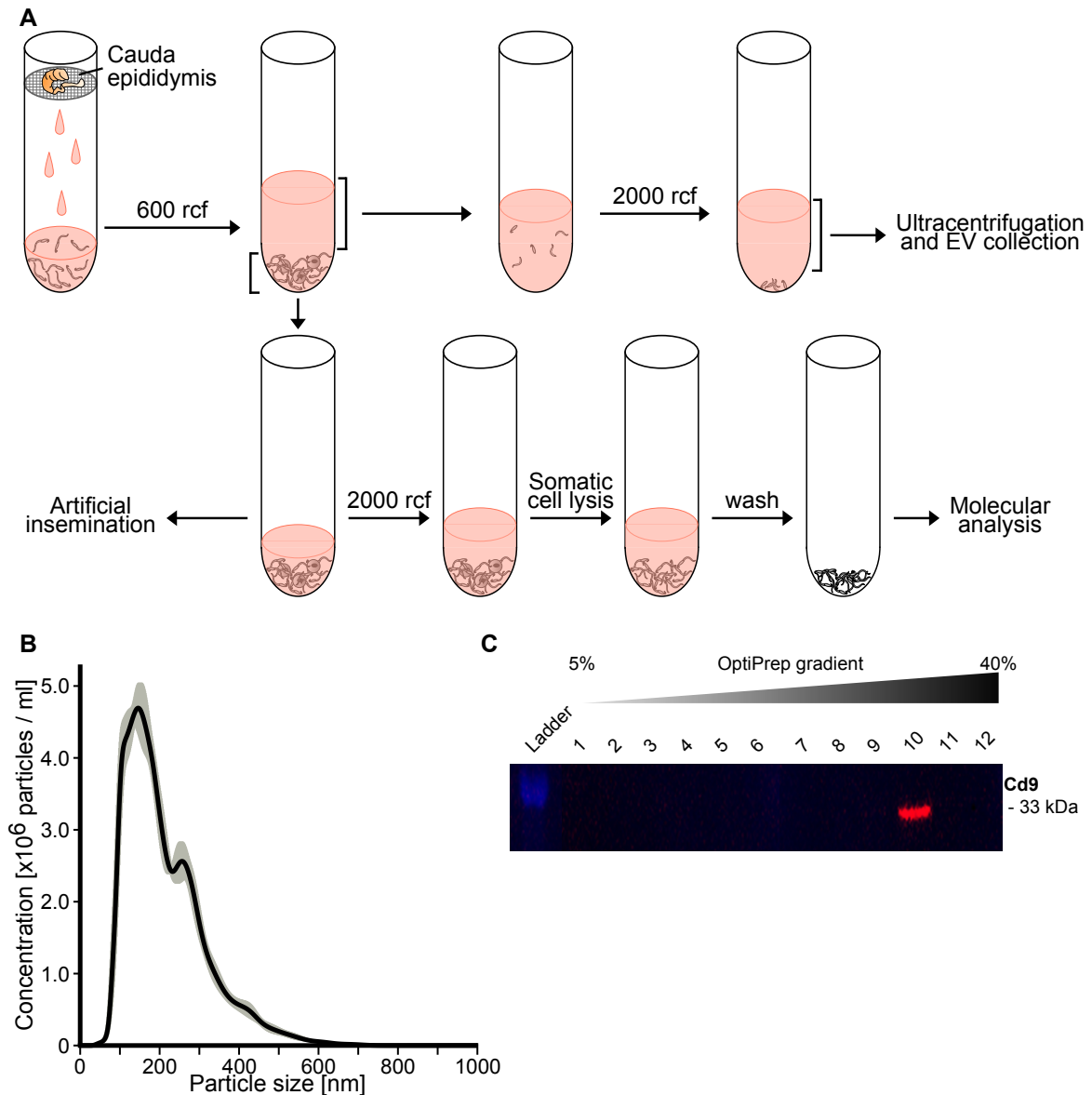
Figure 2. Collection of mature sperm allows to analyse associations of sperm DNAm with transcript expression in sperm and embryo.

A Heatmap of marker genes for mature sperm (Prm2 and Tnp1), immature sperm (Piwil1 and Sycp3), somatic cells (Hist2h2aa1) and liver (Cyp1a2) to compare collected sperm (n = 10) with whole testis (n = 21) and liver (n = 21) tissues. Gene expression in log(TPM).

B Violin plots of single CpG sperm DNAm at germline specific imprinted loci.

C Median sperm transcript expression (y-axis) plotted against mean sperm DNAm (x-axis) using the whole dataset (n = 10).

D Median embryo transcript expression in log₁₀(TPM) (y-axis) plotted against mean sperm DNAm in log₁₀(TPM) (x-axis) using the whole dataset (n(sperm) = 10, n(embryo) = 28).

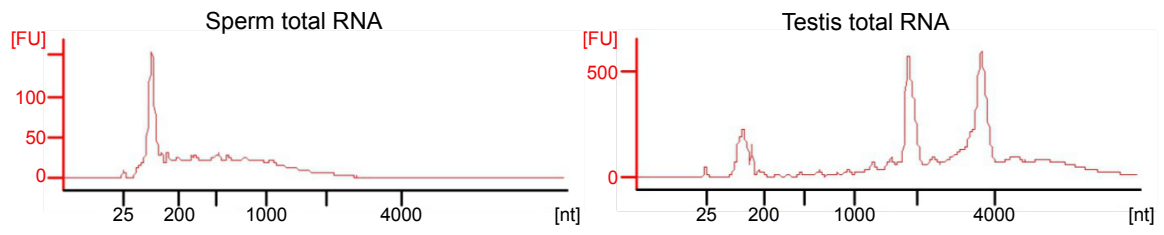


Supplementary Figure 1.

A Full schematic overview of the Omnisperm protocol to collect sperm for AI and molecular analyses and EVs.

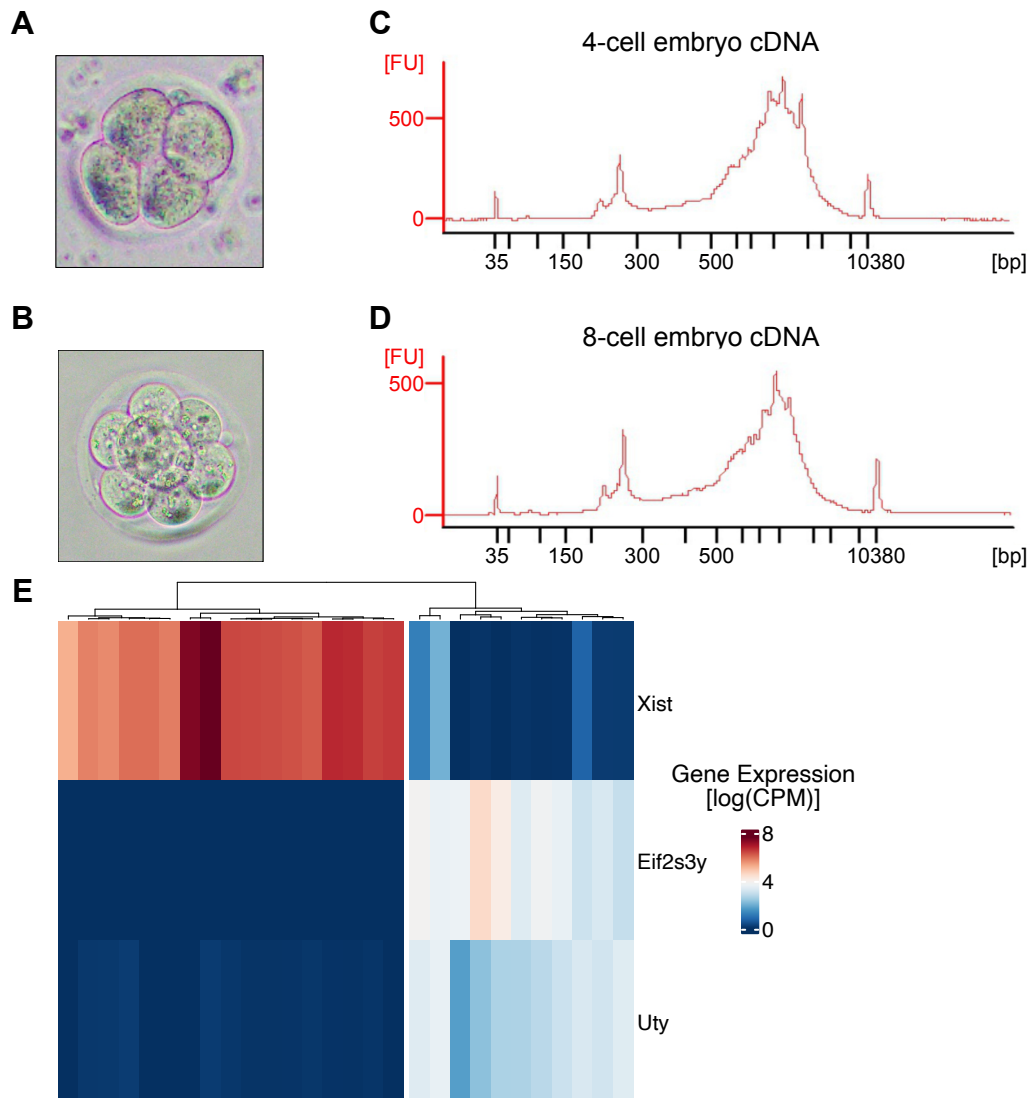
B Nanoparticle tracking results shown as concentration of detected particles according to their size in nm. The size of isolated extracellular vesicles ranges from 50 nm to 600 nm, with a majority of particles with a size around 150 nm ($n = 5$ individual males). Gray area indicates ± 1 SEM.

C Western blot of enriched epididymosomes across fractions (1-12) collected after gradient ultracentrifugation (5-40 % OptiPrep gradient) stained for the epididymosome surface marker Cd9.



Supplementary Figure 2.

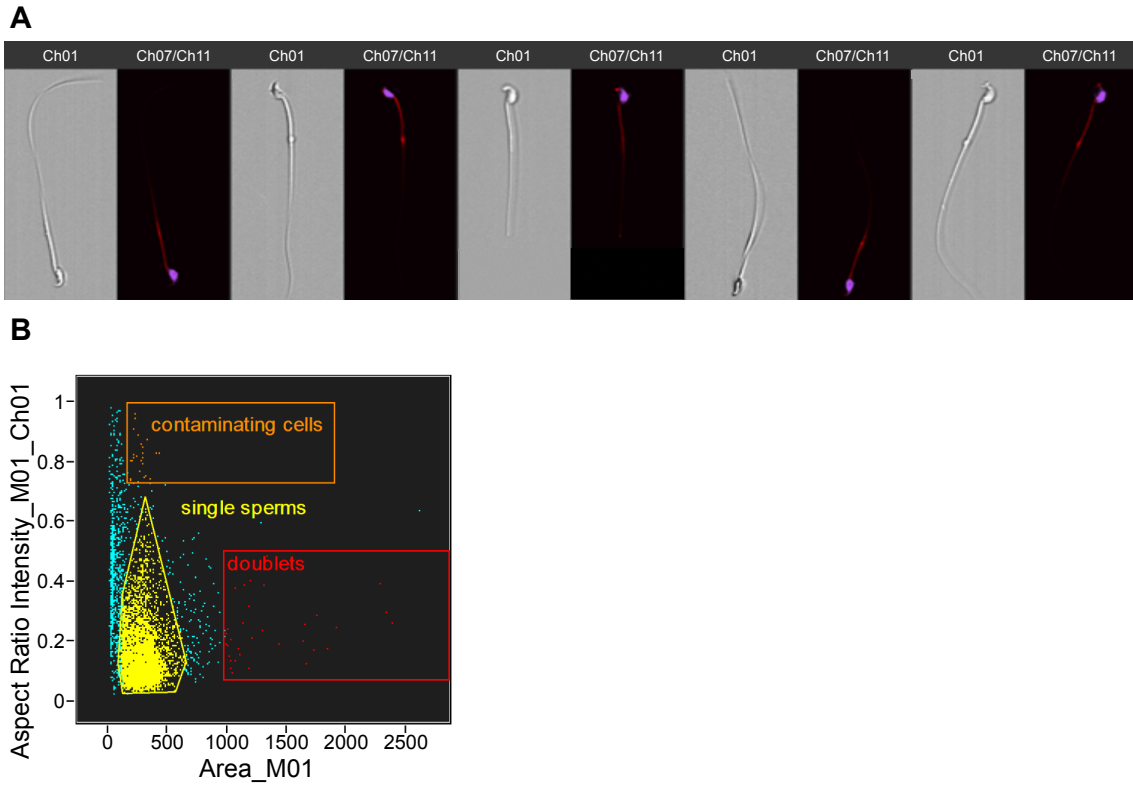
Electropherograms of RNA from sperm RNA and whole testis RNA, in fluorescence units (FU) for given nucleotide length (nt).



Supplementary Figure 3.

A-B Representative pictures of 4-cell and 8-cell embryos collected from AI fertilized females.
C-D Representative electropherograms of single embryo RNA sequencing cDNA libraries generated from 4- or 8-cell embryos.

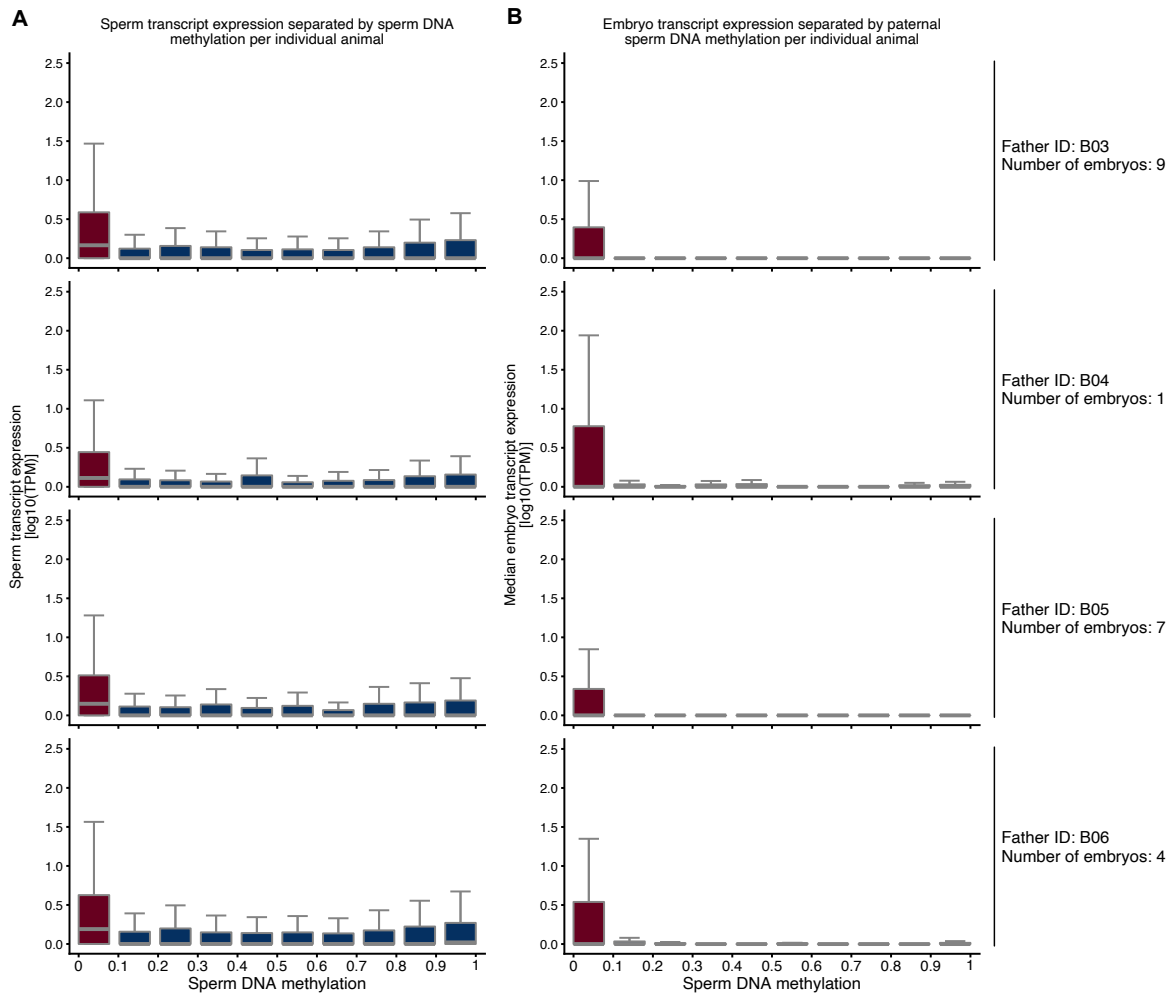
E Heatmap of sex specific genes expressed in single embryos to determine sex. Gene expression in log(CPM).



Supplementary Figure 4.

A Brightfield (Channel 1) and overlaid fluorescence images (Channel 7 and 11) of sperm stained with Hoechst 33342 (blue) and MitoTracker Deep Red (red) acquired by imaging flow cytometry.

B Imaging events were quantified based on the detected aspect ratio (with the value 1 equaling a completely round object) and their size in μm^2 .



Supplementary Figure 5. Association of sperm DNAm and transcript expression in sperm and embryo in sperm of individual male and their respective embryos.

A Sperm transcript expression (y-axis) plotted against sperm DNAm (x-axis) of four representative males. Transcript expression in $\log_{10}(\text{TPM})$.

B Median transcript expression of the embryos derived from one father (y-axis, 1 – 9 embryos per father) plotted against mean sperm DNAm of the father (x-axis). Transcript expression in $\log_{10}(\text{TPM})$.

5.3 Methods

Animals & MSUS

Animal experiments were conducted in strict adherence to the Swiss Law for Animal Protection and were approved by the cantonal veterinary office in Zürich under license number 57/2015 and 83/2018. C57Bl/6J mice were obtained from Janvier (France) and bred in-house. Mice were housed in groups of 3 to 5 animals in individually ventilated cages. Animals were kept in a temperature- and humidity-controlled facility

on a 12h reversed light/dark cycle (light on at 20:00, off at 8:00) with food (M/R Haltung Extrudat, Provimi Kliba SA, Switzerland) and water *ad libitum*. Cages were changed once per week. Half of the male animals used for sperm collection underwent a paradigm to model postnatal trauma, as described here [27]. The conducted analyses were not affected by animals undergoing postnatal trauma.

Sperm and tissue collection

The intraperitoneal cavity of adult males was cut open with scissors from the sternum to the penis. Cauda epididymis and vas deferens were freed from adipose and connective tissue. The epididymal luminal fluid was extruded from vas deferens with a pair of fine forceps and deposited on cauda epididymis. The empty vas deferens was then cut off and removed. The cauda epididymis was sliced with 20 cuts and placed in 1 ml of M2 medium (Sigma, M7167) in a 2 ml Eppendorf tube and placed at 37 °C for 15 minutes. The tube was gently flicked to detach the tissue from the tube wall and the whole content immediately poured on a 70 µm cell strainer (Falcon, 352350) on top of a 50 ml Falcon tube to allow filtrate collection. The tissue on the nylon mesh was gently rinsed with warm M2 medium using a 1000 µl pipette for a total of 14 ml M2 medium. The filtrate was transferred to a 15 ml conical Falcon tube and the remaining cauda epididymis was snap-frozen for further analysis. The filtrate was centrifuged in a pre-warmed centrifuge at 600 rcf for 5min. The supernatant was transferred to a fresh 15 ml Falcon tube for extracellular vesicles extraction. The sperm pellet was left in 400 µl M2 (a smaller volume can be chosen to increase sperm concentration) and gently resuspended with a wide-bore pipette tip to minimize shearing and sperm cells damage. An aliquot should be used at this stage to determine sperm concentration and visually confirm that spermatozoa are still motile and not damaged before artificial insemination. The spermatozoa were kept at 35-37 °C throughout the procedure and processed within one hour for artificial insemination.

For the collection of liver and testis samples, the intraperitoneal cavity of adult males was cut open with scissors from the sternum to the penis. Testis and a lobe of the liver were freed from adipose and connective tissue and snap frozen until further processing.

Epididymosomes collection

To remove cellular debris, the supernatant from sperm collection was subjected to a series of centrifugations of 2'000 rcf for 10 min and 10'000 rcf for 30 min. Supernatants were ultracentrifuged at 120'000 rcf at 4 °C for 2 h (TH 64.1 rotor, Thermo Fisher Scientific). The pellets were washed in PBS at 4 °C and again ultracentrifuged. The pellets were resuspended in 60 µl of PBS. For particle quantification, 10 µl was diluted to a 1:1000 concentration in filtered (0.22 µm) PBS. The number and size distribution of epididymosomes was measured on Nanosight NS300 (Malvern, UK) at 20 °C.

Artificial insemination

Artificial insemination was performed as previously [28] with slight modifications. To ensure that females ovulate, vaginal smears from acyclic virgin females were collected and oestrus stage assessed shortly before insemination. A 100 µl pipette was used to gently flush the opening of the vaginal canal with sterile PBS and collect the liquid on a glass slide. Only females with vaginal cytology characterized by cornified epithelial cells typical of oestrus were used for insemination. 30 µl of the sperm suspension was loaded into a 200 µl pipette tip (Biorad, 223-9915). Two in-house manufactured Teflon tubes of different size (small speculum: 13 mm; large speculum: 10 mm) were used as speculums to guide the pipette tip through the vagina and localize the cervix. Each female mouse was placed on an angled wire cage top and gently pulled up by the tail to expose the vaginal opening. The smaller speculum (inner diameter, 3.28–3.58 mm, wall 0.38 mm) was first inserted into the vagina until the cervix was reached (slight resistance is felt). The small speculum was then removed and the large speculum (inner diameter, 2.06–2.31 mm, wall 0.38 mm) inserted. The cervical opening was localized by gentle probing with the tip of the pipette, and once in place, the tip was inserted into the cervix for a total of 2 cm and the sperm suspension slowly injected. After removing the large speculum, a small cotton tampon moistened in 0.9 % saline solution was inserted into the vaginal opening to mimic the mating plug and replace the need of mating to a vasectomized male. All inseminations were performed under red light during the active phase of the mice. 3 female mice were inseminated with the sperm of one male.

Embryo collection

Four to eight-cell embryos were collected from the oviducts of inseminated females, 42 hours following mating. In brief, female mice were euthanized with 5 % isoflurane

and the oviducts were dissected out and placed in 24-well plates in M2 media at 37 °C. The oviducts were flushed with M2 media by inserting a slightly bent hypodermic 30 G needle through the infundibulum. The procedures were carried out using a stereomicroscope equipped with reflected white light for better visualization of the infundibulum opening. Individual embryos were assessed by light microscopy for cell stage and morphological integrity. Intact four to eight cell embryos were freed from any attached cells, transferred in 4 µl of Buffer RLT+ and frozen.

Sperm DNA / RNA extraction

Sperm was lysed in 200 µl lysis buffer (190 µl Buffer RLT+ (Qiagen, 1053393) and 10 µl 0.5 M TCEP (Sigma, 646547))[29]. The lysate was homogenized for 2 min at 20 Hz using a 0.5 mm stainless steel bead and a TissueLyser II (Qiagen, 85300) then incubated for 5 min at room temperature. Complete lysis of sperm heads was confirmed by microscopy.

For DNA extraction, 50 µl of sperm lysate was used with the DNeasy Blood & Tissue Kit (Qiagen, 69506) according to the manufacturer instructions. DNA concentration was determined using a NanoDrop 2000 (ThermoFisher). DNA integrity was analysed on a 2200 TapeStation (Agilent) with the Genomic DNA ScreenTape analysis according to manufacturer instructions.

For RNA extraction, 100 µL of sperm lysate were mixed with 1 mL TRIzol Reagent (Life Technologies, 15596026). 200 µL chloroform was added, and samples were shaken and incubated at RT for 10 min. After centrifugation at 12000 rcf for 15 min, the aqueous phase was transferred to a fresh tube. 500 µL chloroform was added, and samples were shaken and incubated at RT for 3 min. After centrifugation at 12000 rcf for 15 min, the aqueous phase was transferred to a fresh tube and 10 µL glycogen was added. 500 µL isopropanol was added, tubes were inverted four times and incubated at RT for 10 min and centrifuged at 12000 rcf for 10 min. Supernatant was decanted and samples were washed twice with 75 % ethanol, resuspended in 30 µL nuclease free water and incubated at 55 °C for 15 min. RNA concentration and integrity were analysed on a 2100 Bioanalyzer (Agilent) with the RNA 6000 Pico Kit (Agilent) according to manufacturer instructions.

Sperm whole genome bisulfite sequencing

Libraries for whole genome bisulfite sequencing were prepared using 100 ng genomic DNA using Ovation UltraLow Methyl-seq DR Multiplex System (NuGen) according to manufacturer recommendation. In brief, DNA was fragmented into 200bp fragments by ultrasonication, followed by purification with Agencourt beads into 14 µl nuclease-free water. End-repair reaction was performed in a preheated thermal cycler by incubating the fragmented DNA at 25 °C for 30 min followed by 10 min at 70 °C. Methylated adaptors were ligated by incubating in a preheated thermal cycler at 25 °C for 30 min followed by 10 min at 70 °C. Post-ligation purification was performed using the Agencourt beads as previously, then samples were eluted in 16 µl of nuclease-free water. Another repair reaction was conducted for 10 min at 60 °C then DNA was subjected to bisulfite conversion by Ovation UltraLow Methyl-seq DR Multiplex System. Following spin-column purification of bisulfite-converted DNA, the optimal number of PCR amplification cycles was determined with a qPCR assay. Linear Rn versus cycle number was plotted and the cycle number corresponding to 1/2 of the maximum fluorescent intensity was calculated and used for PCR amplification. Libraries were purified using the Agencourt RNA Clean XP beads and eluted in 20 µl nuclease-free water. Libraries quality and quantity were assessed using the Bioanalyzer 2100 (Agilent Technologies) on DNA 1000 Chips. Profiles typically displayed a peak around 300 bp, corresponding to 150-200 bp inserts. Paired-end sequencing was performed on an Illumina HiSeq 2500 and 300 million paired-end reads were sequenced per sample.

Sperm total RNA sequencing

Total RNA libraries were generated starting from 1 ng of DNase treated (AM1906, Invitrogen) sperm RNA using SMARTer Stranded Total RNA-seq Kit v2 – Pico Input Mammalian (Takara Bio) according to manufacturer instructions. In brief, RNA was fragmented in first strand buffer at 94 °C for 90 s. After addition of template switching oligo and reverse transcriptase, samples were incubated at 42 °C for 90 min. Unique Dual Illumina Indexes were added in 5 PCR cycles. Libraries were purified with AMPure XP beads (Beckman Coulter) and rRNAs depleted with ZapR v2 at 37 °C for 60 min. Final libraries were PCR amplified in 12 cycles and purified with AMPure beads. Libraries were quantified with Qubit dsDNA HS kit and profiles assessed using Agilent High Sensitivity DNA Kit. Sequencing was performed on an Illumina HiSeq 4000 and 20 million paired-end reads were sequenced per sample.

Single embryo sequencing

Embryo RNA-seq libraries were generated using G&T-seq followed by smart-seq2 protocols [30, 31]. In brief, individual embryos were lysed in Buffer RLT+ and gDNA separated from polyA-RNA using magnetic beads (Invitrogen) labelled with dT30VN (MicroSynth). After washing, cDNA was reverse transcribed by Superscript II (Life Technologies) and template switching oligo (IDT) at 42 °C for 90 min and 10 cycles (50 °C for 2min, 42 °C for 2min). cDNA was PCR amplified (20 cycles) using KAPA HiFi HS (Roche) and purified using Ampure XP beads. cDNA library profiles were assessed using Agilent High Sensitivity DNA Kit. Sequencing was performed on the Illumina HiSeq 4000 and 20 million paired-end reads were sequenced per sample.

Whole testis and liver RNA sequencing

Liver and testis tissue pieces were homogenized in 1 ml Trizol by steel beads using a TissueLyser. RNA was extracted as described above for sperm.

PolyA⁺ RNA libraries were prepared by Beijing Genomics Institute (BGI, Shenzhen, China) using their BGISEQ-500 RNA-Seq library preparation protocol. 100 bp paired-end sequencing was performed on the BGISEQ-500 platform.

Sperm DNAm data preprocessing

Reads were trimmed with TrimGalore (-q 30, -l 30) and mapped with Bismark using Bowtie2 to the mm10 reference genome. CpG methylation was assessed using bismark_methylation_extractor and used for further analysis with custom scripts and R packages.

Sperm RNA data preprocessing

Reads were trimmed with TrimGalore (-q 30, -l 30) and quantified using Salmon (--seqBias, --posBias, --gcBias, --dumpEq, --numBootstraps 30).

Embryo RNA data preprocessing

Reads were trimmed with TrimGalore (-q 30, -l 30) and quantified using Salmon (--seqBias, --posBias, --gcBias, --dumpEq, --numBootstraps 30).

Epididymosomes characterization

For immunoblot analysis, fractions were prepared. Iodoxanol (OptiPrep) density media (Sigma-Aldrich, St Louis, MO, USA) was used to prepare an OptiPrep gradient (40 %, 20 %, 10 %, 5 %) by diluting OptiPrep with 0.25 M sucrose, 10 mM Tris. The UC pellets resuspended in PBS were layered onto the OptiPrep gradient and ultracentrifuged at 100'000 rcf at 4 °C for 18 h. 12 fractions were collected from top to bottom, and each fraction was diluted with filtered cold PBS and subjected to 120'000 rcf ultracentrifugation for 2 h at 4 °C. The PBS-resuspended pellet was mixed with 10x RIPA (Cell Signaling Technology) and incubated for 5 min at 4 °C. Equal amount of protein was mixed with 4x Laemmli Sample Buffer (Bio-Rad Laboratories, USA) and samples were loaded on 4-20 % Tris-glycine polyacrylamide gels (Bio-Rad, CA, USA). Membranes were blocked in 5 % SureBlock (LubioScience GmbH, Zürich, Switzerland) in Tris-buffered saline with 0.05 % Tween-20 (Sigma-Aldrich, St Louis, MO, USA) for 2 h at room temperature and incubated with primary-antibodies overnight at 4 °C (anti-CD9 [1:3000; System Biosciences, Palo Alto, CA, USA], anti-GAPDH [1:5000; Cell Signaling, Davers, MA, USA; 14C10]). Next, membranes were washed 3 times in TBS-T, and incubated with a corresponding HRP-conjugated secondary antibody (anti-rabbit [1:10000; Santa-Cruz Biotechnology, cs2357], anti-mouse [1:10000; Upstate Biotechnology, 12-349]) for 2 h. WesternBright Sirius western blot detection kit (Advansta, Menlo Park, CA, USA) was used to visualize the signals, following analysis on ImageLab software (Bio-Rad, Hercules, CA, USA).

Electron microscopy

Extracellular vesicles were prepared by negative stain for electron microscopy. The negative staining of extracellular vesicles was performed with methylcellulose. Briefly, the carrier grid was glow-discharged in plasma for 10 min and then washed with a 100 ul drop of PBS, followed by incubation in 1% glutaraldehyde (GA) in water for 5 min and washing with water 5 times for 2 min per wash. The grid was then incubated in 1% UAc (uranyl acetate) for 5 min and kept on ice in Methylcellulose/UAc (900 ul Methylcellulose 2 % and 100 ul 3 % UAc) solution. After incubation with Methylcellulose/UAc, excess liquid was removed with a filter paper. The grid was air-dried in a gridbox on ice for 5 min. Imaging was performed with a Transmission Electron Microscope.

5.4 Conflict of interest

The authors declare that the research was conducted in the absence of any commercial or financial relationships that could be construed as a potential conflict of interest. Funders had no role in the design of the study; in the collection, analyses, or interpretation of data; in the writing of the manuscript, or in the decision to publish the results.

5.5 Author contributions

MR, JB and IMM designed experiments. MR established sperm collection and characterization. MR, IL, GvS and FM performed animal experiments. MR, IL, AJ and EK collected sperm. MR, IL and JB performed AI. MR, IL, DK and MO collected embryos. MR and NO processed samples and prepared sequencing libraries. MR and AA collected and characterized epididymosomes. LCS, PG and DT performed bioinformatic analyses. MR, JB and PL interpreted experimental results. IMM, JB, JT and JvB acquired funding for the study. MR, LCS, JB, IL and IMM wrote the manuscript. Authors discussed the results and approved the final version of the manuscript.

5.6 Acknowledgements

The authors thank Dr. Silvia Schelbert for administrative support, Dr. Claudia Dumrese from the UZH Cytometry Facility for help with imaging flow cytometry, Dr. Catharina Aquino and Dr. Emilio Yánguez from the Functional Genomics Center Zurich for sequencing services, Dr. Andres Käch and Teresa Colangelo from the UZH Center for Microscopy and Image Analysis for electron microscopy services, and the animal caretakers of the Laboratory Animal Services Center.

5.7 References

1. Lehti MS, Sironen A. Formation and function of sperm tail structures in association with sperm motility defects. *Biol Reprod.* 2017;97:522–36.
2. Sutovsky P. Sperm-egg adhesion and fusion in mammals. *Expert Rev Mol Med.* 2009;11.

3. Tarozzi N, Nadalini M, Coticchio G, Zaca C, Lagalla C, Borini A. The paternal toolbox for embryo development and health. *Mol Hum Reprod.* 2021;27.
4. Ozil JP, Banrezes B, Tóth S, Pan H, Schultz RM. Ca²⁺ oscillatory pattern in fertilized mouse eggs affects gene expression and development to term. *Dev Biol.* 2006;300:534–44.
5. Baum JS, St. George JP, McCall K. Programmed cell death in the germline. *Semin Cell Dev Biol.* 2005;16:245–59.
6. Kumar N, Singh A. Trends of male factor infertility, an important cause of infertility: A review of literature. *J Hum Reprod Sci.* 2015;8:191.
7. Tesarik J, Mendoza C, Greco E. Paternal effects acting during the first cell cycle of human preimplantation development after ICSI. *Hum Reprod.* 2002;17:184–9.
8. Fainberg J, Kashanian JA. Recent advances in understanding and managing male infertility. *F1000Research* 2019 8670. 2019;8:670.
9. Martin JA, Brady MPH, Hamilton E, Sutton PD, Ventura SJ, Menacker F, et al. Births: Final data for 2004. *Natl Vital Stat Reports.* 2006;55:1–101.
10. Gapp K, Jawaid A, Sarkies P, Bohacek J, Pelczar P, Prados J, et al. Implication of sperm RNAs in transgenerational inheritance of the effects of early trauma in mice. *Nat Neurosci.* 2014;17:667–9.
11. Anway MD, Cupp AS, Uzumcu N, Skinner MK. Epigenetic transgenerational actions of endocrine disruptors and male fertility. *Science.* 2005;308:1466–9.
12. Lismer A, Dumeaux V, Lafleur C, Lambrot R, Brind'Amour J, Lorincz MC, et al. Histone H3 lysine 4 trimethylation in sperm is transmitted to the embryo and associated with diet-induced phenotypes in the offspring. *Dev Cell.* 2021;56:671-686.e6.
13. James ER, Carrell DT, Aston KI, Jenkins TG, Yeste M, Salas-Huetos A. The role of the epididymis and the contribution of epididymosomes to mammalian reproduction. *Int J Mol Sci* 2020, Vol 21, Page 5377. 2020;21:5377.
14. Machtinger R, Laurent LC, Baccarelli AA. Extracellular vesicles: roles in gamete maturation, fertilization and embryo implantation. *Hum Reprod Update.* 2016;22:182–93.
15. Alshanbayeva A, Tanwar DK, Roszkowski M, Manuella F, Mansuy IM. Early life stress affects the miRNA cargo of epididymal extracellular vesicles in mouse. *Biol Reprod.* 2021;105:593–602.
16. Sharma U, Sun F, Conine CC, Reichholf B, Kukreja S, Herzog VA, et al. Small

RNAs are trafficked from the epididymis to developing mammalian sperm. 2018. <https://doi.org/10.1016/j.devcel.2018.06.023>.

17. Kossack N, Terwort N, Wistuba J, Ehmcke J, Schlatt S, Schöler H, et al. A combined approach facilitates the reliable detection of human spermatogonia in vitro. *Hum Reprod*. 2013;28:3012–25.

18. Tian P, Zhao Z, Fan Y, Cui N, Shi B, Hao G. Changes in expressions of spermatogenic marker genes and spermatogenic cell population caused by stress. *Front Endocrinol (Lausanne)*. 2021;12:1268.

19. Uno S, Endo K, Ishida Y, Tateno C, Makishima M, Yoshizato K, et al. CYP1A1 and CYP1A2 expression: Comparing ‘humanized’ mouse lines and wild-type mice; comparing human and mouse hepatoma-derived cell lines. *Toxicol Appl Pharmacol*. 2009;237:119–26.

20. Xie W, Barr CL, Kim A, Yue F, Lee AY, Eubanks J, et al. Base-resolution analyses of sequence and parent-of-origin dependent DNA methylation in the mouse genome. *Cell*. 2012;148:816–31.

21. Moore LD, Le T, Fan G. DNA methylation and its basic function. *Neuropsychopharmacol* 2013 381. 2012;38:23–38.

22. Jodar M, Selvaraju S, Sendler E, Diamond MP, Krawetz SA. The presence, role and clinical use of spermatozoal RNAs. *Hum Reprod Update*. 2013;19:604–24.

23. Corral-Vazquez C, Blanco J, Aiese Cigliano R, Sarrate Z, Rivera-Egea R, Vidal F, et al. The RNA content of human sperm reflects prior events in spermatogenesis and potential post-fertilization effects. *Mol Hum Reprod*. 2021;27.

24. Hammoud SS, Nix DA, Zhang H, Purwar J, Carrell DT, Cairns BR. Distinctive chromatin in human sperm packages genes for embryo development. *Nature*. 2009;460:473–8.

25. Jenkins TG, Carrell DT. The sperm epigenome and potential implications for the developing embryo. *Reproduction*. 2012;143:727–34.

26. Brykczynska U, Hisano M, Erkek S, Ramos L, Oakeley EJ, Roloff TC, et al. Repressive and active histone methylation mark distinct promoters in human and mouse spermatozoa. 2010. <https://doi.org/10.1038/nsmb.1821>.

27. Franklin TB, Russig H, Weiss IC, Grff J, Linder N, Michalon A, et al. Epigenetic transmission of the impact of early stress across generations. *Biol Psychiatry*. 2010;68:408–15.

28. Bohacek J, Von Werdt S, Mansuy IM. Probing the germline-dependence of

epigenetic inheritance using artificial insemination in mice. *Environ Epigenetics*. 2016;2:1–10.

29. Roszkowski M, Mansuy IM. High efficiency RNA extraction from sperm cells using Guanidinium Thiocyanate supplemented with Tris(2-Carboxyethyl)Phosphine. *Front cell Dev Biol*. 2021;9.

30. Picelli S, Faridani OR, Björklund ÅK, Winberg G, Sagasser S, Sandberg R. Full-length RNA-seq from single cells using Smart-seq2. *Nat Protoc* 2013 91. 2014;9:171–81.

31. Macaulay IC, Teng MJ, Haerty W, Kumar P, Ponting CP, Voet T. Separation and parallel sequencing of the genomes and transcriptomes of single cells using G&T-seq. *Nat Protoc*. 2016;11:2081–103.

Acknowledgements

I. My first and foremost thank you goes to Isabelle for offering me this chance to pursue my doctoral studies under her supervision. I thank her for always encouraging independence and initiation in the different projects, and letting me explore different directions due to my pure curiosity. I also thank her for always being available and providing a more experienced guidance through tough and important decisions throughout the project. Undoubtedly, thanks to her and other interactions in the team, not only have I learnt to be a more independent and project-driven thinker, but I have also improved my soft-skills. I also learnt from her the power of simplicity in any project – dissecting every concept or results to its smallest parts, the basics or its core; this in turn taught me to understand better and faster other projects, that are outside of our field of study.

I would like to thank Magdalini and Gerhard for accepting to co-supervise my project, for participating in my annual committee meeting, and for providing valuable feedback throughout my PhD. Their expertise and suggestions have immensely contributed to my yearly progress and kept me on track with the objective.

I would next like to thank Rodrigo Arzate for playing such a crucial role in the last few years of my doctoral journey. Your passion for science and teaching has been fundamental during these years, and I have learnt a lot from you. Thank you for all your support and guidance, I will be forever grateful.

I also would like to thank Pierre-Luc and Deepak for their advice, support and contribution in my journey of data analysis throughout initial years of my studies.

I would also like to thank Tom for being the professor of the first lab course I have taken in my life and sparking curiosity and enjoyment in conducting experiments. Your support during my undergraduate years and later on during my PhD have been invaluable for me. Professor Graham and Professor Locler, thank you for seeding the knowledge that served me for years. Here also I would like to thank Xevi and Rudi for their support and mentorship during my initial arrival to ETHZ, and for encouraging exploration of new domains.

I want to thank our team for creating such a lovely atmosphere to work in. Kristina, Anastasiia, Lola – thank you for being the best PhD support group one could imagine. I will never forget all the challenging but also fun moments we shared together. Leo, Maria, Andy, Franci, Chiara, Dennis, Nancy, Alessandra, Bogdan, Gabriel, Jana, Viviana, Rahel, Ionelia, Lisa, Basil – thank you all for being such a great team to work in.

And all the former lab members - Gretchen, Irina, Martin, Ali, Eloise, Lukas, Bisrat – thank you for being there for the young PhDs and sharing your knowledge and experience. And all the other members – Silvia Schelbert, Fabio, Niha, Serena, Maria Gullien, Alberto – thank you for being there.

I would also like to thank Gerhard, Johannes, Kathi, Denis and all of their lab members for being great colleagues and making INS a great institute to be part of.

Special thanks go to Pawel and his team for being great people and supporting me through several experiments. When I think of a great team spirit and environment, I think of you guys.

And, thank you HIFO for being such a lovely place to be at, all the professors and students, and special thanks for the SOLA team for letting me join you in your yearly SOLA runs.

II. The second part of my acknowledgements go to the people who were not involved directly with the thesis work but played a role just as important.

Many thanks go to Adrienne, Rodrigo, Nina, Gina and all the other members of my bu family for being the most fun and accepting friends one could ask for thousands of kilometers away from home. Also Khawlah, Nazgulya and Dana, Mika, Asselya, Azimkhan – thank you guys for all the beautiful memories. I want to thank Michael, Clara, Valentin, Ivan and Gorge for being truly inspiring and great friends, and making the months of bme pass like a day.

I would like to thank Benjamin for being the best roommate and lifetime friend one could ask for. Your support during my time in Paris, coming to CH, also invaluable advices in decision-making and problem-solving later on have been crucial. I am grateful to have such a friend in my life. In addition, many thanks go to the family of Dupays – for the Christmases, the winning lottery tickets, the Versailles runs and many more.

I want to thank Samy for always being there for me and giving me the best career and life advices. Your hard-work and positive attitude have always been infectious and have shaped a part of me today. I will forever be grateful for having you in my life and am looking forward for many more memories in the future.

I want to thank my mentor Daniel for being a great advisor and a supportive friend. Your passion to ideas in science and technology, as well as openness, respect and kindness to others, inspire me.

All other friends that have been there for me – Dimi (thank you for always being supportive and positive), Simon (thank you for always being there for me and I wish you all the best, looking forward for the years ahead), Ankit (thank you for your warm welcome in CH and all the fun times), Nan (thank you for being the older sister I never had and being encouraging and supportive), Oliver (for walks with Daisy and all the fun times), Zhazira (for all the fun childhood memories and your love and support during my PhD), Gulnara (for your support in NYC and pushing me in business ventures), Gemma, Charel and Jean-Philippe (for being great people and a lovely family to be with), Eric, Olivia, Moritz (thank you for your support and wish you all the best in your professorship!), Gulnara Meiramovna, Sampath, Zeinaf, Dyugu, Amanzhol, Islam (for being my career buddy), Mattia and Darren (for always being positive and fun). People from demello's that made my transition swift and joyful – XiaoBao (thank you for everything), Gregor, Julie, Rudi and Justina.

Next, I want to thank the family Hess for being my family here in Switzerland. Angela, Markus, Selina, Fabian, Chayannis, Aran, Liselotte and Robert, and Loona (of-course..!) – thank you guys for welcoming me into your family with open arms, for your warmth and support, for all the fun holidays together. I will forever be grateful for your kindness. Angela – thank you for all your understanding and support, for being a great mother and a friend, I truly cherish our relationship.

I want to thank David for his kindness, patience and support during all these times, for teaching me how to cherish and appreciate the beauty of simplicity in life and to be more grounded, for making the most challenging times in life lighter, easier and not so challenging after all...!, for always believing in me and for being there through highs and lows of this journey.

I would next like to thank my closest family – Askar, Aslan, Anuar, Karakoz, Ayaru und Danial. Also our dearest Alpha and Kuzmich. Thank you guys for being the most amazing family one could ask for, for your support and for the fun times we spent together. I am looking forward to many more of them in the future.

“Аскар - Асико Сикоко Жумуртка - спасибо тебе за твою поддержку. Ты подталкивал меня в первые годы учебы и поддерживал меня в продолжении учебы в Штатах, покупал мне книги для подготовки к SAT, за все это я тебе бесконечно благодарна. Я счастлив видеть, что ты вырос в такого замечательного человека и преуспеваешь в карьере и личной жизни.

Аслан - спасибо тебе за то, что ты всегда был самым спокойным, сильным и мудрым из нас четверых и всегда делился со мной своей жизненной мудростью. И, конечно же, за то, что смеялся надо мной за то, что я вписала свое имя в книгу Жалаира.

Анчик - мой дорогой младший брат, ты всегда будешь моим младшим братом, и я буду любить тебя больше всех. Спасибо тебе за то, что делился своими финансовыми знаниями, всегда был готов обсудить новые бизнес-идеи, поддерживал меня и приезжал ко мне в Швейцарию. Я желаю тебе скорейшего выздоровления после операций на глазах и желаю тебе всего наилучшего в твоей карьере и личной жизни.

Каракоз - добро пожаловать в семью! Спасибо тебе за то, что ты такой красивый, добрый и умный человек и являешься прекрасным партнершей моего брата. Я желаю тебе достичь всех твоих мечтаний в будущем и надеюсь, что однажды вы сможете переехать в Европу.

Аяру и Даниал - самые лучшие пополнения в нашей семье! Продолжайте заставляя нас улыбаться каждый день, вы - будущее!

Кузьмич и Альфа - мы всегда будем помнить вас.”

I also would like thank: *“Спасибо дяде Канату, тете Гуле, тете Зауреш, дяде Асхату, тете Заиде, тете Оле, дяде Марату, Алишеру, Данияру, Аскеру, Даурену и Даулету - за то, что сделали мое детство незабываемым. Дядя Канат - за то, что не давал спать и заставлял делать зарядку рано утром; тетья Гуля - за то, что научила быть начальником; Тетья Зауреш - за твои советы по жизни и потрясающую стряпню; дядя Асхат - за то, что всегда был самым артистичным и веселым; Тетья Оля - за то, что ты самый знающий и структурированный человек, и за летние крошки; тетья Заида - за то, что ты самая веселая; дядя Марат - за то, что написал лучшую книгу о Жалаирах; Данияр - за то, что поддерживал и был отличным братом и приветствовал нас в Алматы; Алишер - Аля Каля Маля - за то, что был отличным младшим братом.”*

Last but not least, I would like to thank my parents – Serikbek and Gulshat for everything they have taught me, for their unconditional love and support. Words cannot express the gratitude and love I have for you two. *“Рахмет, аяулы анам Гүлшат пен ардақты әкем Серікбек. Ең алдымен мені осы дүниеге әкелгеніңіз үшін, мені және бауырларымды өсіріп, әрқашан қасымызда болғаныңыз үшін рахмет. Екіншіден, мені әрқашан жақсы көріп, моральдық қолдау көрсеткеніңіз үшін рахмет. Сіздердің қолдауларыңыз болмаса, мен бүгінгідей болмас едім. Екеуіңізді құрметтеймін, жақсы көремін, осы дүниеде бұдан да көп қызық, бақытты сәттерді өткізулеріңізге тілектеспін. Менің докторлық қорғауым кезінде қатыса алмайтыныңызды білу мені қынжылтады. Мен екеуіңмен тағы бір рет саяхаттап, көбірек естелік қалдыруды күте алмаймын.”*

And anyone else, whose name I might have forgotten to mention, you all know who you are. Thank you for being there for me throughout this journey.

Curriculum Vitae

Anara Alshanbayeva

Contact anara.alshanbayeva@gmail.com,+4178 695
Linkedin 63 26
Address <http://linkedin.com/in/anara-alshanbayeva>
Date of Birth Zürich, Switzerland
CH 20.02.1992
Permit B



Summary

A doctoral scientist, with background in research, multi-omics data analysis and public health. A great team player, with experience in international collaborative projects and fund acquisition for a number of research projects.

Experience

- | | |
|----------------------|--|
| 01/2018 -
03/2023 | Doctoral Researcher in Neuroepigenetics - ETH Zürich, Switzerland <ul style="list-style-type: none">• Designed and managed the PhD research project• Performed analysis of multi-omics data• Supervised and organized projects of master and bachelor students• Represented the lab at local and global scientific events |
| 02/2017 -
10/2017 | Scientific Assistant in single-cell biology - GENETHON, France and ETH Zürich, Switzerland <ul style="list-style-type: none">• Managed and coordinated a project in single-cell biology for Genethon• Collected and analyzed data for an EU grant submission• Designed and fabricated a microfluidic system for single-cell capture and performed experiments |
| 01/2016 -
08/2016 | Data analysis intern in clinical immunology - Institute Curie, France <ul style="list-style-type: none">• Created an automated patient data analysis pipeline in R• Trained team clinical immunology team members in automated data analysis• Collaborated with internal and external departments |
| 01/2015 -
04/2015 | Neuroscience intern - Paris Descartes University, France <ul style="list-style-type: none">• Studied traumatic brain injury through organotypic cerebellar cultures |
| 09/2014 -
05/2015 | UROP scholar - Boston University, USA <ul style="list-style-type: none">• Investigated the role of transcription factor NF-κB modulation in sea anemones |
| 05/2014 -
09/2014 | Undergraduate researcher in molecular biology - Boston University, USA <ul style="list-style-type: none">• Studied the function of N- and C-terminal non-conserved residues in transactivation by sea the anemone (<i>Nematostella vectensis</i>) NF-κB transcription factor |
| 06/2013 - | Intern - National Laboratory of Biotechnology, Kazakhstan |

08/2013 06/2012 - 08/2012	<ul style="list-style-type: none"> Processed blood samples for a clinical trial and isolated DNA, RNA <p>Program assistant - National Medical Holding, Kazakhstan</p> <ul style="list-style-type: none"> Built a database of courses for the MBA Program in Health Management at Eurasian National University (database approved by the Ministry of Education and Science of Kazakhstan)
---------------------------------	---

Education

01/2018 - Present	Doctor of Sciences, ETH Zürich, Institute of Neuroscience, Switzerland
2015 - 2017	MSc in Biomedical Engineering, ENSAM and Paris Descartes University, France
2011 - 2015	BSc in Cellular, Molecular Biology and Genetic, Boston University, USA Minor: Public Health

Experience

Bioinformatics	Single-cell, small and long RNA-sequencing analysis in R and Bash. Metabolomic and Lipidomic data analysis.
Microfluidics	Design, fabrication and operation of a single-cell capture microfluidic system. Culture of cells in microfluidic chips.
Biology	<i>In vitro</i> fertilization, embryo culture, cell culture, common molecular biology techniques (Western blot, qPCR, Immunohistochemistry, cloning, DNA & RNA extraction, immunohistochemistry, immunocytochemistry), fluorescent microscopy, organotypic brain cultures, ultracentrifugation, density gradients.
IT skills	R, Bash, Affinity Designer, MS Office, Inkscape, Matlab.
Animals	Writing licenses, organization of breedings and documentations, experiments.
Soft skills	Result-oriented, analytical, data-driven, empathetic, creative, communicative.

Certifications

2022	CORE: Business Analytics, Economics for Managers, Financial Accounting. Harvard University.
2021	Computational RNA Biology. Swiss Institute of Bioinformatics.
2020	Computational Statistics. ETHZ.
2020	Good Clinical Practice (Modules 1 and 2). Universitätsspital Zürich.
2011	Asia Pacific Leaders Program certificate. Korea University.
2010	American Language Program certificate. Columbia University.

Extracurricular and Leadership Roles

09/2022 - 11/2022	Team leader, Bridge Program. Led a team of 4 consultants for a project in life sciences for a swiss startup, ETH Zürich.
2021 - 2022	Committee member, Graduate Consulting Club, ETH Zürich.
2021 - 2022	President of PhD Students, Brain Research Institute, University of Zürich.
2020-2022	Active participant of Fix the Leaky Pipeline (Inclusion Program), ETH Zürich.
02/2020	Doctorate student representative, Life Sciences Annual Event, University of Zürich.
2015 - 2016	Self-employed instructor (SAT Math courses), France.
2014 - 2015	Board member, Boston University Ballroom team, USA.

2012-2015 Performance in external and internal university ballroom competitions. Board member, Boston University Kazakh Student Society, USA. Organization of cultural activities, fund-raising, advertisement, dance performances.

Awards and Honors

2018 ANR (France) – SNSF (Swiss) Lead Agency Grant.
2018 Research Scholarship for Master Thesis, ETH Zürich, Switzerland.
2016 - 2017 French Embassy Excellence Scholarship, France (6 Nominees from Kazakhstan per year).
2014 - 2015 Undergraduate Research Program Opportunities (UROP). Boston University. Awarded twice.
2010 - 2014 Presidential award “Bolashak” of the Republic of Kazakhstan (Full coverage of Undergraduate studies).
2010 “Gold Medal” for excellent completion of High School. Graduated in the top 2% in the country.

Languages

English: fluent German: B2 French: A2 Russian: fluent Kazakh: native

Publications

Anar Alshanbayeva, Leonard Steg, Alaa Othman, Francesca Manuella, Rodrigo G. Arzate-Mejia, Nicola Zamboni, Isabelle M Mansuy. Circulating extracellular vesicles as soma-to-germline carriers of information on early life experiences. *In prep.*
Anar Alshanbayeva, [Deepak K Tanwar](#), [Martin Roszkowski](#), [Francesca Manuella](#), [Isabelle M Mansuy](#). Early life stress affects the miRNA cargo of epididymal extracellular vesicles in mouse. *Biol. Reprod.*, 593-6021, (2021).
Martin Roszkowski, Irina Lazar-Contes, Pierre-Luc Germain, Deepak Tanwar, Anara Alshanbayeva *et al.* OmniSperm: Multi-omics analyses of sperm and offspring production from a single male. *In prep.*
Mansfield, K.M., Carter, N.M., Nguyen, L. *et al.* Transcription factor NF-κB is modulated by symbiotic status in a sea anemone model of cnidarian bleaching. *Sci Rep* 7, 16025 (2017).
Anar Alshanbayeva, Thomas Gilmore, *et al.* N- and C-terminal non-conserved residues contribute to transactivation by a sea anemone (*Nematostella vectensis*) NF-κB transcription factor. *BIOS* 86, 165-175 (2015).